

**A NEW PALEOCLIMATE RECORD FOR NORTH WESTLAND, NEW ZEALAND,  
WITH IMPLICATIONS FOR THE INTERPRETATION OF SPELEOTHEM BASED  
PALEOCLIMATE PROXIES**

*A thesis submitted in partial fulfilment  
of the requirements for the degree of:*

**Master of Science in Geology**

*at the*

The University of Canterbury

*by*

**Andrea Jean Logan**

**University of Canterbury  
2011**

---



Frontispiece – The Main Entrance to Metro cave.



# **Table Of Contents**

Acknowledgments	v
Abstract	vii
List of Figures and Tables	viii
<b>Chapter 1 – Introduction</b>	<b>1</b>
<b>Chapter 2 – Literature Review</b>	<b>4</b>
2.1 Speleothems as Terrestrial Proxies of Paleoclimate	4
2.1.1 Introduction	4
2.1.2 Caves and Speleothems	4
2.1.3 Dating of Speleothems	8
2.1.4 Speleothems as Paleoclimate Proxies	10
2.1.5 Stable Oxygen Isotopes in Speleothems	12
2.1.6 Stable Carbon Isotopes in Speleothems	17
2.1.7 Summary	19
2.2 New Zealand Quaternary Paleoclimate	20
2.2.1 Introduction	20
2.2.2 Climate Drivers	20
2.2.3 Late Quaternary Climate Events	21
2.2.4 Late Quaternary Climate from Speleothems	25
2.2.5 Summary	27
2.3 Speleothem Fluid Inclusions	28
2.3.1 Introduction	28
2.3.2 The Formation of Fluid Inclusions	28
2.3.3 Fluid Inclusions and Paleoclimate	29
2.3.4 Extracting Fluid Inclusions from Speleothem Calcite	30
2.3.5 Summary	33
<b>Chapter 3 – Field Methods</b>	<b>34</b>
3.1 Introduction	34
3.2 Geological Setting	34
3.3 Regional Climate and Vegetation	39
3.4 Previous Research at Te Ananui/Metro Cave	40
3.5 Field Methods	40
3.6 Description of the Stalagmites	43
<b>Chapter 4 – Analysis Methods and Results</b>	<b>46</b>
4.1 Introduction	46
4.2 Hendy Tests	46
4.3 Drip Water Analyses	50
4.4 Trace Element Analysis	51
4.5 Stable Isotopic Analysis of Calcite	58
4.6 Fluid Inclusion Extraction Method	60
4.6.1 Introduction	60
4.6.2 Development Phase 1	61
4.6.3 Development Phase 2	65
4.6.4 Summary	67

<b>Chapter 5 – Metro 1 Age Model</b>	<b>68</b>
5.1 Introduction	68
5.2 Experimental Age Estimate	68
<b>Chapter 6 – Interpretation and Discussion</b>	<b>72</b>
6.1 Introduction	72
6.2 Interpreting Stable Isotopic Composition	73
6.2.1 Stable Oxygen Isotopes	73
6.2.2 Temperature Reconstruction from the M1 Stalagmite	75
6.2.3 Stable Carbon Isotopes	77
6.3 Interpreting Trace Element Composition	78
6.4 M1 Trace Element Dilution/Enrichment Models	81
6.5 Paleoclimate from the M1 Stalagmite	85
6.6 Discussion of M1 Paleoclimate	89
6.6.1 Comparison with Two South Island Stalagmite Records	89
6.6.2 Modern Geochemical Variability versus Past Variability	91
6.7 Summary	92
<b>Chapter 7 – Conclusions and Future Research</b>	<b>94</b>
<b>Thesis References</b>	<b>98</b>
<b>Appendix 1 – Trace element data from top and base sections of M1</b>	<b>CD</b>
<b>Appendix 2 – M1 stable carbon and oxygen data</b>	<b>CD</b>

## **Acknowledgments**

The completion of this thesis has been made possible by the help and support of many people. Firstly I would like to thank my three supervisors, for all their assistance and guidance. My primary supervisor, Dr. Travis Horton, has been an endless source of ideas, encouragement, and advice. Your support, especially in the lab, has taught me a huge amount about stable isotope geochemistry. You have been not just an excellent supervisor, but a great mentor also. Thanks to Dr. Andrew Lorrey for all the assistance with trace element analyses, and work towards getting dates, even though they have taken a lot longer than we thought! The numerous hours you have spent reading through my chapters and providing feedback have been invaluable. Thanks also to Dr. Mark Quigley for helping out with field work, helping me to set deadlines for my work, and for being there to bounce ideas off.

I have been fortunate to receive several grants and funds for this research, in particular the Mason Trust fund for my field work, the S.J. Hastie scholarship award, and the UC Masters scholarship. I am also very grateful for funding from the Department of Geological Sciences to attend the GSNZ conference in Auckland, 2010, and to the Geoscience Society of New Zealand and the New Zealand Federation of Graduate Women for travel grants to attend the AGU Fall Meeting, December 2010, in San Francisco.

I would also like to thank Lindsay Main and Alice Shanks for introducing me to the world of caves, in particular for taking me on my first trip through Metro cave. Without all your expertise and advice about working in caves, this project would not have been possible. I would also like to thank the West Coast Department of Conservation staff for granting me a sampling permit, and in particular DOC Ranger Chippy Wood for your assistance with field work.

I am also very grateful to Canterbury University Department of Geological Sciences staff for all your technical assistance. Rob Spiers has been a fantastic help with both sourcing cave sampling equipment, and cutting and polishing the stalagmites. Thanks also to Chris Grimshaw for providing me with all the compressed air I needed.

Finally I would like to thank all my family and friends for your constant support, especially those who were happy to be dragged over to Charleston and kept underground for a day of field work. I would also like to thank my parents and friends for the time you have spent listening to me attempting to explain my project, and encouragement to keep at it. Also thanks to my grandparents for your love and extra travel support. Lastly, I am especially grateful to my fiancé, Ollie, for your endless love and support throughout this, and future projects.

# **Abstract**

New Zealand speleothems can be used as proxy records of terrestrial Southern Hemisphere climate change and can be compared to records from the Northern Hemisphere to evaluate the timing of significant climatic events, and the driving influences of the Antarctic and North Pacific. The interpretation of paleoclimate from stalagmite geochemistry is a complex process. The majority of stalagmite records from New Zealand are based on calcite stable isotope composition, however, recent research into stalagmite trace element composition has shown that multi-proxy records aid paleoclimate interpretations. The complexity of the many processes affecting the geochemistry of calcite forming in a cave system requires assumptions to be made about cave environment conditions.

This thesis presents a new high-resolution paleoclimate record based on stable isotope and trace element composition from a West Coast, New Zealand, stalagmite. The assumptions underlying the interpretation of such a record are examined and compared to local environmental field data. In addition, a new method of extracting and analysing calcite fluid inclusions is explored, in order to address some of the issues associated with unknown past stable isotope composition of cave drip water. Field data from the local cave area have demonstrated high natural variability in the stable isotope composition of rainfall, cave drip water, dissolved inorganic carbon, and modern cave calcite. The high modern natural variability raises questions about the validity of assumptions of the stability of the cave environment. The high-resolution record of calcite stable isotope and trace element composition indicates that changes in precipitation amount, the atmospheric temperature of rainfall precipitation, and local environmental water balance are the dominant controls on stalagmite geochemistry on the West Coast. The comparison of this single stalagmite paleoclimate record to other single and multiple stalagmite records from the same region indicate that data from single stalagmites show more variation in past climate, and can be best understood when the modern variability is accounted for with in-depth field measurements of the local environmental processes.

# **List of Figures and Tables**

**Figure 2.1:** Diagrammatic representation of the karst system highlighting the general areas of calcite dissolution and precipitation (Fairchild et al. 2007).....6

**Figure 2.2:** Diagrammatic representation of the processes related to fractionation of  $\delta^{18}\text{O}$  values in water through the hydrological system from the ocean to the cave (Lachniet 2009).....16

**Figure 2.3:** Master North-West South Island (NWSI) speleothem record of  $\delta^{18}\text{O}$  values from eight South Island speleothems (Williams et al. 2010). The record has been corrected for the ice volume effect – taking into account the change in the ocean  $\delta^{18}\text{O}$  values during the LGM (Williams et al. 2005). 56 TIMS dates with  $2\sigma$  error bars are also shown (Williams et al. 2010).....26

**Figure 3.1:** General location of Te Ananui/Metro Cave in the South Island context, approximate location of cave is starred.....35

**Table 3.1:** The data on environmental conditions inside the cave during the 2010 winter, with some extra data from January 2011. Unfortunately relative humidity was not measured during the summer trip.....43

**Figure 3.2:** Geological map of the Charleston area with Te Ananui/Metro cave starred. Map taken from digital version of Greymouth Q-Map series (Nathan et al. 2002). Partial key to mapped geological units is as follows (from GNS Geological Legend, available online):

Q1: Postglacial deposits

Q2-Q10: Quaternary river/alluvial sedimentary deposits

Regional Unconformity

Mbo: O’Keef Formation: Blue-grey micaceous muddy sandstone grading up into yellow-brown sandstone

On: Nile River Group: Limestone, predominantly shallow water bioclastic varieties

Ers: Kiata Formation: Shallow marine sand and sandstone

Eb: Brunner Coal Measures: Quartz sandstone, conglomerate, and carbonaceous shale with lensoid coal seams

Regional Unconformity

Krg: Rahu Suit: Biotite or biotite-muscovite granite

Krm: Rahu Suite: Leucocratic muscovite granite

Krt: Rahu Suit: Biotite granodiorite and tonalite

Ckg: Karamea Suite: Foliated biotite granite, locally containing K-feldspar megacrysts

Dkn: Karamea Suite: Foliated biotite-muscovite granite-gneiss

θgp: Greenland Group: Pecksniff Metasedimentary Gneiss.....36

**Figure 3.3:** Survey map of Te Ananui/Metro Cave (Smith 2004). Locations of the four stalagmites collected in May 2010 are marked. Entrance to the cave is gained through the Triclops Entrance, the Main Entrance is only accessible through the cave. The sites of M1 and M2 were also the sites used for drip water collection, drip rate monitoring, temperature and humidity readings.....37

<b>Figure 3.4:</b> Structural map of the region showing location of major faults and folds (Ghisetti & Sibson 2006). Approximate location of Te Ananui/Metro Cave is also plotted (star).....	38
<b>Figure 3.5:</b> Graph of mean annual temperature and annual precipitation from the Westport climate station over the last 50 years (Data from CliFlo, accessed 2/06/2011). Gaps are due to no data from some years.....	39
<b>Figure 3.6a:</b> Stalagmite M1, high resolution scan of the quarter used later for stable isotopic analysis, surface is polished.	
<b>Figure 3.6b:</b> Stalagmite M2, high resolution scan of one quarter, polished surface.	
<b>Figure 3.6c:</b> The two dead speleothems; larger stalagmite collected from near the Hall of Refugees, shorter speleothem is the top piece of a column (oriented vertically) collected from near Split Ledge passage. Split faces unpolished.....	45
<b>Figure 4.1a-e:</b> Graphs of Hendy Test results ( $\delta^{18}\text{O}$ and $\delta^{13}\text{C}$ values) for 5 layers up the M1 stalagmite.	
<b>Figure 4.1f:</b> Correlation of $\delta^{18}\text{O}$ and $\delta^{13}\text{C}$ up the growth axis of the M1 stalagmite.....	48
<b>Table 4.1:</b> Shows the data analysed from the drip water gathered June-July 2010. The naming of the sites was based on the order visited in the cave, so is slightly different to the naming of the stalagmites – M1 stalagmite was collected from Site 2 (Eureka Hall), while M2 stalagmite was collected from Site 1 (Dragon’s Teeth). Data on the isotopic composition of May precipitation from Westport and Greymouth were kindly passed on by Joshua Blackstock (MSc candidate, UC).....	49
<b>Figure 4.2:</b> Plot of analysed stable isotope composition from Metro cave drip water, local rainwater and modern calcite. Precipitation values indicate the local meteoric water line. Global Meteoric Water Line is from Craig (1961). Recent calcite plotted on this graph is the raw data of the upper-most 10 points analysed.....	51
<b>Figure 4.3a-b:</b> Graphs of trace element and stable isotopic values up the length of the basal section. Light grey line is raw trace element concentration data, black line is the 5pt running mean of the raw data offset by +1 SD. Intervals are marked where there is significant departure of raw trace element concentrations above the offset 5pt running mean. Intervals are labelled A – D, with N representing “normal” intervals.....	52-53
<b>Figure 4.3c-d:</b> Graphs of trace element and stable isotopic values up the length of the top section. Light grey line is raw trace element concentration data, black line is the 5pt running mean of the raw data offset by +1 SD. Intervals are marked where there is significant departure of raw trace element concentrations above the offset 5pt running mean. Intervals are labelled E – J, with N representing “normal” intervals.....	54-55
<b>Figure 4.4a-b:</b> The base section (4.4a) and the top section (4.4b) of the M1 stalagmite analysed for trace element concentration and for dating. The insert to the side shows the detrital Th concentration and the areas picked for dating. Points 1 and 2 are preferred sites for dates. The intervals of above normal trace element concentration from figures 4.3a-d are also plotted. Figure provided by Dr. Andrew Lorrey, NIWA.....	57-58
<b>Figure 4.5:</b> High-resolution scan of Metro 1 stalagmite showing the placement of all the drill holes for stable isotopic analysis of the calcite.....	59

<b>Figure 4.6:</b> 557 data points of $\delta^{18}\text{O}$ and $\delta^{13}\text{C}$ values up the growth axis of the M1 stalagmite. Black lines indicate positions where Y concentrations increase (from left to right, in intervals C, D, E, G, and I).....	59
<b>Figure 4.7:</b> A – sketch of the first set-up for fluid inclusion extraction. B – sketch of the second set-up for fluid inclusion extraction.....	61
<b>Figure 4.8:</b> Samples of SMOW and GISP standard water analysed through the set-up for Method 1. All samples analysed fall within the accepted variability for the standard.....	63
<b>Figure 4.9:</b> Yield plot produced using Method 1. Aliquots of SMOW standard water were analysed through the method described above, with increasing samples of water added.....	63
<b>Figure 4.10:</b> Plot of fluid inclusion data from one calcite sample from the Waitomo stalagmite. The fluid inclusion data from periodic cold trap injections are blue and red points (data provided by Kurt Joy, UC). The orange point is the average isotopic composition of all the water extracted from the sample over the total decrepitation time (about 4 hours). The global mean water line is plotted as a comparison to the Waitomo data.....	64
<b>Figure 4.11:</b> Fluid inclusion data ( $\delta\text{D}$ and $\delta^{18}\text{O}$ ) from two 30mg calcite chips taken 270mm (F1) and 155mm (F2) from the base of the M1 stalagmite. The 10 points of calcite isotope data ( $\delta^{18}\text{O}$ and $\delta^{13}\text{C}$ ) around these locations are also graphed, as are the modern cave drip water $\delta^{18}\text{O}$ and $\delta\text{D}$ for comparison. The GMWL and the LMWL from figure 4.2 are also shown.....	66
<b>Figure 5.1:</b> Plot of ice volume corrected (dark blue) M1 calcite $\delta^{18}\text{O}$ values with uncorrected (light blue) $\delta^{18}\text{O}$ values (Peltier 2004).....	69
<b>Figure 5.2:</b> Experimental age model for the M1 stalagmite, based on the growth rates of stalagmites in Punakaiki caves 30km south of Metro cave. M1 Stable isotope record is normalised to the Late Holocene (4 Ka), and ice volume corrected following adjustments made according to the global ICE-5G (VM2) model (Peltier 2004). Holocene HW3 stable carbon and oxygen data were kindly provided by Dr. Tom Whittaker, and the age data from this stalagmite were not used in the average growth rate model to enable comparison with an independent time series (Whittaker et al. 2011). Grey bars mark cold periods in the Southern Alps identified through cosmogenic and $^{10}\text{Be}$ dating (Schaefer et al. 2009; Kaplan et al. 2010; Putnam et al. 2010).....	70
<b>Figure 6.1:</b> Temperature reconstruction using two different calcite-water fractionation equations (Kim 1997; Demeny 2010) and the stable oxygen isotope data from the M1 stalagmite.....	76
<b>Figure 6.2:</b> Fe concentration in the base (left) and top (right) sections of the M1 stalagmite. Note the log-scale in the top section (right). There has clearly been a shift between the base and top sections from larger magnitude oscillations to smaller scale oscillations, lower concentration, and larger peak spikes.....	81



**Figure 6.3a:** Dilution/enrichment plots of trace elements against Y concentration in ppm. Five separate intervals are plotted over all the data from the top and bottom sections of the M1 stalagmite. Intervals B and C are from the base of the M1 stalagmite and intervals H, I, and J are from the top section.....82

**Figure 6.3b:** Dilution/enrichment plots of stable oxygen and carbon isotopes and trace elements (Sr) against Y concentration in ppm. Five separate intervals are plotted over all the data from the top and bottom sections of the M1 stalagmite. Intervals B and C are from the base of the M1 stalagmite and intervals H, I, and J are from the top section.....83

**Figure 6.4:** Comparison of the M1 stable oxygen and carbon isotope record with stable isotope records from a Punakaiki stalagmite (HW3) and the North West South Island Master speleothem record (PW NWSI) (Williams et al. 2010; Whittaker et al. 2011). Data were kindly provided by Dr. Tom Whittaker for HW3, and by Prof. Paul Williams for the NWSI Master record. Grey bars represent periods of known Holocene glacial advances in the Southern Alps (Schaefer et al. 2009; Kaplan et al. 2010; Putnam et al. 2010).....88

# **Chapter 1: Introduction**

Climate is one of the large drivers of change on our planet. Throughout the rock record we can see many examples of times when changes in global climate have lead to extinctions and evolutionary changes, both in deep time and during the Quaternary (Davis & Shaw 2001; Zachos et al. 2001; Wing et al. 2005; Parmesan 2006). Although the overall temperature at the surface of the Earth has not changed much during the Cenozoic, the climate has oscillated from glacial conditions with ice covering the poles and many mountainous areas, to interglacials with no ice at the poles (Zachos et al. 2001; Rabassa et al. 2005; Sugden et al. 2006). Climate also plays a large role in shaping the land as the primary tools of erosion (wind, water and glaciers) are subject to local, regional and global changes (Chinn 1996; Drost et al. 2007). The close and complex interactions between climate and the Earth and oceans have long been a major area of research, as understanding the natural processes and variability of climate is necessary before we can evaluate anthropogenic impacts. In addition, our attempts to predict future climate change scenarios are based on knowledge of natural variability and regional change (Jansen et al. 2007). Today we can observe many environmental changes globally that are the result of changing climate; but without a knowledge of the past we cannot know if the current retreat of mountain glaciers, or the increased frequency of tropical storms, are normal fluctuations or an indication that a natural threshold is being approached with potentially significant flow-on effects.

Paleoclimate research seeks to build our knowledge of the magnitude, duration and causes of past climatic changes, through investigation of proxy records that supplement and extend both written and oral history. There are many potential proxies that can be studied on a variety of spatial and temporal scales, such as tree rings, lake and ocean sediments, bubbles of air trapped in ice, and coral reefs (Beck et al. 1997; EPICA Community Members 2004; McCarroll & Loader 2004; Barrows et al. 2007). At present some of the most detailed records of past climate have been constructed from analysis of ice cores in Antarctica and Greenland (Dansgaard et al. 1993; EPICA Community Members 2004), and the longest climate records are from deep ocean sediments (Zachos et al. 2001). However, while these records indicate changes occurred in the ocean and in polar regions over different time scales, they fail to provide detailed assessments of the changes that have occurred on land. Proxy records from mid-latitude and tropical regions are necessary to investigate the impact of past climate

change in terrestrial regions. Limestone and karst, usually with accompanying cave systems, are found throughout the world's continents, and the climate conditions through time can be preserved in the geochemical composition of each layer in calcite deposits (Ford & Williams 1989). Hence the analysis of the stable isotope and trace element composition of stalagmites, and other cave speleothems, provide a valuable proxy for understanding past climate in many key terrestrial regions of the world.

New Zealand and South America, spanning the southern mid-latitudes, contain large karst systems where climate reconstruction studies can be carried out. These areas are important due to the lack of Southern Hemisphere terrestrial representation when compared to the rest of the world. Paleoclimate analyses of New Zealand stalagmites contribute to our understanding of climate change in the Southern Hemisphere during the last 230 Ka (Williams 1996; Hellstrom et al. 1998; Williams et al. 2004, 2005; Alloway et al. 2007; Whittaker et al. 2011). While there are fewer records available than in the Northern Hemisphere, the Southern Hemisphere records that are available provide valuable comparative information on the influence of Antarctica on global climate versus that of Northern Hemisphere sources of climate change (Denton et al. 1999; Turney et al. 2003; Williams et al. 2005; Shulmeister et al. 2006). Well-dated stalagmites can be used to investigate whether climate events such as the Younger Dryas, or Dansgaard-Oeschger cycles occurred simultaneously or were earlier/later than their northern counterparts (Williams et al. 2004; Whittaker 2008). Probing these archives in New Zealand can lead on to other important questions about how climate warming and cooling was initiated in the past, and this can help to establish cause and effect relationships of regional to global atmospheric and oceanic circulation.

This thesis presents a new speleothem-based paleoclimate record from North Westland in the South Island of New Zealand, and is aimed at advancing our knowledge of local/regional climate changes and the processes that lead to recording climate signals in stalagmites. The study of paleoclimate proxies is often based on various assumptions about a physical system. Each new analysis helps to validate past work, challenge past assumptions, and refine the processes responsible for the variability captured in a climate proxy archive. For example, a key assumption in stable isotope speleothem paleoclimate research is that the cave environment remains fairly stable relative to the intra-annual fluctuations outside the cave, and that the isotopic composition of water entering a cave remains representative of the stable isotopic composition of local annual rainfall. This assumption underlies the hypothesis that

modern speleothem calcite, and fluid inclusion isotopic compositions, are not significantly different than modern cave drip-water isotopic compositions. If this can be demonstrated for a cave, then isotopic equilibrium was likely achieved between the drip water and the precipitating calcite. In this case, changes in stalagmite (and fluid inclusion) isotopic composition through time should reflect changes in cave climate during calcite formation.

This thesis was designed to monitor a cave environment for several months, including collection of drip water isotopic composition, temperature, and relative humidity data, to assess the stability of a cave system over a year. Such monitoring data will facilitate our understanding of multiple environmental variables that can help in defining cave processes that lead to the formation of speleothems in the cave environment. It is also well known that there can be considerable variation in drip water chemistry between locations at both large and small scales in a karst system (Williams et al. 1999; Williams et al. 2004; Williams 2008). Further tests of the stability of the cave environment, and whether isotopic equilibrium between the drip water and calcite was achieved, can be made by comparing the stable isotopic composition of recently formed fluid inclusions with the composition of modern drip-water. The analysis of fluid inclusions trapped in speleothem calcite will enable interpretation of the stable isotopes in terms of changes in both temperature and precipitation amount (see sections 2.3 and 4.6). Published methods for analysing speleothem fluid inclusions require large samples (~300mg), which are not comparable to the sampling resolution achievable (0.5mm) when drilling calcite for stable isotopic analysis. Therefore, this research also targeted the development of a new method combining online and offline mass spectrometric techniques to extract and analyse fluid inclusions from speleothem calcite. The goal of this research facet was to greatly reduce the sample size necessary and increase the efficiency of the fluid inclusion extraction method.

# **Chapter 2 – Literature Review**

## **2.1. Speleothems as Terrestrial Proxies of Paleoclimate**

### **2.1.1 Introduction**

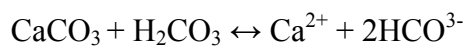
Speleothems have been recognised as important archives of paleoclimate for decades (Siegel & Reams 1966; Fornaca-Rinaldi et al. 1968; Hendy & Wilson 1968; Thompson et al. 1976). They can record detailed changes in local conditions throughout their time of growth, which can in some cases be over 500 000 years (Ka) (Ayliffe et al. 1998; Woodhead et al. 2010). Speleothems are found in terrestrial locations, so their records of climate are often more variable than those from polar ice cores or deep sea marine sediments due to the heterogeneous conditions of terrestrial climate systems. However, as speleothems record climatic variability in the cave region they are often of increased value, from the human perspective, as a consequence. The processes involved in the formation of caves and speleothems are reasonably complex (Ford & Williams 1989), and an understanding of them is necessary for interpreting how climate changed in the past. This chapter will cover a review of the formation of caves and speleothems, how speleothems are dated, and how changing cave processes can be inferred from the geochemistry of speleothem calcite.

### **2.1.2 Caves and Speleothems**

Caves are common, though sometimes overlooked, features found all over the world. They can form in a variety of different rock types, but are most common in crystalline bedrock of carbonate origin (most commonly limestone) where cave systems can reach spectacular proportions (Ford & Williams 1989). The world's longest and deepest caves reach over 600 km in length and over 2 km in depth. In New Zealand the most extensive cave systems are found in North-West Nelson (Kahurangi National Park) with the surveyed length of Bulma cave at 67.2 km, and the Ellis Basin system at just over 1 km deep (NZSS 2011).

Large karst systems can take tens of thousands to millions of years to form through the dissolution of limestone by water (Figure 2.1) (Ford & Williams 1989). When water interacts

with carbon dioxide (CO<sub>2</sub>) it forms weak carbonic acid with a pH of about 5.7 (Gillieson 1996). CO<sub>2</sub> mixes with water in the atmosphere and also when the water percolates down through vegetation, soil, and partly broken down rock (regolith) that overlies the cave. This layer is termed the epikarst (Figure 2.1). The dissolution of limestone occurs through an equilibrium reaction (Gillieson 1996):



The addition or loss of CO<sub>2</sub> from water drives the reaction to either dissolve limestone (addition) or precipitate calcite (loss) (Svensson & Dreybrodt 1992). In the soil and epikarst environments sources of CO<sub>2</sub> such as the atmosphere, plants, and microbial decomposition of organic matter, cause an abundance of carbonic acid – resulting in dissolution of the surrounding rock (Figure 2.1). Deeper in the cave the situation is reversed, where CO<sub>2</sub> is lost through degassing, causing super-saturation of calcite ions and precipitation of calcite (Figure 2.1).

Dissolution of limestone and the growth of caves differs between temperate zones and the tropics. The tropics support a higher biomass of surface vegetation, and along with a lack of freezing, saprophytic fungi and bacteria in the soil remain active for longer than in temperate zones. This year-round biological activity produces soil CO<sub>2</sub> concentrations of up to 10% in the tropics and around 3% in temperate areas (Gillieson 1996). Tropical caves also tend to have higher rates of calcite precipitation, as more dissolution causes higher concentrations of Ca<sup>2+</sup> ions in the water, thus allowing faster precipitation of calcite (Genty et al. 2001; Baldini et al. 2005).

As water infiltrates from the surface and becomes confined in the epikarst zone, it generally remains at least partially open to sources of CO<sub>2</sub> until it reaches deeper in the cave.

Dissolution will occur until all the carbonic acid has reacted with the CaCO<sub>3</sub> of the rock (Figure 2.1) (Williams 2008). The presence of fractures and cracks in the host rock influences the residence time of the water by changing the ease with which water travels through the epikarst. This greatly affects the geochemical composition of the water entering caves and cavities deeper underground. There are some cases where dissolution of limestone can occur at greater depths in a cave such as where a large stream or river is flowing down into the rock. The rapidly flowing water is constantly supplying new carbonic acid, which is free to react

with the calcium carbonate at deeper levels (Williams 2008). However, the most common process occurring deeper in cave systems is precipitation of calcite.

Calcite precipitation occurs when the water enters a cavity or cave deeper underground where the air does not contain such a high concentration of CO<sub>2</sub> (Figure 2.1) (Gillieson 1996; Fairchild et al. 2007; Baldini et al. 2008; Williams 2008). Consequently the water has a higher concentration of dissolved CO<sub>2</sub> than the cave air, and the resulting gradient causes some of the CO<sub>2</sub> to degas (Baldini et al. 2006). Because the water descending from the surface is saturated with Ca<sup>2+</sup> ions, degassing causes some of it to precipitate as CaCO<sub>3</sub> (Baldini et al. 2006; Baldini et al. 2008). The build-up of calcite at points where drip water enters into the cave causes the growth of speleothems.

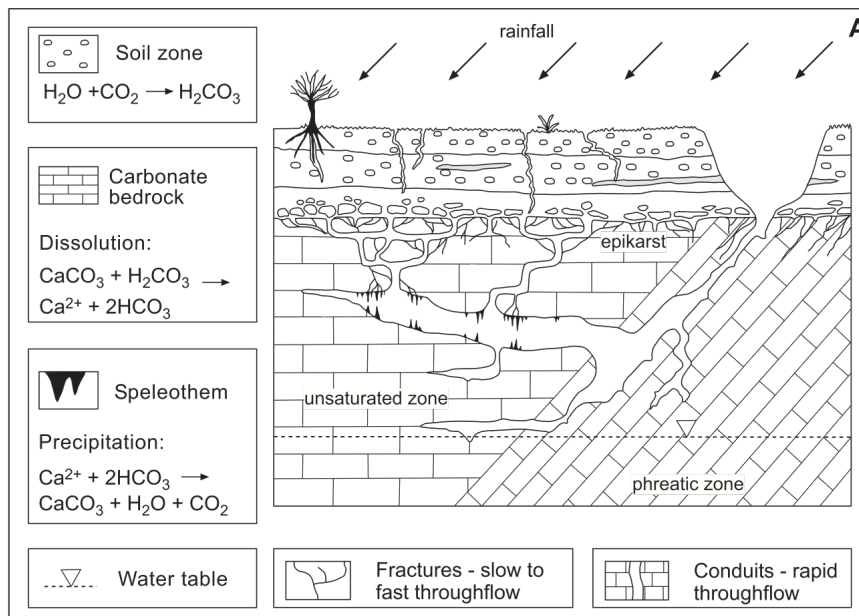


Figure 2.1: Diagrammatic representation of the karst system highlighting the general areas of calcite dissolution and precipitation (Fairchild et al. 2007).

Speleothems come in many different forms, and are separated into three groups. Stalactites form from drip water entry points in the ceiling, stalagmites form from the floor upwards from dripping water, and flowstone forms as sheets of calcite from thin water flows on the walls or the floor (Fairchild et al. 2007). The colour of speleothems can vary greatly depending on the local geochemical and organic conditions contributing to their formation. The presence of organic matter in the drip water often causes the forming speleothem to trap matter between crystals, and has been suggested to cause the brownish colour often observed in many speleothems (Ramseyer et al. 1997). The majority of organic matter found in

speleothems are organic acids such as fulvic acid, and other products of humification (Ramseyer et al. 1997; McGarry & Baker 2000). Other colours can be produced by coatings of iron or manganese oxides, which can indicate oxidation in the source water (Fairchild et al. 2007).

In general, stalagmites are the most common form of speleothem used for paleoclimate research as they tend to form discrete stratigraphically-arranged cone-shaped layers. Flowstone is sometimes used in the same way if it can be sampled using a coring drill angled perpendicular to the deposited growth layers (Hellstrom et al. 1998). Because stalagmites are unique objects in the cave, great care can be taken to choose ones that do not have obvious changes in the location of the drip-water. In the case of a flowstone deposit, it can be difficult to tell if the source water and flow has shifted laterally over time until sampling is carried out. Changes in drip-water foci in speleothems can be due to a number of complicated factors, for example, changing hydrological routes through the limestone or geophysical activity. These changes can often be observed in cross sections of speleothems. Sampling must be carried out perpendicular to the growth axis of the speleothem to ensure a continuous time-series of calcite layers are being analysed.

Cutting a stalagmite in half along the growth axis allows the individual layers to be visible in cross section, and careful analysis up this axis can provide detailed information of the stalagmite's growth history. The type of crystal habit in the stalagmite is related to the local conditions in the cave under which the calcite precipitated. Thinly laminated stalagmites are usually indicative of equilibrium conditions, and depending on the drip rate, the layers can represent annual to even sub-annual deposition, as well as climate event-related layers (Dreybrodt 1980; Genty & Quinif 1996; Frappier et al. 2002; Frappier et al. 2007). Such layers are composed of columnar or fibrous calcite crystals which grow when the stalagmite receives a constant moderate supply of drip water, there is a relatively low supersaturation of calcite, and the cave is at close to 100% humidity (Kendall & Broughton 1978; Frisia et al. 2000). Other fabrics that are sometimes observed in stalagmites include microcrystalline calcite which forms when drip rates are high, but variable, and dendritic fabric which forms when there is great variability in the drip rate and when there is evaporation of the water (Frisia et al. 2000).



The shape of a stalagmite gives some clues to changes in drip rate and local cave conditions over time. The water forms a thin film over the surface of the growing stalagmite, and calcite is precipitated as the water degasses CO<sub>2</sub>. An individual layer is thickest at the apex of the stalagmite, and thins progressively from the centre. Numerical modelling has shown that when the conditions for stalagmite growth remain reasonably constant over time it approaches a columnar form (Romanov et al. 2008). When the drip rate changes through time the form of the stalagmite also alters. The diameter can widen or narrow, and small protrusions can form (Romanov et al. 2008). Columnar stalagmites are more often chosen for climate research as their more stable growth conditions are more likely to preserve climate related signals in the calcite geochemistry than stalagmites with alternate morphologies.

The growth of stalagmites also varies as a function of drip rate, and can range globally between 0.01 – 1.0mm/year (Baker et al. 1998; Genty et al. 2001; McDermott 2004). Because of this large range in growth rates it is not possible to tell how old a stalagmite is without absolute radiometric dating techniques, or some other indicator of age, such as features known to be present prior to stalagmite growth (Genty & Quinif 1996; Baldini et al. 2005). Stalagmites will continue to grow as long as drip water is continuously entering the cave and the environmental conditions result in CaCO<sub>3</sub> super-saturation. They can reach great heights of 7m or more and often interact with other calcite formations forming columns, shawls, and mounds that have built up drip by drip over many thousands of years. If there is a break in the supply of drip water, there is a break in deposition of calcite, and sometimes colour changes can be seen between two periods of calcite deposition. Changes in drip rates can also be reflected in growth model results from well-dated stalagmites, and can often be paired with  $\delta^{13}\text{C}$  values of the stalagmite calcite to indicate hydrological changes in precipitation amount (Hellstrom et al. 1998; Hellstrom & McCulloch 2000).

### **2.1.3 Dating of Speleothems**

An important consideration for paleoclimate research is the suitability of the study material for dating. Precise ages are required to constrain the length of climate change events and compare events from different locations around the world. Stalagmites and other speleothems can be very accurately dated using modern U-series techniques, and several methods have been developed using the decay of uranium to thorium.

The suitability of stalagmites for U-series dating arises from the composition of the calcite. The calcite will incorporate measurable amounts of  $^{234}\text{U}$ , but generally excludes the daughter product  $^{230}\text{Th}$ ; and once the calcite has been deposited the stalagmite acts as a closed system with respect to both parent and daughter isotopes (Richards & Dorale 2003). When there is no inclusion of detrital material in the calcite, the stalagmites have an initial  $^{230}\text{Th}/^{234}\text{U}$  activity ratio of zero, which changes over time as  $^{234}\text{U}$  decays to  $^{230}\text{Th}$  (Hellstrom 2003). By measuring the ratios (including the ratio of  $^{234}\text{U}$  to its parent isotope  $^{238}\text{U}$ ) and using the known decay constants, ages of stalagmites up to ~500 Ka can be calculated from samples between 0.2g – 1g in size (Ayliffe et al. 1998; Schwarcz & Rink 2001; Hellstrom 2003). This method is based on thermal ionisation mass spectrometry (TIMS), developed in the 1980s, and has been the preferred method for age determination of calcite for many years (Edwards et al. 1987; Stirling et al. 1995; Zhao et al. 2001).

An issue that must be addressed in any study determining the age of speleothems is the possibility of contamination of the samples by daughter isotopes not derived from radiogenic decay. Stalagmites may violate one of the assumptions upon which the dating is based, through the incorporation of external  $^{230}\text{Th}$  from detrital material such as clays and humic components from soil (Schwarcz & Rink 2001; Richards & Dorale 2003). Consequently the contaminating  $^{230}\text{Th}$  must be estimated for corrections to the age to be made (Richards & Dorale 2003; Hellstrom 2006). Corrections can be made through isochron determination methods, or through an *a priori* estimate of the isotopic composition of the contaminating phase (Hellstrom et al. 1998; Hellstrom 2006). The contamination from detrital Th can vary depending on location (parent and proximal bedrock) as well as other local environmental factors. A study from New Zealand found that two stalactites known to be 100 years old gave near concordant ages of 2000 and 3000 years old (Whitehead et al. 1999). They found from other samples that very young speleothems could include  $^{230}\text{Th}$  without accompanying  $^{232}\text{Th}$ , resulting in errors in very young speleothems of up to a few thousand years (Whitehead et al. 1999). The large age errors in the young calcite were inferred to be due to the transport of radionuclides in groundwater from old eroding limestone. Groundwater in a limestone aquifer with a high  $^{230}\text{Th}/^{232}\text{Th}$  ratio could conceivably deposit enough  $^{230}\text{Th}$  in 100 years to cause age errors of several thousand years in recently formed calcite (Whitehead et al. 1999). Therefore, in some areas of New Zealand there can be significant uncertainty around the minimum dateable age of speleothem samples, and care must be taken to investigate this if very young samples are studied. Although this can be mitigated somewhat through replicating

analyses, and comparing speleothem results to other proxy records dated using different methods.

Modifications have been added to the basic TIMS method over time in order to improve analytical precision. An important change has been the development of multi-collector inductively coupled plasma mass spectrometers (MC-ICPMS), which greatly increase the efficiency of analysing samples (Hellstrom 2003; Woodhead et al. 2006). Methods which allow parallel ion-counting MC-ICPMS techniques enable the simultaneous measurement of  $^{230}\text{Th}$  and  $^{234}\text{U}$  meaning U/Th ages and uncertainties can be calculated in real time (Hellstrom 2003). These techniques have recently been extended to investigating the use of U-Pb dating on speleothems in attempts to extend the dated paleoclimate records beyond 500 Ka, and potentially up to several million years (Woodhead et al. 2006).

Other developments in dating techniques in order to increase through-put of samples and allow high-resolution dating of speleothems is the use of laser ablation MC-ICPMS (Eggins et al. 2005). Although the data using this technique is not as precise or accurate as that possible through conventional TIMS or solution MC-ICPMS, an entire stalagmite can rapidly be scanned for elements and isotopes of interest (Eggins et al. 2005). The advantage of this is that samples for more accurate dating can be picked out to avoid areas of high detrital Th contamination. This method is also useful for scans of trace element composition in samples for multi-proxy studies (Fairchild et al. 2000; Hellstrom & McCulloch 2000), and both approaches are explored later in this thesis.

#### **2.1.4 Speleothems as Paleoclimate Proxies**

To varying degrees all the observable characteristics of stalagmites provide information on climate changes through time. However, detailed quantitative data governed by thermodynamical conditions can be compiled through analysing the stable isotope composition of the calcite. The stable isotopes of oxygen, hydrogen, and carbon are inherited from the water precipitating the calcite, so the calcite reflects isotopic changes occurring in the water (McDermott 2004). By investigating the relative influences of temperature, precipitation, water balance, vegetation and soil respiration on the stable isotope composition of the water entering the cave, quantitative estimates of past environmental change can be inferred from the stable isotope composition of the speleothem calcite.

Stable isotope ratios are usually expressed in delta notation, in terms of parts per thousand (‰) relative to an international standard (Sharp 2007). For oxygen isotopes:

$$\delta^{18}\text{O} = \left( \frac{{}^{18}\text{O}}{{}^{16}\text{O}}_{\text{sample}} - \frac{{}^{18}\text{O}}{{}^{16}\text{O}}_{\text{standard}} \right) / \left( \frac{{}^{18}\text{O}}{{}^{16}\text{O}}_{\text{standard}} \right) \times 1000$$

The standard used for carbonates is the Pee Dee Belemnite (PDB) and the standard for water is Standard Mean Ocean Water (SMOW). Both standards are now commonly prefixed with “Vienna”, which is now the accepted international standard value as the original standard materials have been exhausted (Sharp 2007; Lachniet 2009).

The use of stable isotopes in paleoclimate research has grown significantly since the early observations of the partitioning of heavy and light isotopologues between different energy states during various natural processes (Dansgaard 1964). For example, when ice forms from water, the heavier isotopes are preferentially incorporated into the solid (lower energy) state, leaving the host liquid relatively enriched in the light isotope (Williams et al. 2005; Lachniet 2009). This means the host liquid  $\delta^{18}\text{O}$  value decreases (becomes more negative) as more  $^{18}\text{O}$  is locked up in ice. Conversely, when water evaporates from the ocean, the vapour constitutes a higher energy state, so preferentially incorporates the lighter  $^{16}\text{O}$ , leaving the ocean with relatively enriched  $\delta^{18}\text{O}$  values (Lachniet 2009). Similar processes also occur in caves when calcite is precipitating from water. A key consideration is that the equilibrium fractionation of the oxygen isotopes between solid and liquid or vapour states is temperature dependent (Dansgaard 1964). When the temperature is colder it is harder for the heavier isotopes to be incorporated into the higher energy phase. For example, theoretically, when the temperature is colder relatively more  $^{18}\text{O}$  should be incorporated into stalagmite calcite, assuming all other conditions remain the same (Hendy 1971; Gascoyne 1992; Fairchild et al. 2006a). Therefore, if we can measure the  $\delta^{18}\text{O}$  value of stalagmite calcite through all the layers, the changes should reflect detailed records of cave temperature change (if no other processes have changed and isotopic equilibrium was achieved). Because caves moderate local temperature fluctuations, the temperature inside the cave should reflect the mean annual local outside temperature (Ford & Williams 1989; Fricke & O'Neil 1999).

The techniques for analysing stalagmite calcite usually involve drilling small sample powders along the growth axis of the stalagmite. Manual drilling using a hand-held dentist drill fitted with a carbide or diamond tipped drill bit can be used to achieve spatial resolutions of about 0.5mm (Spötl & Matthey 2006). Laser ablation and analysis methods can be used for rapid assessment of the isotopic and trace element composition of a stalagmite, with sample spot sizes of 100-150µm (Eggins et al. 2005; Spötl & Matthey 2006). Even smaller samples than this can be produced using a micro-milling technique where the drill is fixed and the sample is mounted on a stage. The stage can moved into the drill by increments as small as 20µm either by hand, or through a computer (Spötl & Matthey 2006).

### **2.1.5 Stable Oxygen Isotopes in Speleothems**

While measurement of the stable oxygen isotope composition of calcite is a well established method, interpretation of these data are much more involved as there are many processes that affect the  $\delta^{18}\text{O}$  value of speleothem calcite. These factors fall into two main categories – the temperature-related effects inside the cave, and the drip water effect (Lachniet 2009).

The temperature-related effects require a specific set of local conditions to be met for equilibrium between the precipitating calcite and the parent water. Specifically, cave air must be at or close to 100% humidity for equilibrium conditions to exist (Lachniet 2009). In addition, the drip rate of the water onto the stalagmite must be slow enough to allow enough time for each drop to equilibrate with the cave air (between 10-100 seconds, Dreybrodt & Scholz 2011), but not so long that further processes, involving degassing of  $\text{CO}_2$  from the drip water, result in isotopic disequilibrium again (i.e. the time between drops must be less than 50 minutes, Dreybrodt & Scholz 2011) (Mickler et al. 2004; Lachniet 2009; Dreybrodt & Scholz 2011). For example, if the degree of ventilation in the area of stalagmite growth is high, changes in the composition of the cave air will likely result in allowing disequilibrium kinetic processes to dominate the  $\delta^{18}\text{O}$  signal (Lachniet 2009; Dreybrodt & Scholz 2011). Thus kinetic isotope effects tend to produce large shifts in the  $\delta^{18}\text{O}$  value of speleothem calcite towards more positive values, thus obscuring any climate signals recorded in calcite chemistry (Mickler et al. 2004; Mickler et al. 2006; Polag et al. 2010).

At present, standard practice to test for equilibrium of the calcite with the drip water is to perform ‘Hendy Tests’, a comparison between the stable oxygen and carbon isotopes, along

individual growth layers (Hendy 1971; McDermott 2004). If equilibrium conditions were achieved during the growth of a discrete layer, then the  $\delta^{18}\text{O}$  should remain relatively constant while the  $\delta^{13}\text{C}$  varies along the layer. In addition, there should be no significant positive co-variation between the  $\delta^{18}\text{O}$  and  $\delta^{13}\text{C}$  along the layer (Hendy 1971; McDermott 2004; Treble et al. 2005). There has been considerable discussion, however, regarding the application of Hendy Tests to collected speleothems (Mickler et al. 2004; Mickler et al. 2006; Dorale & Liu 2009). In practise, it is often difficult to sample along a single growth layer due to the thinning of each layer away from the growth axis, thus mixing of neighbouring layers that can have quite different isotopic compositions complicates the results (McDermott 2004). It has also been demonstrated that equilibrium conditions can exist close to the growth axis, but kinetic fractionation processes can have occurred on the flanks of the stalagmite further demonstrating the challenges of interpreting speleothem carbonate isotopic data (Spötl & Mangini 2002; Dorale & Liu 2009).

Interestingly, Hendy (1971) assumes stalagmite  $\delta^{13}\text{C}$  values are not linked to climate changes. However, it has since been shown that changes in vegetation such as shifts from C3 to C4 plants, and changes in soil respiration rate, are closely linked to local climate conditions. These changes are often captured by the  $\delta^{13}\text{C}$  values of the calcite (Harmon et al. 2007; Dorale & Liu 2009; Lambert & Aharon 2011). An alternative to the Hendy Test for assessing isotopic equilibrium involves performing replicate analyses on multiple speleothems from the same cave (Dorale & Liu 2009). Equilibrium conditions should exist if two stalagmites from different areas of the same cave system show similar isotopic profiles, as kinetic processes are not expected to have affected the two stalagmites in the same way due to heterogeneous water flow-paths from the surface to the cave chambers and cave temperature conditions (Dorale & Liu 2009). However, the replication test is often difficult to apply due to sampling limitations imposed by cave conservation considerations and to economic and time constraints in the laboratory. In addition, stalagmites from the same cave system may not necessarily show the same isotopic profile due to differences in cave ventilation, effects of relative humidity, the partial pressure of  $\text{CO}_2$ , temperature etc. in different parts of the endokarst environment.

Despite these challenges, if Hendy Tests or replication tests or both indicate that equilibrium conditions are likely to have occurred throughout the growth period of the stalagmite, then

there is a simple temperature dependent fractionation of oxygen isotopes (Siegel & Reams 1966).

$$1000\ln\alpha_{(\text{Calcite-H}_2\text{O})} = 18.03 (10^3 T^{-1}) - 32.42 \quad (\text{Kim \& O'Neil 1997})$$

Where  $1000\ln\alpha_{(\text{calcite-water})}$  is the fractionation between the calcite and water, and  $T$  is the temperature in Kelvin (Kim & O'Neil 1997). Interestingly, a new study has suggested that natural formations do not always follow these experimentally derived relationships, and differ depending on the type of environment (Demeny et al. 2010). Through analysis of calcite deposits in many different environments the authors have proposed that for cave deposits between 5°C and 25°C the following equation should be used:

$$1000\ln\alpha = 17500/T - 29.89 \quad (\text{Demeny et al. 2010})$$

These equations present a problem in that there are two unknowns, and the isotopic composition of the drip water from which the calcite is precipitating must be estimated in order to solve for temperature. The fractionation between the calcite and water can either be quantified by measuring the  $\delta^{18}\text{O}$  values of the calcite and fluid inclusions trapped in the stalagmite, or estimated through the relationship of modern drip water with modern calcite. The latter method has been more widely utilised due to the difficulty of extracting and analysing fluid inclusions for  $\delta^{18}\text{O}$  values, but relies on the assumption that the  $\delta^{18}\text{O}$  value of the drip water has not changed substantially through time (Williams et al. 1999; Lachniet 2009). It is well known that the oxygen isotopic composition of meteoric-derived waters is highly variable on a variety of temporal scales. Such natural variability can be corrected for to the first order on glacial-interglacial timescales based on ocean ice volume effects (Williams et al. 2005; Williams et al. 2010). However, on shorter timescales the issue of 'one equation, two unknowns' remains highly problematic.

Under isotopic equilibrium conditions the change in  $\delta^{18}\text{O}$  values of calcite with changes in temperature ( $\Delta\delta^{18}\text{O}_{\text{ct}}/\Delta T$ ) has been approximated at  $-0.24\text{‰}^\circ\text{C}^{-1}$  at 10°C (O'Neil et al. 1969; Kim & O'Neil 1997). The slope becomes less negative at higher temperatures, so in the tropics at 35°C the relationship would be closer to  $\Delta\delta^{18}\text{O}_{\text{ct}}/\Delta T = -0.18$  (Kim & O'Neil 1997). Because the slope of the cave temperature effect is negative, when there is a decrease in cave

temperature, and all other factors remain the same, relatively more  $^{18}\text{O}$  is incorporated into the calcite resulting in more positive calcite  $\delta^{18}\text{O}$  values in colder periods (Sharp 2007; Lachniet 2009).

In addition to the temperature effect, several other factors affect the  $\delta^{18}\text{O}$  value of precipitation entering the cave environment – and hence the resulting speleothem calcite (Figure 2.2). These processes change the  $\delta^{18}\text{O}$  value of the water before it enters the epikarst. For a speleothem located in the mid latitudes (i.e., in a region such as New Zealand), only some of these have a significant effect on the  $\delta^{18}\text{O}$  values in precipitation (Lachniet 2009). For example, the amount effect is only observed in tropical to sub-tropical areas where deep vertical convection due to high sea surface temperatures is common, so does not have an important effect in New Zealand (Higgins & MacFadden 2004; Lachniet 2009).

The stable isotopic composition of rain in New Zealand is affected by the ocean source of the air mass, evaporation, and Rayleigh processes involved in the precipitation of rain. The source effect refers to the observation that air masses sourced from different areas of the ocean have distinct  $\delta^{18}\text{O}$  values (Bowen & Wilkinson 2002; Friedman et al. 2002). The high natural

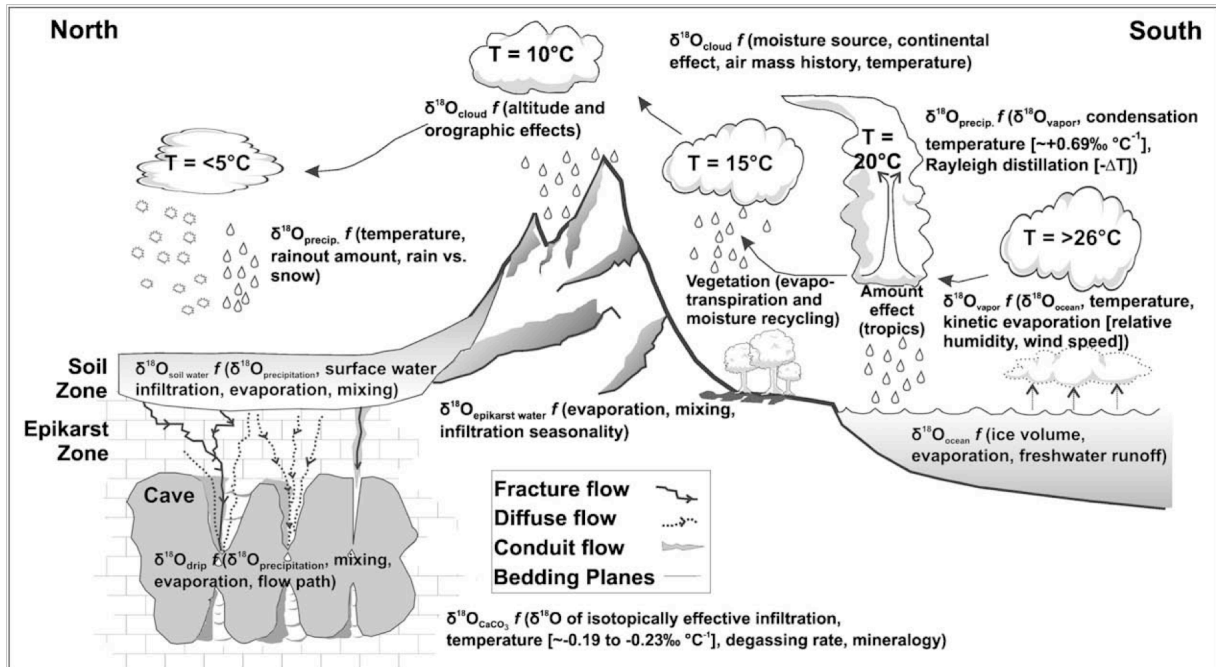


Figure 2.2: Diagrammatic representation of the processes related to fractionation of  $\delta^{18}\text{O}$  values in water through the hydrological system from the ocean to the cave (Lachniet 2009).



variability of  $\delta^{18}\text{O}$  values in New Zealand meteoric precipitation are partially due to the varied source regions from the sub-tropics to the sub-Antarctic (Bowen & Wilkinson 2002). The  $\delta^{18}\text{O}$  value of the ocean also changes on glacial-interglacial timescales, due to the fractionation of oxygen isotopes that occurs when ice is formed, affecting the  $\delta^{18}\text{O}$  value of water entering the cave environment and the isotopic composition of speleothems growing over similar time periods (Williams et al. 2005; Lachniet 2009).

The oxygen isotopic composition of water vapour sourced from the ocean changes further over land (Figure 2.2). The process of condensation involves a decrease in temperature, thus the mean annual temperature at a site controls how much moisture is produced – called the rainfall temperature effect (Fricke & O'Neil 1999; Lachniet 2009). When precipitation is formed, it preferentially includes the heavier isotopes of oxygen due to equilibrium fractionation during condensation, so the first rain falling on land near the ocean will have higher  $\delta^{18}\text{O}$  values than the remaining air mass, though still negative in comparison to the initial ocean source (Harmon et al. 2007; Lachniet 2009). The global relationship between the  $\delta^{18}\text{O}$  value of rainfall and the atmospheric temperature at the altitude of condensation is described as  $\delta^{18}\text{O} = 0.69(\text{MAT}) - 13.6\text{‰}$  (SMOW) (Dansgaard 1964).

However, while the global slope is  $0.69\text{‰}/^{\circ}\text{C}$  many local regions depart significantly from this due to the influence of local conditions. For example, if the air mass is forced to rise through orographic lifting, or travels a long way across a continent, there is progressive cooling and rain-out of the heavy isotopes in a process called Rayleigh distillation; resulting in isotopically lighter precipitation at higher altitudes and with increasing distance from the ocean (Figure 2.2) (Lauritzen & Lundberg 1999; Darling 2004; Lachniet 2009). However, if there is evaporation of rain light  $^{16}\text{O}$  isotopes are preferentially removed, due to equilibrium fractionation, resulting in rainfall with more positive  $\delta^{18}\text{O}$  values. These processes are also affected by changes in seasonality, which further alter mean annual  $\delta^{18}\text{O}$  values, potentially complicating climatic signals recorded in high resolution speleothem records (Harmon et al. 2007; Matthey et al. 2010).

### 2.1.6 Stable Carbon Isotopes in Speleothems

The use of carbon isotopes in paleoclimate reconstructions has increased over the last decade (Lauritzen & Lundberg 1999; Frappier et al. 2002; McDermott 2004). In speleothems, carbon is mainly sourced from the atmosphere, dissolution of host rock, and from forest vegetation, and microbes in the soil above the cave (Frisia et al. 2011). As the  $\delta^{13}\text{C}$  values of the host rock change little across the timescales involved in most paleoclimate studies, the primary controls on speleothem  $\delta^{13}\text{C}$  values have to do with changes in vegetation, soil respiration rate, and processes within the cave system.

Cave systems in areas dominated by plants that use the C3 metabolic pathway for photosynthesis typically show more negative  $\delta^{13}\text{C}$  values than areas dominated by C4 pathway plants. If climatic changes produce a shift in the C3/C4 balance, then differences of ca.  $\sim 7\text{‰}$  in  $\delta^{13}\text{C}$  values can be expected (taking into account the mixing of vegetation derived carbon with host rock derived carbon) (Desmarchelier et al. 2000; Lambert & Aharon 2011). Even if a change between C3 and C4 vegetation does not occur,  $\delta^{13}\text{C}$  values in C3 plants still register changes in relative precipitation; becoming more depleted in  $^{13}\text{C}$  during high rainfall, and more enriched in  $^{13}\text{C}$  during droughts (Frappier et al. 2002; Lambert & Aharon 2011). The fractionation of carbon isotopes in plants is associated with the fixation of  $\text{CO}_2$  by the enzyme RuBisCO (Hartman & Danin 2010). In times of water stress there is reduced conductivity through stomata, leading to more positive  $\delta^{13}\text{C}$  values in plants (Hartman & Danin 2010). In addition, the seasonality of plant productivity in mid to high latitude regions influences the  $\delta^{13}\text{C}$  value of the water entering the cave (Frisia et al. 2011). In summer, plant productivity is high and the amount of soil- $\text{CO}_2$  in the groundwater increases, with the opposite occurring in winter (Lambert & Aharon 2011). The residence time of the water in the soil zone also impacts the  $\delta^{13}\text{C}$  value of the speleothems. Specifically, if recharge from the surface to the groundwater is fast, there is not enough time for isotopic equilibration between soil- $\text{CO}_2$  and atmospheric  $\text{CO}_2$  to be achieved, ultimately making drip water DIC  $^{13}\text{C}$  enriched (McDermott 2004; Lambert & Aharon 2011).

As water percolates below the soil zone, further carbon isotopic fractionation will occur if conditions promote the precipitation of calcite in the epikarst. If calcite is precipitated before reaching the main cave, there will be corresponding changes to the isotopic composition of

the drip water (McDermott et al. 2005; Lambert & Aharon 2011). The prior precipitation of calcite before drip water enters the cave is known to cause the resulting stalagmites to have relatively high  $\delta^{13}\text{C}$  values, and are often associated with increased Mg/Ca values (McDermott et al. 2005).

The conditions for prior calcite precipitation are similar to those that affect the drip water when it finally enters a cave chamber. The precipitation of calcite primarily depends on the partial pressure of  $\text{CO}_2$  ( $p\text{CO}_2$ ) in the cave atmosphere. If cave air  $p\text{CO}_2$  is sufficiently lower than the soil  $p\text{CO}_2$ , to which the water is equilibrated, then carbon dioxide will degas from the drip water causing calcite supersaturation (Ford & Williams 1989; Baldini et al. 2006). The removal of  $\text{CO}_2$  from the drip water through degassing causes fractionation of the carbon isotopes, as the lighter  $^{12}\text{C}$  will be preferentially removed due to kinetic effects (Harmon et al. 2007). The rate of degassing, and so the degree of isotopic fractionation, is controlled by the difference in  $p\text{CO}_2$  between the outside atmosphere and the cave (which can change seasonally), and by the drip rate (Baldini et al. 2006; Lambert & Aharon 2011). In general,  $\text{CO}_2$  degassing from a drop of water will be complete in 10-100 seconds, and so will be in isotopic equilibrium with the cave air before dropping onto a stalagmite (Dreybrodt & Scholz 2011; Lambert & Aharon 2011). If the drip rate is faster than this, then the precipitation of calcite onto the stalagmite will occur while continued degassing causes potentially large kinetic isotope changes (Dreybrodt & Scholz 2011; Lambert & Aharon 2011). For example, if cave ventilation changes on a seasonal basis, the  $p\text{CO}_2$  inside the cave will also change with the circulation of new air (Baldini et al. 2006). This causes increases and decreases in the rate of  $\text{CO}_2$  degassing and ‘forces’ degassing in cases where the  $p\text{CO}_2$  difference between outside and cave atmosphere is increased (Dreybrodt & Scholz 2011; Lambert & Aharon 2011). Thus, it is the combination of  $\text{CO}_2$  degassing, causing calcite supersaturation in the drip water, and the drip rate that controls the speed of speleothem formation in a cave.

Due to the complexity of these processes influencing stalagmite  $\delta^{13}\text{C}$  values, records are best interpreted on a case-by-case basis after first investigating all the local conditions. In some cases elevated  $\delta^{13}\text{C}$  values can be linked to wet periods causing incomplete equilibration between soil  $\text{CO}_2$  and percolating water, and in other cases dry periods causing evaporation in the cave result in high  $\delta^{13}\text{C}$  values (McDermott et al. 2005). If seasonal changes in temperature exert a strong control on the productivity of the vegetation and soil biomass

above a cave, then this may prove to be the controlling factor on the changes in  $\delta^{13}\text{C}$  value in stalagmites (Hellstrom et al. 1998; Hellstrom & McCulloch 2000; Harmon et al. 2007).

### **2.1.7 Summary**

This section has highlighted the complexities involved in interpreting stalagmite stable isotopic data in terms of climate, due to the many complicating factors that influence the chemistry of stalagmite calcite:

- a. Stability of the cave environment (Chapter 1)
- b. Achievement of isotopic equilibrium during the precipitation of calcite (Hendy Test vs Replication Test) (Chapter 2.1.5)
- c. 'One equation, two unknowns' problem (Chapter 2.1.5)
- d. Cave temperature effect (Chapter 2.1.5)
- e. Ocean source and ice volume effects (Chapter 2.1.5)
- f. Rainfall temperature effect (Chapter 2.1.5)
- g. Rayleigh distillation and evaporation of rainfall (Chapter 2.1.5)
- h. Seasonal changes in water stress and plant productivity and soil respiration (Chapter 2.1.6)
- i. Residence time of percolating water in the soil zone and epikarst (Chapter 2.1.6)
- j. Prior calcite precipitation in the epikarst (Chapter 2.1.6)
- k. Drip rate onto a stalagmite (Chapter 2.1.6)
- l. Degassing of  $\text{CO}_2$  in the cave environment (Chapter 2.1.6)

The large amount of cave research that has been conducted since the 1960s has been the foundation for many important paleoclimate records around the world (Dorale et al. 1998; Treble et al. 2005; Frappier et al. 2007; Zhou et al. 2008b). However, our understanding of the complexities of cave and karst systems is still growing, and knowledge that has been gained from one cave system may not always be applied to others. The intricacy and highly variable results of stable carbon and oxygen isotope fractionation processes reinforces the necessity of viewing speleothems as part of a large system intimately connected with the surrounding environment.

## **2.2. New Zealand Quaternary Paleoclimate**

### **2.2.1 Introduction**

New Zealand is a geologically young landmass formed at the Pacific and Australian tectonic plate boundary in the Southern Hemisphere. Two major islands make up the majority of the landmass above sea level from 34°25 S to 46°37 S, while the nearest neighbouring continent (Australia) is just over 2100km away. New Zealand's isolation means the ocean has a strong influence on climate, and this is accentuated by the NE-SW oriented axial ranges that run the length of the South Island and extend up the North Island. The Southern Alps reach up to 3754m at the highest point, and act as a barrier to the prevailing westerly winds, resulting in a very wet West Coast and a strong rain shadow effect to the east (Salinger & Mullan 1999). The uplift of the Southern Alps began about 5 Ma, and is continuing at a rate of about 10mm per year (Little et al. 2005). Consequently, throughout the Quaternary the Southern Alps have had a large impact on climate in New Zealand, particularly in the South Island. The climatic gradients are accentuated across this mountain range, and because they are oriented perpendicular to the prevailing circulation, are very sensitive to any change. Studies of Quaternary climate records in New Zealand have aided our understanding of the impact of glaciations and interglacial conditions in the Southern Hemisphere, and allowed investigations into the role of Antarctica in influencing southern climate, as well as interhemispheric linkages. Records of glacial advances currently extend back about 2.5 Ma, but other proxy archives of climate change mainly cover the last 30 Ka (Suggate 1990; Alloway et al. 2007).

### **2.2.2 Climate Drivers**

Major climate oscillations are known to have occurred throughout much of the Earth's history (Zachos et al. 2001; EPICA Community Members 2004). These oscillations have been closely linked with orbital fluctuations and changes in relative insolation, and in response to them the average global temperature of our planet has increased and decreased accordingly. The triggering of positive feedback cycles in many different systems has meant that when the Earth cools ice volume increases at the poles producing an ice age, and when warming is triggered the situation is reversed and polar ice melts. The drivers of climate change act on

many different timescales. The orbital cycles (also known as Milankovitch cycles) activating some of these triggers are the eccentricity, obliquity, and axial precession of the Earth's orbit; with periodicities of 400 Ka and 100 Ka, 41 Ka and 23 Ka respectively (Zachos et al. 2001). There are also other processes known to trigger glacials and interglacials such as tectonic movements (e.g. the opening of the Southern Ocean), changes in the ocean thermohaline system (through catastrophic inputs of fresh water), and release of greenhouse gases (such as large volcanic eruptions or release of methane clathrates) (Buffett 2000; Zachos et al. 2001; Broecker 2003). In the Southern Hemisphere, decadal to multidecadal variability is significant, and the most prominent source of interannual to decadal variability is from El Nino Southern Oscillation (ENSO) (Evans & Allan 1992). In addition, low frequency multidecadal changes are associated with the Interdecadal Pacific Oscillation (IPO) (Salinger et al. 2001), which has spatial characteristics similar to ENSO. The IPO occurs over timescales of about 20 to 30 years, while ENSO cycles are typically on the order of 5 to 7 years (Diaz et al. 2001; Salinger et al. 2001).

### **2.2.3 Late Quaternary Climate Events**

While the evidence from moraines and glacial sediments makes it clear there have been many large glaciations in New Zealand over the past 2.5 Ma or more, there is more detail available for the last 30 Ka. The addition of proxy records to geomorphological and sedimentary data, combined with a variety of dating techniques has allowed a reasonably detailed understanding of this time period in New Zealand to be developed from prior to the Last Glacial Maximum (LGM) to the present.

The LGM was the period of lowest sea level during the last glacial cold period (local nomenclature of Alloway et al. 2007). Global sea level dropped by 120m as temperatures fell and more water was locked up as ice on continents worldwide (Clark & Mix 2002). In New Zealand the LGM is considered to have lasted about 6 000 years between 24 Ka and 18 Ka, and during this time there were multiple glacial advance and retreat phases occurring at different times in different regions (Mix et al. 2001; Barrows et al. 2002; Alloway et al. 2007). During the LGM an ice cap formed over the Southern Alps, and glaciers generally advanced. However, some warmer intervals during the LGM period saw advance and retreat of glaciers throughout the South Island, with variations on the number and timing of advances in different regions (Suggate 1990; Pillans 1991; Suggate & Almond 2005). The amount of

temperature decrease during this time has been the subject of some debate, as different proxy records provide different estimations.

One approach to reconstructing past climate has been to create models of past glacier advances. Varying complexities of models have been developed with the aim of simulating real glacial systems, in order to investigate how much temperature decrease is needed to drive a glacier out to its LGM moraines (Oerlemans 1992, 2005; Anderson et al. 2006). Simulations have suggested that cooling in the LGM was on average between 2.5°C and 4°C lower than today, as well as in general less precipitation and stronger westerly winds (Drost et al. 2007). However, there were differences between regions, so some areas experienced more or less cooling, and different changes in annual precipitation amounts (Drost et al. 2007; Lorrey et al. 2007).

Different proxy records suggest a range of LGM temperature estimates around this average, and support the idea that different regions experienced different climatic changes. Records of sea surface temperatures calculated from foraminifera from four deep sea ocean cores around the New Zealand region show that ocean cooling of about 6°C occurred during the height of the LGM (Nelson et al. 2000; Barrows et al. 2007). Fossil beetle assemblages from LGM sediments in the Canterbury foothills suggested LGM temperatures were no more than 2°C cooler than today in these areas (Marra 2006). However, in the Awarere valley (north of Canterbury) a similar study found temperatures were between 2.5-5°C cooler than today (Marra et al. 2004). Pollen profiles from peat bogs show a retreat of forests and an invasion of grasslands close to 29 Ka, somewhat before the start of the global LGM (McGlone 2002; McGlone et al. 2004; Newnham 2007). The replacement of forests by grasses from around 29 Ka suggests cooler conditions may have started somewhat earlier in New Zealand than in other global locations (Newnham 2007; McGlone et al. 2010). The grasslands are indicative of colder and drier conditions, leading to an estimate of temperatures about 4°C cooler than today (McGlone et al. 2004). It has been proposed that the grassland increase was due to enhanced climate seasonality and bleak conditions, rather than purely temperature and/or precipitation decreases (Drost et al. 2007), and that this period has no modern analogue (Moar 1980).

The termination of the LGM at approximately 18 Ka is well established from cosmogenic dating of LGM moraines, and <sup>14</sup>C dates of pollen bearing sediments (Turney et al. 2003;

Schaefer et al. 2006; Alloway et al. 2007). Temperatures warmed to around 0-2°C lower than today, and rapid re-forestation occurred in many regions (Shulmeister et al. 2003; Newnham 2007; Vandergoes et al. 2008). Warming progressed from 17.5 Ka to close to 14 Ka when many proxy records show some complex climate fluctuations (Alloway et al. 2007). There are moraines in the Lake Pukaki region and along the West Coast that date to the time of this fluctuation, and indications in the pollen record from several other regions that suggest grasses again became more dominant (Alloway et al. 2007). The glacial records indicate that considerable advances occurred between 14 Ka and 11.4 Ka in most regions of the South Island, which coincides with the Antarctic Cold Reversal and the Northern Hemisphere Younger Dryas chronozone (Denton et al. 1999; Ivy-Ochs et al. 1999). Cooling during this period may have been as significant as during the LGM, however, the shorter duration of cooling prevented glaciers reaching their LGM extent (Williams et al. 2005; Anderson & Mackintosh 2006; Alloway et al. 2007). The exact termination of the Late Glacial Reversal (LGR) is somewhat unclear, but is proposed at around 11 Ka (Alloway et al. 2007). Pollen studies have argued for warming beginning somewhat prior to 11.4 Ka based on the establishment of flora assemblages that are noticeably absent from the record when cool, harsh conditions prevail (McGlone 1995; Singer et al. 1998; Turney et al. 2003). Regardless of the exact commencement, warming continued into the Holocene reaching a climatic optimum of mild, moist conditions with drought and frost sensitive assemblages at about 10 Ka (Isla 1989; Newnham et al. 1999; Marra et al. 2004; McGlone et al. 2004). Pollen records from several sites around the South Island have indicated that the Holocene climatic optimum was at least as warm as today, and may have a degree or two warmer, as well as wetter (Marra et al. 2004; McGlone et al. 2004). Conditions cooled slightly to modern values around 8 Ka (McGlone et al. 2004).

While proxy records indicate Holocene climate has remained close to the modern average, significant variations in climate have continued to the present with intervals of cooling/warming, aridity, and changes in atmospheric circulation; however, these have been on a smaller scale than those that took place post LGM (Clare et al. 2002; Mayewski et al. 2004). It has been suggested that most of these climate fluctuations can be linked to changes in solar variability and insolation, with cooling at the poles and increased atmospheric circulation, and increased aridity in the tropics (Clare et al. 2002; Mayewski et al. 2004). These fluctuations have caused several smaller scale glacial advance and retreat phases through the Holocene both in New Zealand and globally, however, the timing and extent of



glacial advances in the South Island have varied between the different regions (Schaefer et al. 2009; Kaplan et al. 2010; Putnam et al. 2010).

In New Zealand today there are distinct differences in regional climate based on geography and the interaction of major geographic features, such as the Southern Alps, with the predominant westerly wind flow (Salinger & Mullan 1999). These different regions experience different synoptic conditions, with recognisable average annual precipitation and temperature patterns, which vary over multi-decadal timescales (Salinger & Mullan 1999; Kidson 2000).

Recent fluctuations in climate are related to decadal/centennial scale oscillations of sea surface temperature and atmospheric circulation (Diaz et al. 2001). In the South Pacific, variations in the Interdecadal Pacific Oscillation (IPO) and El Niño – Southern Oscillation (ENSO) modulate climate over decadal to multi-year timescales (Salinger et al. 2001). Changes in the mode of ENSO and the IPO have significant impacts on average temperature and precipitation in New Zealand, with characteristic regional differences (Lorrey et al. 2007). The development of modern ENSO variability is thought to have occurred around 4 Ka around New Zealand and Australia, while prior to this the variability was much more subdued (Shulmeister & Lees 1995; Gomez et al. 2004). The increase in ENSO strength and variability has caused more variation in climate during the last 4 Ka with increased erosion, and large storms in La Nina years, which have been observed in ocean sediment cores off the North Island of New Zealand (Gomez et al. 2004). Studies of modern glaciers have revealed a strong link between ENSO index (El Nino or La Nina years) and glacier mass balance (Chinn et al. 2005). A case study on the Franz Josef glacier found that during winter accumulation there was a marked increase in the strength of westerly winds, with El Nino conditions prevalent during glacier advance phases, and tendencies to La Nina conditions during retreat phases (Hooker & Fitzharris BB 1999; Chinn et al. 2005). This study indicates that ENSO-related variability in atmospheric circulation can have significant effects on South Island climate on multi-decadal timescales.

The multi-decadal variability of synoptic climate patterns in different regions of New Zealand influence the record preserved in climate proxies. The significant regional differences mean individual proxy records will record climatic changes specific to geographic locality. For example, climate records from the West Coast and North-West Nelson are most likely to be

related to changes in mid-latitude atmospheric circulation and westerly wind strength (Clare et al. 2002; Lorrey et al. 2007; Lorrey et al. 2008). These changes in westerly wind strength are proposed to result from the changing thermal gradient between the poles and the equator during global warming and cooling (Putnam et al. 2010; Whittaker et al. 2011). The sea surface temperature anomalies that drive ENSO index changes in the South Pacific can be amplified on millennial and longer timescales (Mullan 1995). These changes influence the North/South migration of large-scale atmospheric circulation features such as the Subtropical Front and the Inter-Tropical Convergence Zone (ITCZ) (Whittaker et al. 2011). These changes to atmospheric circulation correspond to cool and warm periods affecting glacial advance/retreat patterns in the Southern Alps (Rother & Shulmeister 2006; Putnam et al. 2010; Whittaker et al. 2011).

#### **2.2.4 Late Quaternary Climate from Speleothems**

Speleothem studies have contributed significantly to our understanding of Quaternary climate change, particularly records from North-West Nelson and Waitomo (Figure 2.3) (Williams 1996; Hellstrom et al. 1998; Williams et al. 1999; Williams et al. 2004, 2005). North-West Nelson harbours some of the oldest and most extensive cave systems in New Zealand, and stalagmite deposition there may have been occurring for around 1 Ma (Williams et al. 2010). Many stalagmites have been studied from these caves and the data from eight is compiled into a master record for the South Island, which covers the last 30 Ka (Figure 2.3) (Williams 1996; Williams et al. 2005; Williams et al. 2010). Because of the ease and accuracy of dating speleothems with U-Th techniques these records have been used to anchor the timing of climate events in New Zealand such as the LGM and late glacial reversal, and also as an independent means of comparing events observed in other proxies. However, because of the difficulty in determining quantitative measurements of temperature, qualitative estimates of change are given (Williams et al. 2005). Positive and negative excursions of calcite  $\delta^{18}\text{O}$  are interpreted as indicating periods of warmer and cooler conditions respectively, but are also influenced by changes in precipitation (Williams et al. 2005). The calcite  $\delta^{13}\text{C}$  values are interpreted as representing wetness and biological activity in the region, with decreases in values (increasingly negative) indicating wetter conditions and more biological activity (Williams et al. 2005). However, the relationships are complex, and even though the  $\delta^{18}\text{O}$

values clearly show a cooling event during the late glacial reversal,  $\delta^{13}\text{C}$  values do not register much change.

Of interest, a study also conducted in North-West Nelson interpreted changes in  $\delta^{18}\text{O}$  in the opposite way (Hellstrom et al. 1998). The speleothems were collected from two caves at elevations of 600m and 900m above sea level in the Mt Arthur region, and increasingly negative excursions of  $\delta^{18}\text{O}$  values were interpreted as warming temperatures (Hellstrom et al. 1998). This difference in interpretation of changes in calcite  $\delta^{18}\text{O}$  values stems from the relationship of the cave temperature effect ( $\Delta\delta^{18}\text{O}_c/dT$ ) to the changes in precipitation  $\delta^{18}\text{O}$  values with temperature ( $\Delta\delta^{18}\text{O}_p/dT$ ) at the study site. The change in  $\delta^{18}\text{O}$  value of the calcite with change in temperature is  $-0.24\text{‰}/^\circ\text{C}$  at  $10^\circ\text{C}$  (O'Neil et al. 1969; McDermott 2004). However, the  $\delta^{18}\text{O}$  value of precipitation also changes with temperature. The relationship of  $\Delta\delta^{18}\text{O}_p/dT$  can either be less than or greater than  $\Delta\delta^{18}\text{O}_c/dT$ , so determining what this relationship is at each site controls the interpretation of warming and cooling from calcite  $\delta^{18}\text{O}$  values (McDermott 2004).

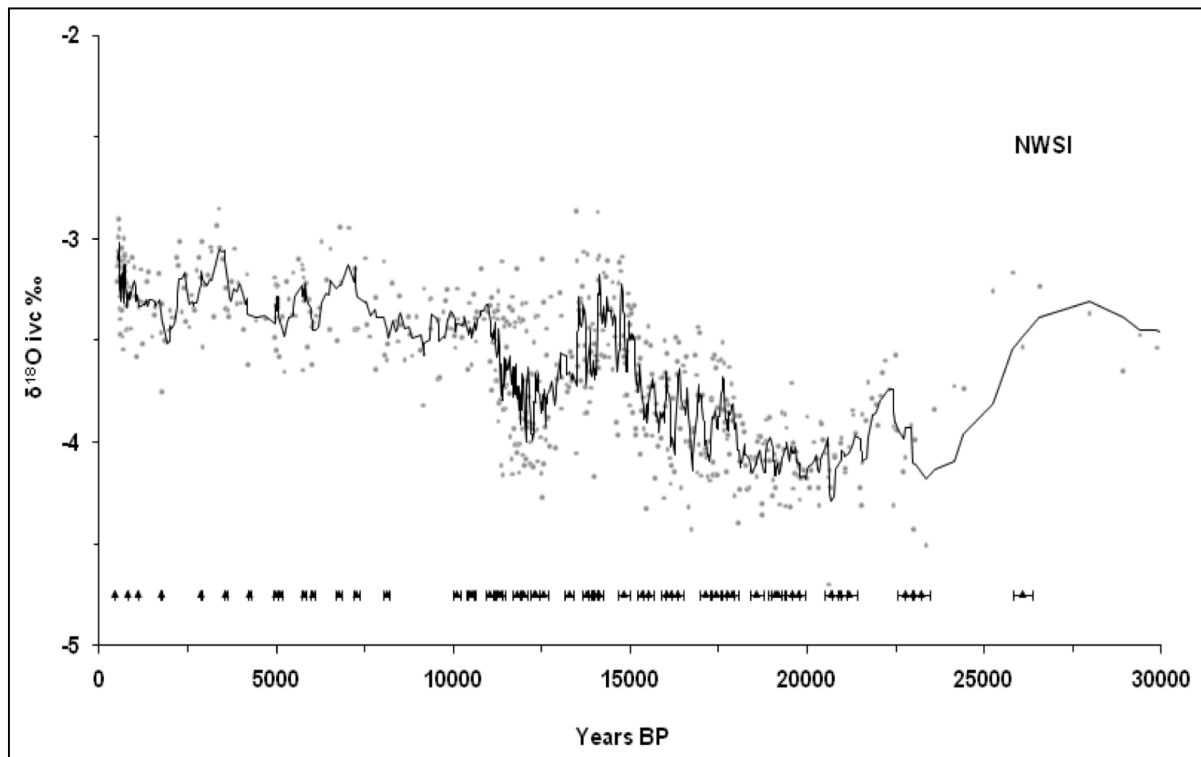


Figure 2.3: Master North-West South Island (NWSI) speleothem record of  $\delta^{18}\text{O}$  values from eight South Island speleothems (Williams et al. 2010). The record has been corrected for the ice volume effect – taking into account the change in the ocean  $\delta^{18}\text{O}$  values during the LGM (Williams et al. 2005). 56 TIMS dates with  $2\sigma$  error bars are also shown (Williams et al. 2010).

In the Mt Arthur region, one cave is about 300m higher than the other, so if the cave temperature effect is dominant the  $\delta^{18}\text{O}$  values should be offset negatively to the lower elevation cave (Hellstrom et al. 1998). However, this was not reported to be the case; i.e.  $\Delta\delta^{18}\text{O}_p/dT < \Delta\delta^{18}\text{O}_c/dT$  (Hellstrom et al. 1998). Conversely, Williams has reported that at other study sites the  $\Delta\delta^{18}\text{O}_p/dT > \Delta\delta^{18}\text{O}_c/dT$ , producing a positive relationship, meaning increases in the  $\delta^{18}\text{O}$  value of calcite are interpreted as increasing temperatures (Williams et al. 2004, 2005). Despite their complex nature, Williams' speleothem records have provided some of the most continuous data available on Quaternary climate change in New Zealand.

The most recently published study is based on a single stalagmite from Hollywood cave near Punakaki, South Island (Whittaker et al. 2011). The stable isotope record from this stalagmite spans marine isotope stages 2-4, and is closely linked to changes in precipitation. The 18 U-series dates allow the timing of cooling and warming periods to be compared to those observed elsewhere, and gives insights into the teleconnections of climate events in the Northern and Southern Hemispheres (Whittaker et al. 2011). Because annual precipitation in New Zealand, especially on the West Coast, is closely linked with westerly wind intensity, and New Zealand speleothem signals have been connected to changes in circulation (Lorrey et al. 2007; Lorrey et al. 2008), this stalagmite record presents insights into past changes in westerly wind circulation and intensity, including data showing close links with North Atlantic cooling (Lorrey et al. 2007; Whittaker et al. 2011).

### **2.2.5 Summary**

Quaternary climate change in New Zealand remains the focus of significant research efforts. The complexity of the changes both between local regions, and compared to changes in the Northern Hemisphere often raise further questions about the drivers of climate. The application of improved and new chronology techniques is constraining the timing of events, and is revealing how regions can respond differently to change. More in-depth understanding of existing proxy records and development of new ones will further contribute to our understanding of such dynamic systems. In comparing the New Zealand record to other areas of the world we can better appreciate the interconnections of climate and earth systems, and improve our decision making for the future.

## **2.3 Speleothem Fluid Inclusions**

### **2.3.1 Introduction**

The study of fluid inclusions is an important aspect in many areas of geology. The fluids trapped in rocks can contain important information about the conditions rocks form in, as well as diagenetic processes. The approach used in studying fluid inclusions depends principally on the temperature system the rocks are found in. The techniques for analysing high-temperature rocks containing fluid inclusions are different to the steps for investigating low-temperature and surface forming rocks and minerals. This review will focus on how fluid inclusions from cave calcite deposits (speleothems) can be used to investigate changes in paleoclimate and past environments. The formation and potential alteration of fluid inclusions in speleothems will be covered, as will methods for extraction and analysis. As there are many good reviews of this subject, this section will concentrate mainly on more current research.

### **2.3.2 The Formation of Fluid Inclusions**

Inclusions are small fluid-filled cavities that form either between or within mineral crystals, and can be water or gas filled, or a mixture of both (Goldstein 2001b; Verheyden et al. 2008). In near surface rocks and minerals such as carbonates and quartz, the fluid inclusions are often water filled. This water can be derived from meteoric precipitation, lake or ground water, seawater, or subsurface fluids associated with burial and alteration, as well as fault fluids (Goldstein 2001b). As crystals grow in the presence of this fluid defects in the crystal lattice allow some bubbles to be trapped, and competition between crystals can cause cavities to form that also trap fluids (Van den Kerkhof & Hein 2001). These inclusions that form when crystals are growing are called primary fluid inclusions, which are effectively a snapshot of the composition of the fluids that were intimately associated with rock formation – as long as no post depositional alteration has occurred (Goldstein 2001a).

Fluid inclusions are an integral part of speleothem formation in caves. As crystals of calcite grow, inclusions of the drip water are trapped. Slight variations in the impurity of the inclusions and the calcite define growth layers, so that patterns of fluid inclusions are

important characteristics defining different speleothem fabrics (Kendall & Broughton 1978). The size of fluid inclusions can vary greatly from less than 1  $\mu\text{m}$  to macroscopic inclusions several millimetres long (Goldstein 2001b; Genty et al. 2002). The density of inclusions in speleothem calcite depends on the formation conditions. The most inclusion rich calcite is white in colour and is usually formed through partial coalescence of the crystals (Kendall & Broughton 1978). Inclusion poor calcite is dark in colour and occurs when calcite crystals completely coalesce, forcing out or preventing inclusion spaces from forming (Kendall & Broughton 1978). The variable size and shape of fluid inclusions can make estimating the volume of fluid in the calcite difficult (Van den Kerkhof & Hein 2001). The general estimate for the volume of fluid inclusions in speleothem calcite ranges between 0.01 and 0.3 wt. % of preserved drip water (Schwarcz et al. 1976; Kendall & Broughton 1978; Harmon et al. 1979; Dennis et al. 2001).

### **2.3.3 Fluid Inclusions and Paleoclimate**

Speleothem fluid inclusions have been recognised as containing important paleoclimate information for many decades. Once fluid inclusions are formed and have been sealed in the calcite crystal lattice, it is generally assumed that the isotopic composition of the inclusion water is representative of the drip water forming the calcite. Many studies have shown that in most caves with high relative humidity the stable isotope composition of the drip water in the cave is representative of the composition of the local rainwater, or it varies in a predictable way (Yonge et al. 1985; Matthews et al. 2000; Mickler et al. 2004; Lambert & Aharon 2011). Consequently, the stable oxygen and hydrogen composition of the fluid inclusion water can be used with the stable isotope composition of the calcite to calculate past temperature and precipitation changes (Gascoyne 1992; Dennis et al. 2001; Lachniet 2009).

It is possible however, that some post-depositional alteration can occur through the exchange of oxygen isotopes between the trapped water and the host calcite (Schwarcz et al. 1976; Dennis et al. 2001; Goldstein 2001b). The most commonly used method of evaluating whether this kind of exchange has taken place is to compare samples of modern drip water with modern calcite and fluid inclusions in the recently formed calcite. This has become more reliable over time as sampling techniques have allowed smaller samples to be analysed.

If the calcite can be shown to have been deposited in isotopic equilibrium with the drip water, then the changes in stable oxygen isotopic ratios can be interpreted in terms of paleoclimate parameters through the well known temperature related fractionation of the light and heavy isotopes (Epstein et al. 1953; Kim & O'Neil 1997; Demeny et al. 2010). The most commonly used calculation for temperature has been experimentally determined by Kim and O'Neil (1997) as:

$$1000 \ln \alpha_{(\text{Calcite-Water})} = 18.03(10^3 T^{-1}) - 32.42$$

where  $\alpha$  is the fractionation factor and  $T$  is temperature in Kelvin (Kim & O'Neil 1997).

This equation requires the knowledge or an estimate of the oxygen isotopic composition of the drip water as well as the calcite, so fluid inclusions were quickly investigated as the best proxy for the isotopic composition of ancient drip water (Schwarcz et al. 1976; Harmon et al. 1979). However, the methods tested in the 1970s and 1980s concluded that oxygen isotopic exchange had occurred between the host calcite and the fluid inclusions, and this discouraged further progress for many years (Schwarcz et al. 1976; Harmon et al. 1979; Goede et al. 1986; Dennis et al. 2001). Without a suitable method for analysing fluid inclusions speleothem studies have used a two-step proxy process, relying on assumptions of isotopic equilibrium to infer estimates of the composition of past drip water from the calcite, and from these inferring changes in climate.

### **2.3.4 Extracting Fluid Inclusions from Speleothem Calcite**

With the development of increasingly more precise and accurate mass spectrometric instruments, new methods for extracting fluid inclusions from speleothems have been proposed over the last decade (Dennis et al. 2001; Vonhof et al. 2006; Verheyden et al. 2008). The release of fluid inclusions from a crystal can be achieved either through the mechanical crushing of the crystal sample (Vonhof et al. 2006; Vonhof et al. 2007), or through thermal decrepitation (Verheyden et al. 2008). Both methods require a system of extracting and isolating the released fluids, to prevent any isotopic exchange and preserve the original composition.

After several early attempts at fluid inclusion extraction (Schwarcz et al. 1976; Harmon et al. 1979; Goede et al. 1986), the catalyst for further fluid inclusion work was a study using a controlled analogue system for speleothems (Dennis et al. 2001). The system of crushing anhydrous Iceland Spar calcite with a glass capillary of water under high vacuum and slightly elevated temperatures (150°C) resulted in recovery of the correct  $\delta^{18}\text{O}$  and  $\delta\text{D}$  of water (i.e. no large isotopic depletion took place during extraction) (Dennis et al. 2001). Keeping the system apparatus at temperatures above 100°C prevented the adsorption of released water to any of the surfaces, including the freshly crushed calcite, hence the analysed water retained the correct isotopic composition (Dennis et al. 2001).

The recent development of a new crushing method advanced the analysis of speleothem fluid inclusions further by allowing the sample preparation and analysis to occur in one step through continuous flow mass spectrometry (Vonhof et al. 2006). The use of continuous flow technology allows faster processing of samples and more accurate analyses. Tests on the set-up (Amsterdam Device) showed that liquid water yielded accurate results, as did analyses of  $\delta\text{D}$  of fluid inclusions from speleothem calcite (Vonhof et al. 2006).  $\delta^{18}\text{O}$  values were not initially measured, however, subsequent studies presented  $\delta^{18}\text{O}$  results of speleothem fluid inclusions after slight modifications to the method (Vonhof et al. 2007; van Breukelen et al. 2008; Griffiths et al. 2010). Errors reported from these studies are  $\pm 2\%$  for  $\delta\text{D}$  values and  $\pm 0.5\%$  for  $\delta^{18}\text{O}$  values (Vonhof et al. 2006; Vonhof et al. 2007).

While this method has been used successfully to analyse speleothem fluid inclusions, there are some limitations associated with it. The minimum sample size required for an accurate analysis is 300mg, and larger samples are required for calcite with lower weight percent water (van Breukelen et al. 2008; Griffiths et al. 2010). This greatly restricts the temporal resolution achievable from a speleothem, and can make correlation with calcite stable isotopic data difficult as calcite can be sampled at scales of around 0.5mm or finer (Spötl & Matthey 2006). In addition, the crushing may not release all the water trapped in the calcite, especially micro-inclusions, and this may result in some isotopic fractionation between the water that is released and any water remaining in the crushed sample.

A different approach to extracting fluid inclusions from speleothem calcite can be achieved by thermal decrepitation. Decrepitation of fluid inclusions occurs when the internal pressure



of the fluid inclusion overcomes the critical toughness of the crystal wall, causing it to fracture (Lacazette 1990). This can occur through heating a solid sample to temperatures higher than those at which the fluid inclusion formed (Lacazette 1990). Decrepitation fractures will remain open and propagate in the direction of least resistance as long as the stresses from the internally pressurised fluid remain higher than the critical toughness of the crystal (Lacazette 1990). Because calcite can also accommodate the stretching of fluid inclusions with increases in temperature, it has been suggested that temperatures of around 150°C or greater are needed to cause the majority of fluid inclusions to decrepitate (Ujiie et al. 2008).

Methods currently in use to release fluid inclusions from calcite through heating are also called thermal decomposition or calcination methods, because they involve heating the samples above the decomposition temperature of calcite (~900°) (Yonge 1982; Matthews et al. 2000; Verheyden et al. 2008). The advantage of this method over crushing is that the water yield is much higher, so smaller samples can be used. However, some studies using this method found  $\delta D$  values were depleted by 20‰ – 30‰ compared to the measured values of cave drip water (Yonge 1982; Matthews et al. 2000; McGarry et al. 2004). A study of water release patterns showed that water liberated after the decomposition temperature of calcite is reached is most likely structural water with a very depleted isotopic composition (Verheyden et al. 2008). Any structural water released consequently decreases the values of any measured fluid inclusion water. Other process that can affect the value of fluid inclusion  $\delta^{18}O$  is the formation of anhydrous lime (CaO) at temperatures above 600°C, and isotopic exchange between water and CO<sub>2</sub>, which can also be significant at high temperatures (Sharp 1992; Rodriguez-Navarro et al. 2009). In the presence of water the anhydrous lime will undergo hydration reactions, and in the closed system for extracting fluid inclusions the only water available is that released from inclusions, resulting in isotopic fractionation of the water (Sharp 1992; Rodriguez-Navarro et al. 2009). Due to these problems when calcite is heated to high temperatures, the most recent decrepitation methods recommend heating the speleothem samples to a maximum of 550°C (Verheyden et al. 2008). However, this method still presents some issues when high resolution analyses are required, because the smallest samples used were about 1g (1cm<sup>3</sup>) of calcite (Verheyden et al. 2008).

A very different approach to analysing fluid inclusions can be used when the fluid inclusions are large. Macroscopic fluid inclusions spanning several millimetres in a speleothem were

identified through the movement of bubbles trapped within them (Genty et al. 2002). They could be extracted by simply drilling a hole to the inclusion and sampled with a syringe (Genty et al. 2002). Unfortunately, such large fluid inclusions have rarely been observed as many do not have gas bubbles, and it is not known how commonly these form (Genty et al. 2002).

### **2.3.5 Summary**

Speleothem fluid inclusions are a useful tool for paleoclimate studies as they commonly represent, in an unaltered form, the isotopic composition of drip water entering a cave. They are readily incorporated within calcite as precipitation in a cave occurs, unless the conditions of formation cause calcite crystals to completely coalesce. However, this seems to be less common, as the vast majority of speleothems are reported to contain at least 0.01 wt% water (Dennis et al. 2001). The stable oxygen and hydrogen isotopic composition of speleothem fluid inclusions can be used to infer changes in climate parameters through time. If the speleothem calcite has formed in isotopic equilibrium with the drip water, then the fluid inclusion isotopic composition can be used to calculate reasonably accurate changes in temperature and precipitation through the growth period of the speleothem (Kim & O'Neil 1997; Demeny et al. 2010). If kinetic conditions prevailed during speleothem growth, then the fluid inclusions offer some insight into the changing hydrological conditions in the cave and regional environment.

The under-utilisation of fluid inclusions for this type of paleoclimate work has primarily been due to the lack of a method that can efficiently produce reliable results of fluid inclusion composition. New methods proposed in the last five years are beginning to address this problem. With the increasing interest in multi-proxy records of climate, the ongoing development of fluid inclusion studies will lead to some exciting new insights into climate change and the links between local processes in the cave system.

## **Chapter 3: Field Methods**

### **3.1 Introduction**

The majority of speleothems collected in New Zealand for paleoclimate research have come from caves either in North-west Nelson, or Waitomo in the North Island. In focusing this thesis on South Island paleoclimate a cave was selected that could be compared with the records from North-west Nelson, but had not previously been sampled for stable isotope analyses. This led to an investigation of the caves south of Westport, but north of Punakaiki. This area of the West coast has extensive limestone formations and many cave systems. Ease of access was a consideration for the field work which narrowed the selection to Te Ananui/Metro Cave (called Metro Cave hereafter) near Charleston (Figure 3.1).

### **3.2 Geological Setting**

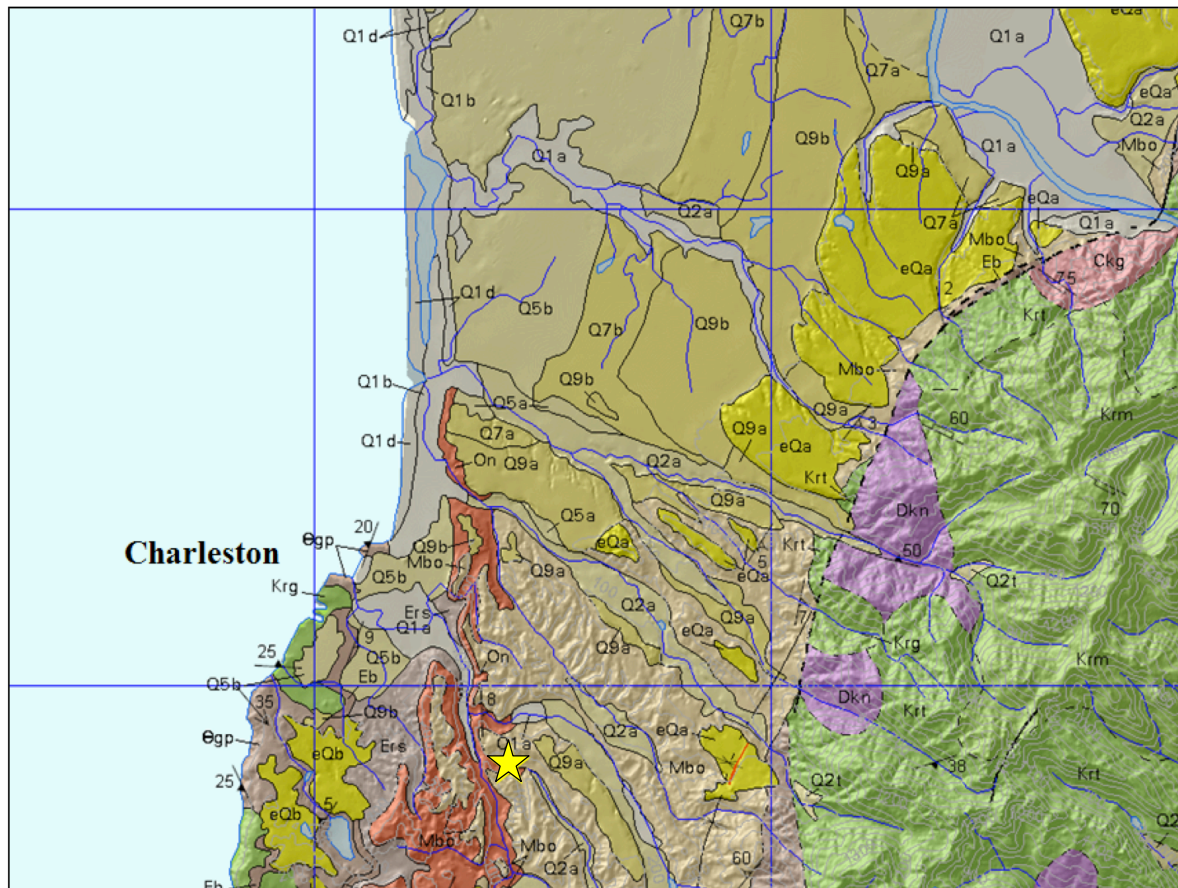
Metro Cave is located in the Nile River valley, 5km east of Charleston on the West Coast of the South Island, New Zealand (Figure 3.1). The cave sits at close to 60m above sea level and is reasonably large, with 8km of passageways and 7 entrances (Figure 3.3). It was formed near the contact of the Tiropahi and Potikohua Limestones of the Oligocene age Nile River Group (Figure 3.2) (Williams 1980). These units are areally extensive and reach up to 200m and 600m respectively at their thickest points south of the Nile River, however both units thin to the north (Williams 1980; Crawford 1994). The Tiropahi Limestone is an impure massive foraminiferal biomicrite, with variable susceptibility to karst formation (Crawford 1994). This is overlain by the Potikohua Limestone, which is made up of a massive basal member and a flaggy upper member. The basal member is a sandy polyzoan biosparite and is visible in the lower passages of Metro Cave (Crawford 1994). The upper member consists of well indurated, sometimes fossiliferous flags separated by thin seams of poorly cemented quartz-arenite (Crawford 1994). The upper member displays a wide range of karst landforms throughout its extent, and is clearly a key component in the style of cave breakdown in some chambers of Metro Cave (Crawford 1994). Atop these formations is the Miocene age Blue Bottom Group, of which the O'Keefe Formation unconformably overlies the Nile River Limestones above Metro Cave (Crawford 1994). The O'Keefe Formation is a blue-grey micaceous fine sandstone-siltstone (Williams 1980).

Metro Cave was formed by the subterranean capture of Ananui Creek – a tributary to the Nile River. Once the caprock was eroded away from the limestone, dissolution occurred through fissures and cracks eventually forming a complex system of passages known as a floodwater maze (Williams 1980). In addition to the down-cutting of Ananui Creek, the Nile River also rapidly incised the bedrock, causing Ananui Creek to constantly re-adjust to the lowering base level. This re-adjustment is visible in the cave system as a series of stepped passages. The earliest major passages and the old stream submergence leading to them are about 30m above the present Main Entrance of the stream (Williams 1980). The age of Metro Cave is still somewhat speculative, however, an age bracket has been suggested from the oldest speleothems dated from the cave, and from mapping of coastal marine terraces above the cave (Williams 1982). The plateau above Ananui Creek is about 100-150m above sea level and has been mapped as an extension of coastal terraces thought to have formed during the Terangian Interglacial around 200Ka (Williams 1980). The formation of Metro Cave cannot have begun while the area was submerged, as the formation of the passages required the capture of a stream. The oldest speleothems in the cave were dated in the 1980s, resulting in a U-Th date of  $120 \pm 45$  Ka from one of the oldest sections of the cave, implying that the early cave passages were sufficiently developed for speleothem formation by this time (Williams 1982).



Figure 3.1: General location of Te Ananui/Metro Cave in the South Island context, approximate location of cave is starred.





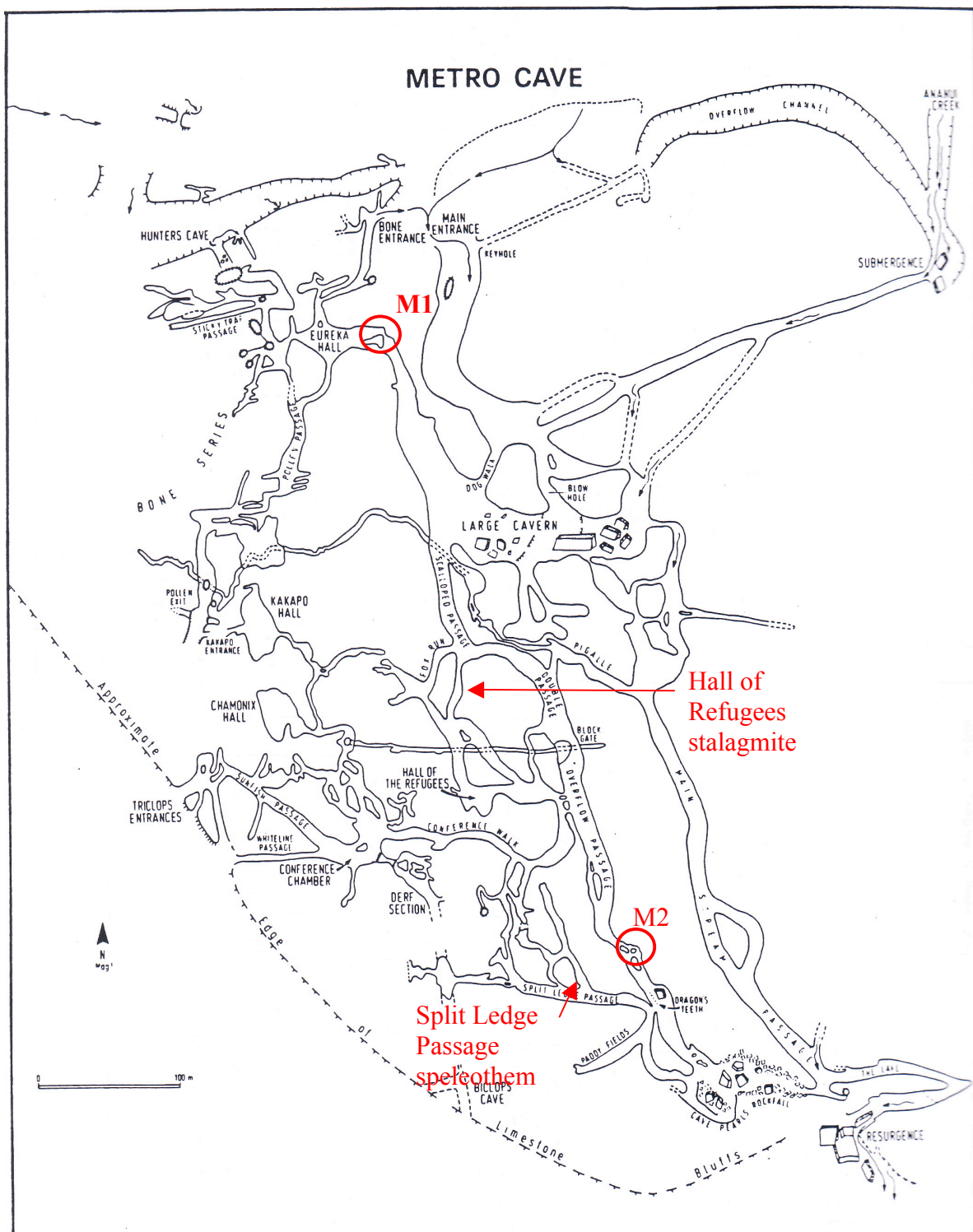


Figure 3.3: Survey map of Te Ananui/Metro Cave (Smith 2004). Locations of the four stalagmites collected in May 2010 are marked. Entrance to the cave is gained through the Triclops Entrance, the Main Entrance is only accessible through the cave. The sites of M1 and M2 were also the sites used for drip water collection, drip rate monitoring, temperature and humidity readings.

The Paparoa karst is bounded by two major faults – the Cape Foulwind fault to the west and the Lower Buller fault to the east (Figure 3.4). The Cape Foulwind fault is a high-angle east-dipping inverted normal fault just offshore of the west coast, with greater than 2000m reverse throw (Ghisetti & Sibson 2006). This fault, along with the Lower Buller fault and others in the region, was re-activated when uplift began and caused anticlinal folding of the sedimentary basin that formed in the hanging wall during the previous extensional phase (Ghisetti & Sibson 2006). The uplift and crustal shortening caused by transpression across the Pacific-Australian boundary in the last 7 Ma resulted in the exposure of the Oligocene-Miocene sedimentary sequences (Ghisetti & Sibson 2006). Continued uplift through the Quaternary has resulted in a relatively simple tilted succession along the coast, with the limestone dipping east at about 5-10° (Crawford 1994). Further south the sequence is folded into the asymmetric Barrytown syncline. The rate of uplift through the Quaternary was estimated from the height of raised coastal terraces, and from dated stalagmites in caves linked to those terraces (Williams 1982). These data produced differential uplift rates of about 0.27mm/yr near Westport and close to 0.14mm/yr further north (Williams 1982).

Figure 3.4: Structural map of the region showing location of major faults and folds (Ghisetti & Sibson 2006). Approximate location of Te Ananui/Metro Cave is also plotted (star).

### 3.3 Regional Climate and Vegetation

The northern West Coast of the South Island has a mild temperate climate. The mean annual temperature at Westport is 12.5°C with average summer and winter temperatures around 17°C and 8°C respectively (Figure 3.5). The prevailing wind direction is from the west, off the Tasman Sea, with seasonal variations between sub-tropical and sub-antarctic influences. Annual precipitation averages about 2000mm at Westport, and increases with elevation towards the Southern Alps (Williams et al. 2005).

The vegetation in the study region is predominantly native mixed beech/podocarp/broadleaf forest, with a thick understory of ferns (Moar & Suggate 1996). During the last several glacial cycles, this region has experienced large changes in the forest composition and structure. However, the area has always remained dominated by C3 vegetation as New Zealand has very few native plants that use the C4 pathway, and these are confined to coastal dune areas (McGlone 1995; Williams et al. 2005). During the height of the last glaciation the vegetation in this region was a mix of grassland/shrubland with the dominant pollen groups including *Poaceae*, *Cyperaceae*, and *Asteraceae*, although *Nothofagus* pollen was still present in small amounts suggesting some pockets of beech may still have existed (Moar & Suggate 1996). This cold-adapted vegetation was succeeded by a progression back to forests as temperatures

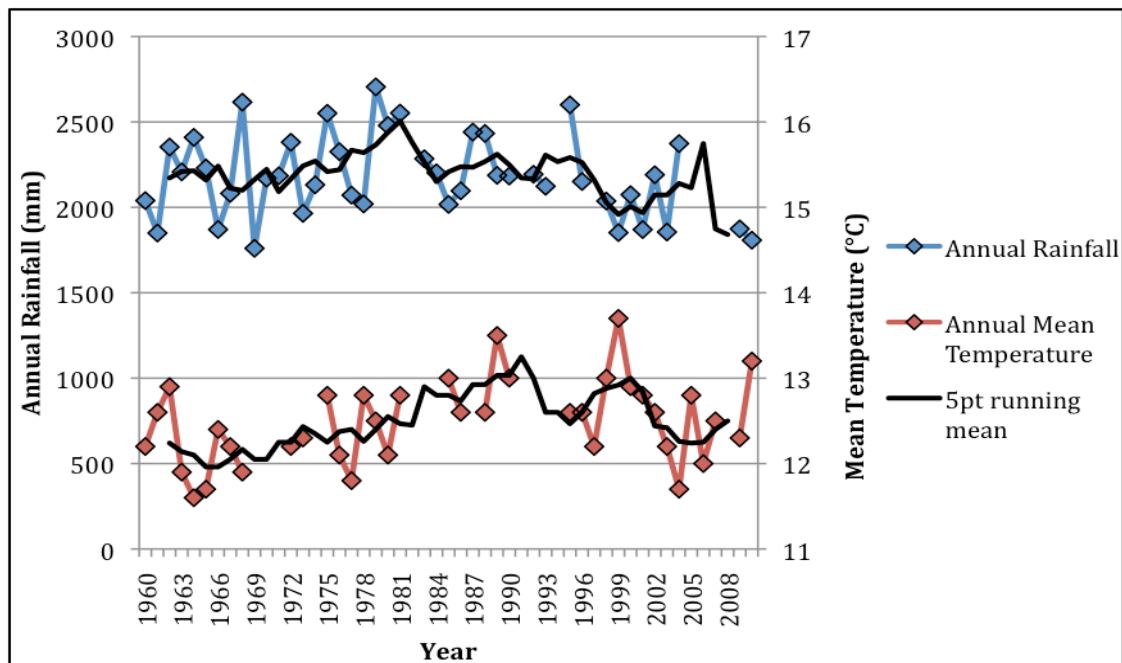


Figure 3.5: Graph of mean annual temperature and annual precipitation from the Westport climate station over the last 50 years (Data from CliFlo, accessed 2/06/2011). Gaps are due to no data from some years.



warmed during the interglacial transition, with the mildest conditions marked by the appearance of *Dacrydium cupressinum* at the Holocene climatic optimum (Moar & Suggate 1996). In recent times there have been various periods of logging disturbing the forest in the area prior to the formation of Paparoa National Park.

### **3.4 Previous Research at Te Ananui/Metro Cave**

Several scientific studies have focused on Metro Cave, the first major one being a survey commissioned by the old New Zealand Forest Service (Williams 1980). This study was conducted to investigate what impact proposed extensive logging would have on the cave system, which was already an attraction to tourists and visitors. A thorough investigation of the cave deposits, fossils, geomorphology and hydrology of the cave system, and cave ecology was conducted, in order to provide information on the impact of visitors and land use in the region (Williams 1980). A subsequent trip to collect samples from speleothems in Metro Cave for dating resulted in 9 U-Th dates from different levels of the cave, with a spread of ages from  $120 \pm 45$  Ka to  $18 \pm 4$  Ka (Williams 1982). These were used to constrain the rate of Quaternary uplift in the region (Williams 1982). Some pollen sampling work has also been carried out in Metro Cave, as has significant fossil studies focusing on the avian faunas (Worthy & Holdaway 1993). Further study on the hydrology and geomorphology of the Paparoa karst was carried out as part of PhD research through the University of Auckland in the early 1990s, although the main field area was just south of Metro Cave (Crawford 1994).

### **3.5 Field Methods**

After a conservation push to recognize and protect more of New Zealand's unique landforms and species, a large section of the Paparoa karst was included in Paparoa National Park – established in 1987. Metro Cave is now often used by recreational cavers, and guided parties can enter the cave with concession holders Norwest Adventures Ltd. However, as the cave is now gated, all access is granted by permit from the regional Department of Conservation (DOC) office. Permission to sample speleothems from Metro Cave for this study required an application for a low-impact research and collection permit. This was applied for in February 2010, and after some consultation was approved in April 2010 with the following conditions:

- a. Group size is not to exceed 4 people including the permit holder.
- b. Up to six stalagmites may be collected, four of which may be “live” (actively dripping).
- c. Only a battery powered, diamond tipped saw may be used in the collection of “live” stalagmites.
- d. The remaining stalagmites to be collected must already be broken.
- e. Only stalagmites in less frequently visited areas to be collected.
- f. A DOC staff member is to present on all stalagmite collection trips.
- g. Stalagmites collected should not be more than 70cm tall.
- h. Up to seven drip-water samples may be collected on a fortnightly basis from 25<sup>th</sup> April until the 31<sup>st</sup> July 2010.

During the time period covered by the collection permit six trips in total were made into Metro Cave.

The initial trip into Metro Cave was conducted with DOC ranger Chippy Wood to explore the cave further and to identify potential stalagmites for collection. Chippy Wood was also present on the subsequent trip a fortnight later to collect two “live” and two “dead” (already broken) stalagmites. Collection of the “live” stalagmites involved the use of a hand-held Hitachi 18v battery powered disk grinder. Water to cool the saw while it was running was sourced from within the cave to minimize the impacts of introduced water in the cave environment. Plastic bags were laid around the stalagmites while cutting was in progress to reduce the build up of calcite dust on neighbouring speleothems. Each of the stalagmites were wrapped in bubble wrap and placed in cardboard boxes packed out with polystyrene foam to be carried out of the cave. They were taken back to the University of Canterbury and split in half for preliminary analysis.

The subsequent four trips to Metro Cave were to collect drip water and measure the drip rate, as well as taking temperature and relative humidity readings (table 3.1). Drip water from straws close to where the two “live” stalagmites were taken was collected in 5ml vials. The drip rate at the site of stalagmite M2 was measured by noting the time that a drip landed on the base of the cut stalagmite from the source straw for at least four consecutive drips. This method of measuring the drip rate was not possible at the site of stalagmite M1 as the straw

directly above the cut stalagmite did not drip at all on any of the trips after the stalagmite had been collected; although the straw had been observed to drip on the initial trip identifying stalagmites, and on the final trip into the cave a drop was present for more than 20 minutes. Consequently, the closest neighbouring straw 20cm away dripping onto another stalagmite was measured for a drip rate. A glass slide was also set on the base of both cut stalagmites and left for eight weeks so that any new calcite would precipitate on the glass and could be petrographically analysed and compared to the respective stalagmites.

Following this period of field work it was decided that an extension to the permit should be applied for, in order to collect some more drip water and take readings in the summer. This was granted and one further trip was made in early January 2011 (Table 3.1). The glass plates were also recovered at this time, however, while there was some calcite deposition on the glass plate from the M2 site, there was no deposition on the glass at the site of the M1 stalagmite.

The preliminary analysis of the collected stalagmites was made on the basis of their internal morphology. The two “live” stalagmites (M1 and M2) were cut in the Geology department at the University of Canterbury, however, the equipment could not cope with the larger two “dead” stalagmites. These were taken to Decra Arts Ltd, a Christchurch based stone working company specialising in kitchen bench tops and gravestones, for sectioning.

<b>Table 3.1</b>				
Trip 1 1/06/10 Winter		Outside entrance	Site M1	Site M2
	Humidity (rel %)	87.4	87.7	85.1
	Temperature (°C)	9.9	10.4	13.0
	Average Drip Rate (mins)		3.00	3.72
Trip 2 16/06/10 Winter		Outside entrance	Site M1	Site M2
	Humidity (rel %)	100.0	100.0	97.0
	Temperature (°C)	9.2	8.4	11.3
	Average Drip Rate (mins)		3.21	3.42
Trip 3 14/07/10 Winter		Outside entrance	Site M1	Site M2
	Humidity (rel %)	92.0	100.0	100.0
	Temperature (°C)	7.0	6.9	9.4
	Average Drip Rate (mins)		3.47	5.60
Trip 4 27/07/10 Winter		Outside entrance	Site M1	Site M2
	Humidity (rel %)	88.0	100.0	100.0
	Temperature (°C)	11.6	8.2	10.5
	Average Drip Rate (mins)		3.00	3.83
Trip 5 5/01/11 Summer		Outside entrance	Site M1	Site M2
	Humidity (rel %)	-	-	-
	Temperature (°C)	18.0	11.0	12.0
	Average Drip Rate (mins)		2.55	5.05
<b>Averages</b>		Outside entrance	Site M1	Site M2
	Humidity (rel %)	91.9	96.9	95.5
	Temperature (°C)	9.4	8.5	11.1
	Average Drip Rate (mins)		3.17	4.14

Table 3.1: The data on environmental conditions inside the cave during the 2010 winter, with some extra data from January 2011. Unfortunately relative humidity was not measured during the summer trip.

### 3.6 Description of the Stalagmites

Stalagmite M1 was a live stalagmite cut from near Eureka Hall (Figure 3.2). It is 28cm long and was growing below a step in the roof down which water was dripping as part of a line straws/stalagmites. The series of stalagmites was at the edge of a breakdown pile, so the stalagmites were all cemented onto loosely piled broken flags. This part of the chamber was situated well back from the various entrances, and was quite low, only about 1m in height, so was well sheltered from drafts. Water was observed beading on the roof. Once split open, M1 revealed a highly laminated structure with about 2-3 macroscopic layers per millimeter (Figure 3.4a). This stalagmite was chosen for further tests of equilibrium deposition and paleoclimate analysis.

Stalagmite M2 was the second live stalagmite cut from an alcove near the Dragons Teeth (Figure 3.2). M2 is 15cm long and it was growing on an open shelf with a continuing passage from the back that curved round to rejoin the rest of the larger passages. The height of the alcove was just under 1m high. Considerable cave coral/popcorn was growing on the floor and on some of the straws. Once split, M2 showed a variety of fabrics, from layers with distinct depositional breaks at the base to dendritic crystals, followed by highly laminated layers towards the top, with about 5 layers per millimeter (Figure 3.4b). This stalagmite was not chosen for further analysis because the dendritic crystal fabric clearly shows the stalagmite must have been affected by kinetic fractionation, and so is not so suitable for paleoclimate investigations.

The stalagmite taken from the back passage to the Hall of Refugees was already broken. It is 58cm long and when cut in half shows three distinct growth periods visible in the layering (Figure 3.4c). The first is a highly laminated sequence, capped by an obvious depositional boundary. The calcite layers in the section above this are thicker and the crystals show a more feathery form, especially towards the top of some layers. The final top section of the stalagmite is again highly laminated. Despite the good possibility that this stalagmite could provide useful paleoclimate information it was not chosen for further investigation, as it was determined that detailed analysis would take too long for the scale of this project.

The final speleothem collected came from near the Split Ledge passage. The piece collected, 39cm long, was already broken and lying on the cave floor just by its base. The bottom edge of the piece and the top edge of the base matched up well, so this was confirmed to have broken off in place. However, in attempting to place the broken piece back on top of its base it was discovered the roof in this section had lowered too much for this to be done. Once the piece was split it could be seen that this was actually the top piece of a column (Figure 3.4c). The majority of the piece collected was the stalactite with the tapering end visible within the layers of calcite that had formed as the join of the column, so just below the broken section in the base would have been the original stalagmite. Because the piece collected was mainly made up of a stalactite, it was not chosen for further analysis due to the difficulty of sampling across layers. As only the M1 stalagmite was analysed for this thesis, the other stalagmites collected from Metro cave are in storage at the University of Canterbury in Christchurch.

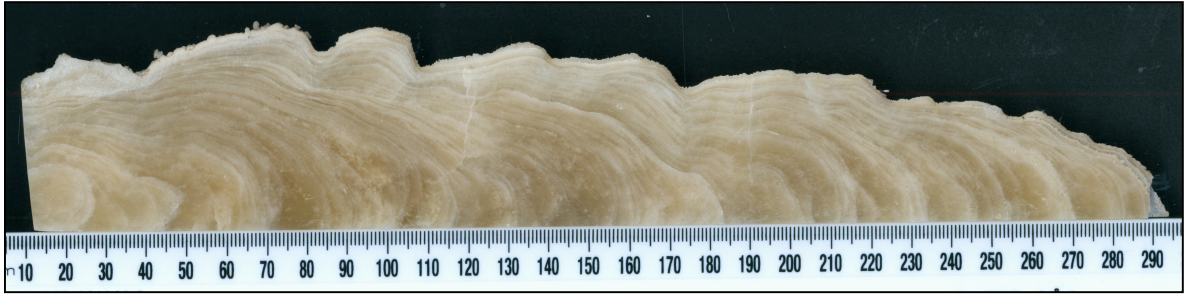


Figure 3.6a: Stalagmite M1, high resolution scan of the quarter used later for stable isotopic analysis, surface is polished.

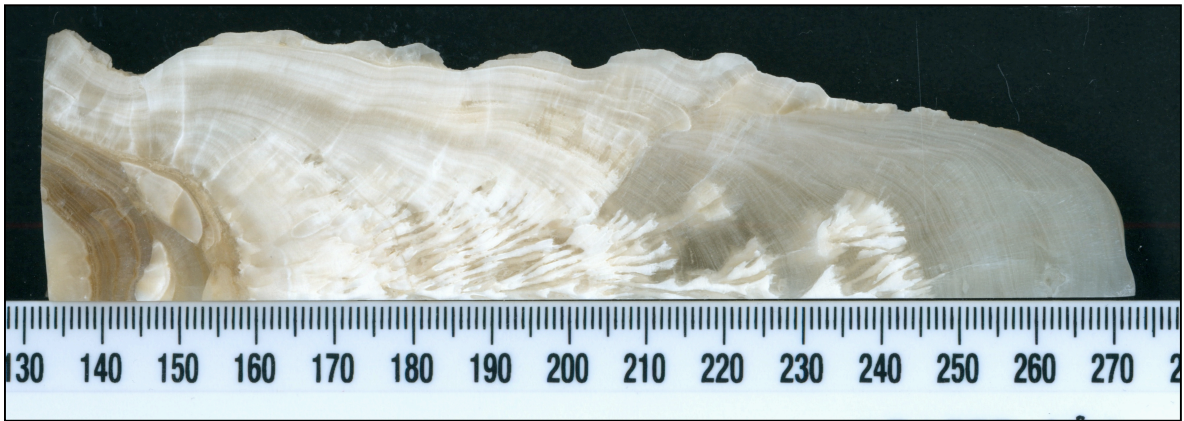


Figure 3.6b: Stalagmite M2, high resolution scan of one quarter, polished surface.



Figure 3.6c: The two dead speleothems; larger stalagmite collected from near the Hall of Refugees, shorter speleothem is the top piece of a column (oriented vertically) collected from near Split Ledge passage. Split faces unpolished.

# Chapter 4: Analysis Methods and Results

## 4.1 Introduction

This chapter presents the laboratory methods used to analyse the M1 stalagmite and the results from the various tests. Initial tests involved evaluating how useful the stalagmite would be for a paleoclimate study, and assessments of the modern hydrological environment in the cave system. Further geochemical analyses were carried out on the stalagmite to obtain trace element and stable isotopic data and to find out the age range of its growth. The final section of this chapter outlines the developmental work carried out on a new method to extract and analyse the stable hydrogen and oxygen isotopic composition of water from fluid inclusions trapped in the calcite. Results are presented for the method testing and initial fluid inclusions analysed. However, the final stage of this work has been delayed following the disruption caused by the earthquakes in Canterbury in 2010 and 2011.

## 4.2 Hendy Tests

A Hendy Test is one of the few ways to geochemically test whether a stalagmite formed in isotopic equilibrium with the drip water or not. It involves evaluating the degree of co-variation of stable carbon and oxygen isotopes along a single layer of precipitated calcite, and up the growth axis of the stalagmite (Hendy 1971). A stalagmite has been deposited in isotopic equilibrium with the cave drip water if the  $\delta^{18}\text{O}$  values remain constant along the layer while the  $\delta^{13}\text{C}$  values vary irregularly; i.e. there is no positive correlation between  $\delta^{18}\text{O}$  and  $\delta^{13}\text{C}$  values along the layer (Hendy 1971; McDermott 2004). Also there should be no positive correlation between the carbon and oxygen isotopes up the growth axis (Hendy 1971). These criteria are based on the assumption that while  $\delta^{18}\text{O}$  values can be expected to change when climate changes, the  $\delta^{13}\text{C}$  of soil  $\text{CO}_2$  does not – i.e. is not linked to climate (Hendy 1971; Dorale & Liu 2009). Consequently, if there is a strong correlation between  $\delta^{18}\text{O}$  and  $\delta^{13}\text{C}$  along a single calcite layer in a stalagmite and up the growth axis, then the conditions under which the calcite has been precipitating were not in equilibrium with the drip water and kinetic fractionation processes have affected both isotope species. If a speleothem has not been deposited in isotopic equilibrium with the drip water then it is likely

that any changes in the stable isotopes that could have been linked to climate change have been overprinted by the stronger changes associated with kinetic fractionation.

The Hendy Test has been used widely as a measure of isotopic equilibrium in speleothems, however, the practicalities of carrying out the tests can sometimes produce uncertain results. It is possible for a stalagmite to fail the Hendy Test and still be a useful representative of climate change. In some cases it is very difficult to sample only along one layer, so mixing of calcite from several layers may show a false positive co-variation of oxygen and carbon isotopes (Dorale & Liu 2009). In other cases it is possible for the centre of the stalagmite close to the growth axis to have been deposited in isotopic equilibrium, but for kinetic fractionation to have occurred on the flanks of the stalagmite (Dorale & Liu 2009). In addition, it has since been shown that changes in climate can change the  $\delta^{13}\text{C}$  value of soil  $\text{CO}_2$  through changing productivity of vegetation and soil microbes, and sometimes even through changes in the vegetation to plants with different photosynthetic pathways (e.g. C3 to C4 plants) (Dorale et al. 1998; Lambert & Aharon 2011). Hence a stalagmite with positive co-variation between  $\delta^{13}\text{C}$  and  $\delta^{18}\text{O}$  values up the growth axis may also represent strong environmental change in the local region. Bearing these possible caveats in mind, the Hendy Test is still one of the only methods using geochemical data available to test for isotopic equilibrium.

In order to evaluate whether equilibrium conditions were achieved throughout the growth of the M1 stalagmite, Hendy Tests were carried out on five layers up the M1 stalagmite, and the  $\delta^{18}\text{O}$  and  $\delta^{13}\text{C}$  values from all the samples up the growth axis were plotted together (Figures 4.1a-f). Sampling was performed using a 1mm carbide drill tip in a hand-held dremel drill, and 10 samples were drilled 0.5cm apart along a layer. This means the furthest samples were 5cm away from the centre of the growth axis. Some samples were discarded after technical issues were found in some of the isotope analysis runs, but there are still at least five points per layer. Lines 3 and 5 “pass” the Hendy Test, whereas lines 1, 2 and 4 show some positive correlation between  $\delta^{18}\text{O}$  and  $\delta^{13}\text{C}$  values (Figure 4.1a-e). The slight positive co-variation up the growth axis is not enough to be significant and may be accounted for by some probable mixing of calcite from different layers (Figure 4.1f). If only the values up to 3-3.5cm (up to sub-samples 6-7) away from the growth axis are considered, then all lines pass the Hendy



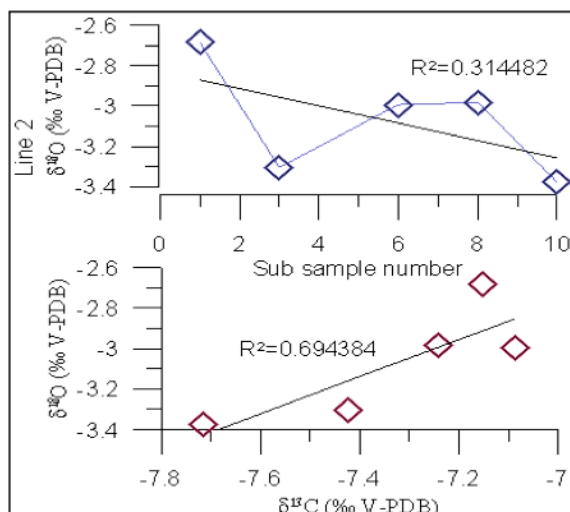


Figure 4.1a: Hendy Test line 1, 87.5mm up from base

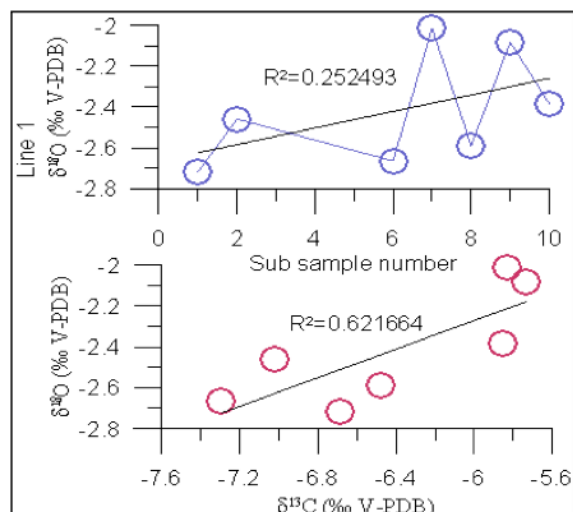


Figure 4.1b: Hendy Test line 2, 133mm up from base

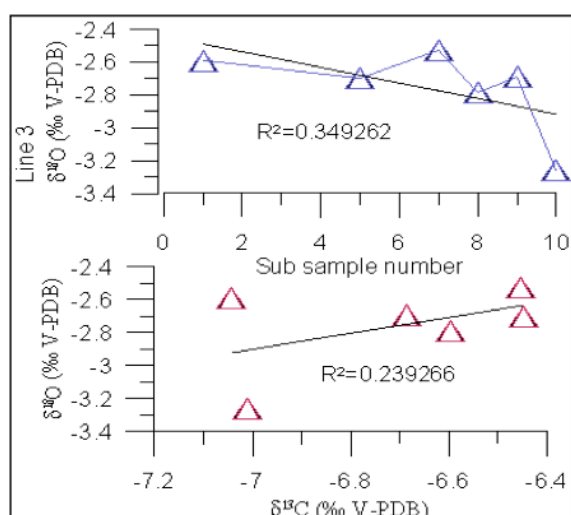


Figure 4.1c: Hendy Test line 3, 158mm up from base

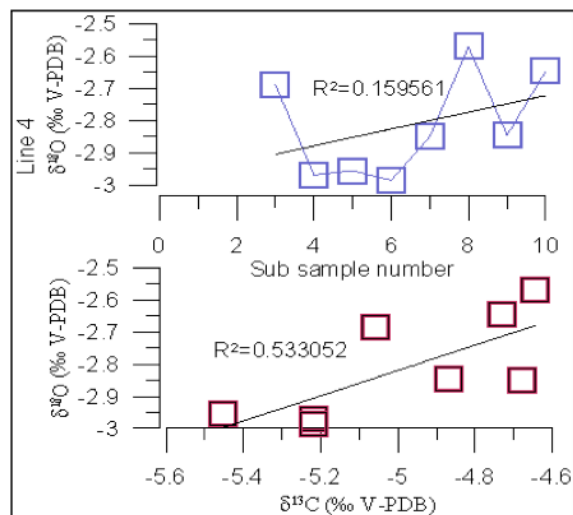


Figure 4.1d: Hendy Test line 4, 220mm up from base

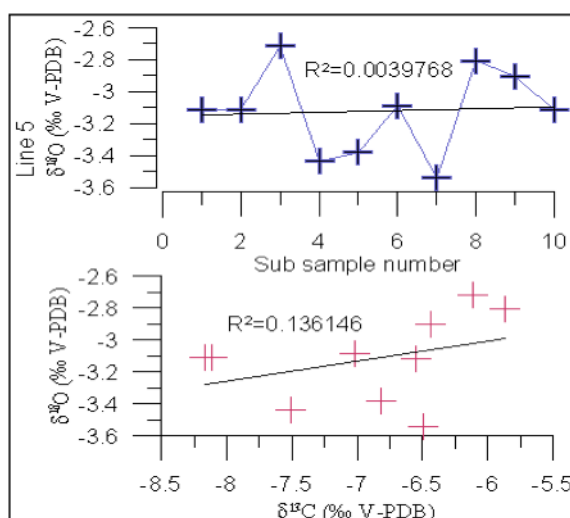


Figure 4.1e: Hendy Test line 5, 250mm up from base

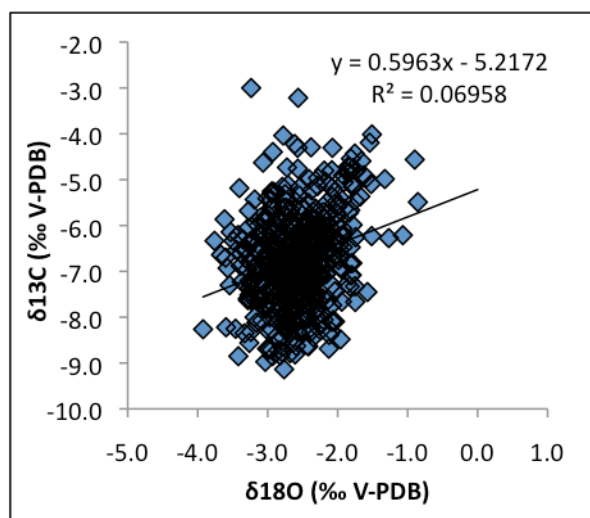


Figure 4.1f: Correlation of  $\delta^{18}\text{O}$  and  $\delta^{13}\text{C}$  up the growth axis of the M1 stalagmite

Test. All the sampling of calcite up the growth axis was carried out within this zone close to the growth axis.

The Hendy Tests indicate that isotopic equilibrium between the drip water and the precipitating calcite was achieved in the zone of the growth axis. From about 3.5cm away from the growth axis, the stable isotopic composition of nearly all the layers analysed indicate that some positive co-variation occurred, suggesting that kinetic isotopic fractionation may have affected the calcite precipitated down the sides of the stalagmite. By analysing a 'moving window' up the M1 stalagmite, we were able to evaluate the likelihood of equilibrium conditions existing at regular intervals throughout the growth of the stalagmite.

<b>Table 4.1</b>			
<b>Sample ID</b>	<b><math>\delta D</math></b>	<b><math>\delta^{18}O</math></b>	<b><math>\delta^{13}C</math> DIC</b>
S1DT.01-06-10	-11.75	-2.67	-5.36
S1DT.16-06-10	-12.76	-2.96	-2.87
S1DT.14-07-10	-8.60	-2.62	-6.33
S1DT.27-07-10	-5.53	-2.05	-3.32
S2EH.01-06-10	-14.67	-2.96	-4.39
S2EH.16-06-10	-15.32	-3.11	
S2EH.14-07-10	-15.78	-3.25	-8
S2EH.27-07-10	-3.95	-1.88	
<b>Average</b>	<b>-11.05</b>	<b>-2.69</b>	<b>-5.05</b>
Cave Waterfall.01-06-10	-17.95	-3.64	
S1DT.puddle.01-06-10	-10.47	-2.72	-3.09
Nile River	-35.81	-5.19	
Westport - May	-43.86	-5.41	
Greymouth - May	-31.52	-4.28	
<b>Average</b>	<b>-37.69</b>	<b>-4.84</b>	

Table 4.1: Shows the data analysed from the drip water gathered June-July 2010. The naming of the sites was based on the order visited in the cave, so is slightly different to the naming of the stalagmites – M1 stalagmite was collected from Site 2 (Eureka Hall), while M2 stalagmite was collected from Site 1 (Dragon's Teeth). Data on the isotopic composition of May precipitation from Westport and Greymouth were kindly passed on by Joshua Blackstock (MSc candidate, UC).

### 4.3 Drip water analyses

All the drip water collected from Metro cave was analysed for  $\delta D$  and  $\delta^{18}O$  composition at the University of Canterbury, and the  $\delta^{13}C$  values of dissolved inorganic carbon (DIC) of some samples were also measured (Table 4.1).

The drip water data indicate that even over the two-month period of water collection the stable isotope composition of the water entering the cave was highly variable (Table 4.1, Figure 4.2). It is also isotopically heavier than the average monthly precipitation in the region, suggesting the residence time of the water in the soil and karst is long enough for environmental processes to cause isotopic fractionation. This can also be seen in the difference between the water analysed from the cave waterfall, which consists of water flowing almost directly from the surface above the cave and the drip water measured in the cave chambers where the live stalagmites were collected. Notably, the drip water  $\delta^{18}O$  values have the same range as the modern calcite layers of the M1 stalagmite (Figure 4.2). The most recent calcite from the M1 stalagmite (final 10 points) also has a very similar average  $\delta^{18}O$  value (-2.87‰) to the  $\delta^{18}O$  value of the drip water (-2.80‰) from the same site. The large variability in the drip water DIC values is also indicative of a large amount of natural variability in the cave environment. Although the drip water  $\delta^{13}C$  values match the range of the modern calcite  $\delta^{13}C$  values, the 5‰ range indicates the large variability in the modern environment is being transferred to the calcite precipitating in the cave, and questions the assumptions of environmental stability in caves on the West Coast of New Zealand.

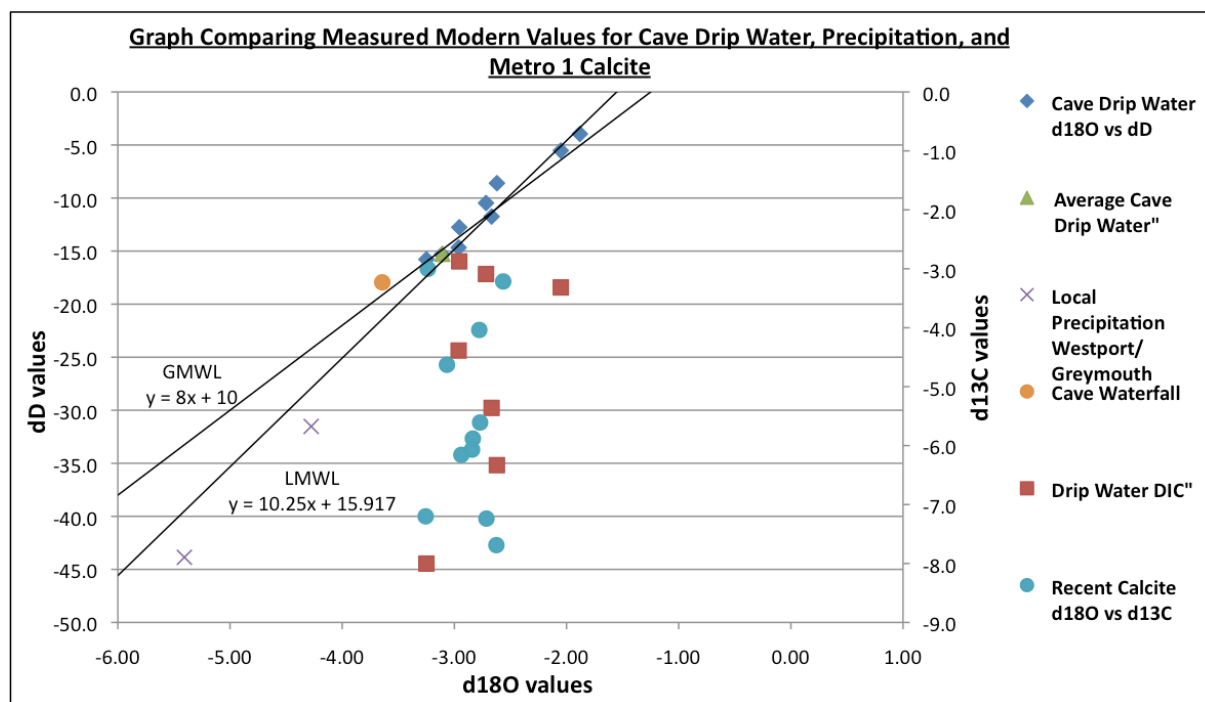


Figure 4.2: Plot of analysed stable isotope composition from Metro cave drip water, local rainwater and modern calcite. Precipitation values indicate the local meteoric water line. Global Meteoric Water Line is from Craig (1961). Recent calcite plotted on this graph is the raw data of the upper-most 10 points analysed.

#### 4.4 Trace Element Analysis

Trace element data from speleothems can also contribute information about environmental processes affecting stalagmites, and as such can be used to help in interpret changes in climate. Knowledge of the concentrations of U and Th in a stalagmite can also be used to pick the cleanest calcite for dating. Determining the age of the M1 stalagmite is an important part of establishing what kind of climate signals may have been preserved in the calcite. In order to establish which areas of the M1 stalagmite would be most suitable for uranium-thorium dating, trace element concentrations along the growth axis of the stalagmite were targeted. A one centimetre thick section was cut off the face matching the one drilled for stable isotopic analysis, and split into four for laser ablation trace element analysis and dating. The sections were polished using a wet rotary disc sander and 1200 grit grinding paper at NIWA in Auckland and digitally scanned in preparation for trace element analysis by Dr. Andrew Lorrey. They were then sent to the University of Melbourne, Australia, for laser ablation analysis which was done at a resolution of 27 $\mu$ m. The trace element data are courteously provided by Dr. Russell Drysdale. In addition to  $^{232}\text{Th}$  and  $^{238}\text{U}$ , other trace elements analysed were  $^{25}\text{Mg}$ ,  $^{57}\text{Fe}$ ,  $^{65}\text{Cu}$ ,  $^{66}\text{Zn}$ ,  $^{88}\text{Sr}$ ,  $^{89}\text{Y}$ ,  $^{138}\text{Ba}$ ,  $^{139}\text{La}$ , and  $^{208}\text{Pb}$  (Appendix 1). These have been graphed for the top and bottom sections of the M1 stalagmite (Figure 4.3a-d).

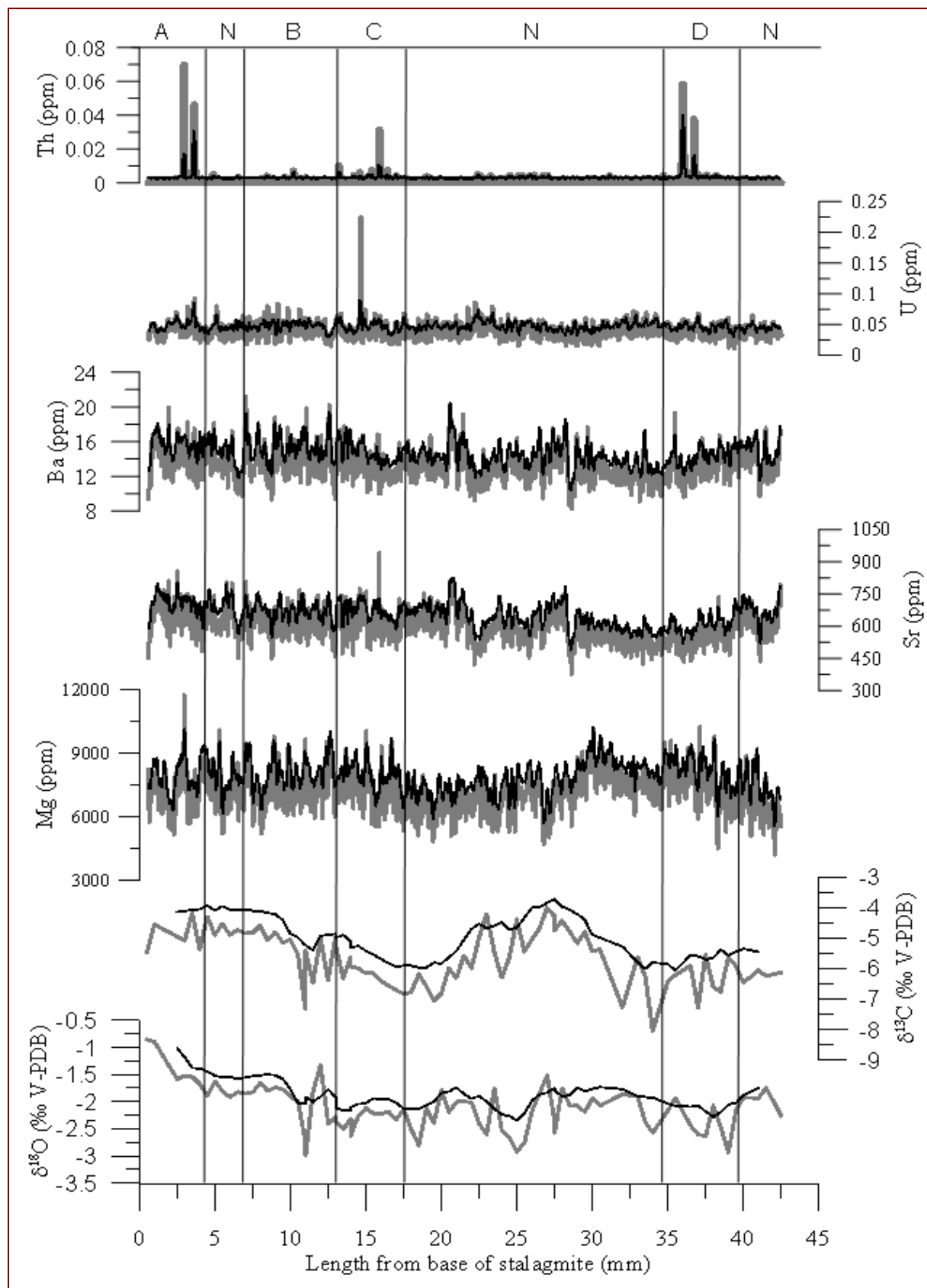


Figure 4.3a: Graphs of trace element and stable isotopic values up the length of the basal section. Light grey line is raw trace element concentration data, black line is the 5pt running mean of the raw data offset by +1 SD. Intervals are marked where there is significant departure of raw trace element concentrations above the offset 5pt running mean. Intervals are labelled A – D, with N representing “normal” intervals.

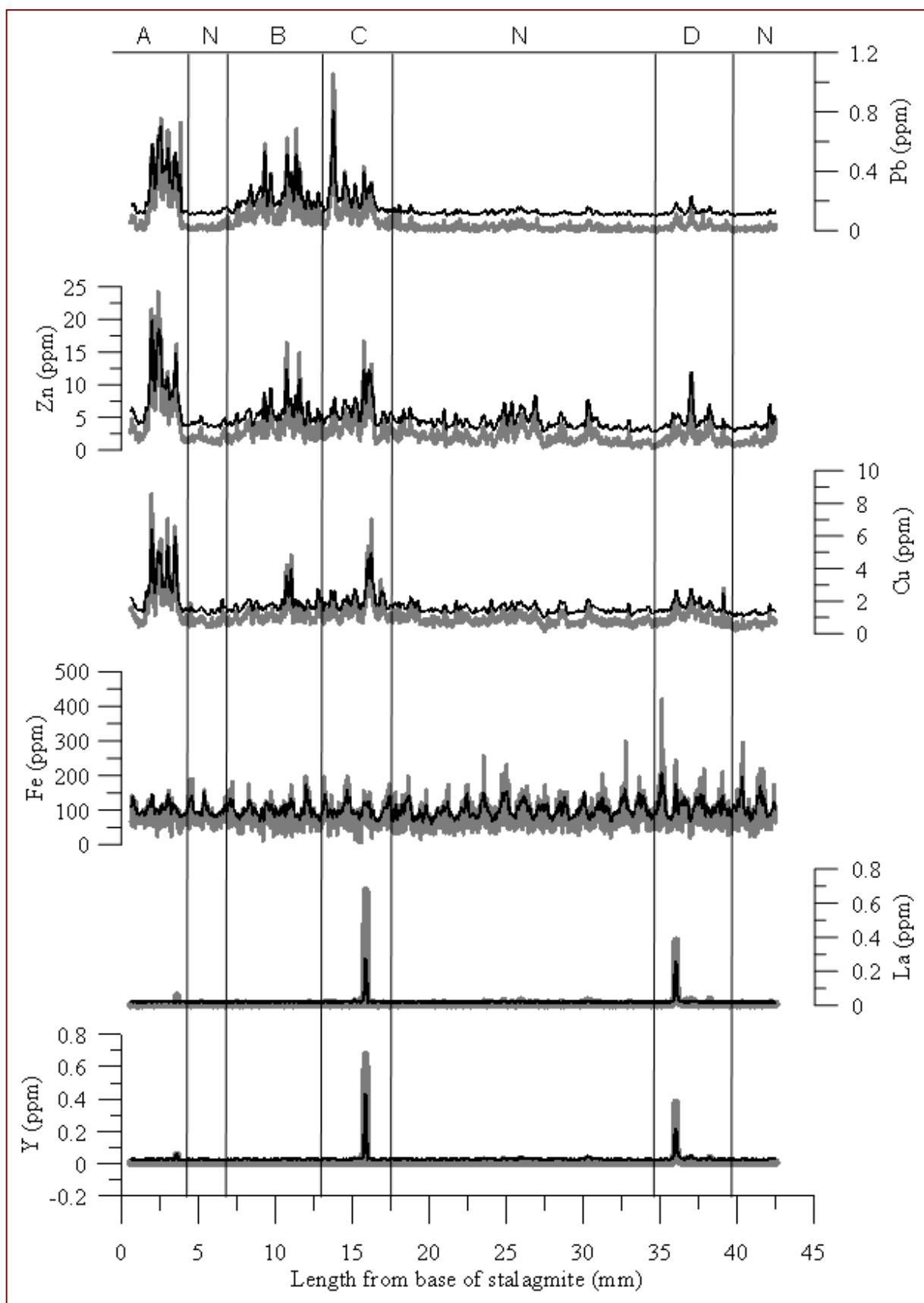


Figure 4.3b: Graphs of trace element concentrations up the length of the basal section. Light grey line is raw trace element concentration data, black line is the 5pt running mean of the raw data offset by +1 SD. Intervals are marked where there is significant departure of raw trace element concentrations above the offset 5pt running mean. Intervals are labelled A – D, with N representing “normal” intervals.

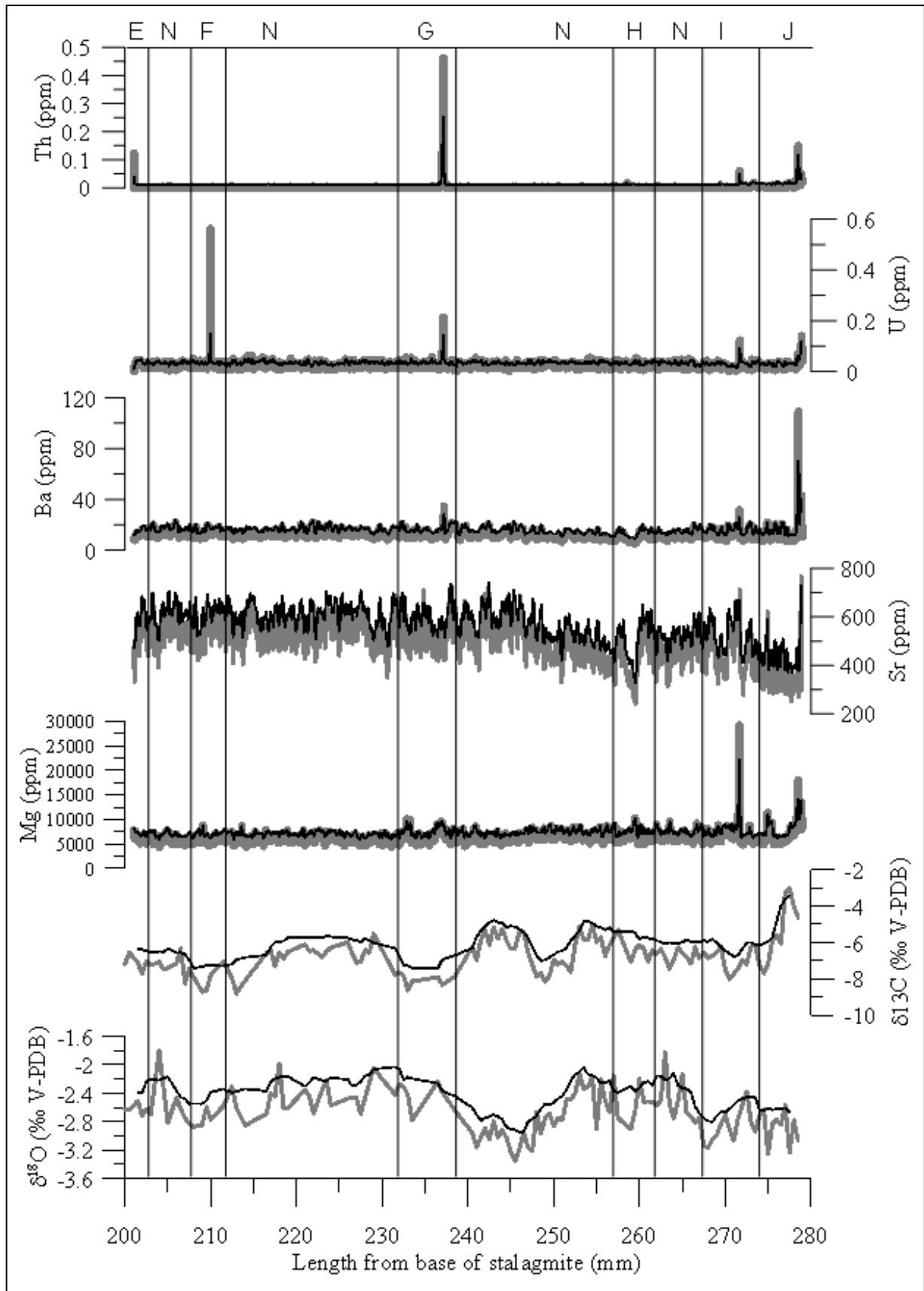


Figure 4.3c: Graphs of trace element and stable isotopic values up the length of the top section. Light grey line is raw trace element concentration data, black line is the 5pt running mean of the raw data offset by +1 SD. Intervals are marked where there is significant departure of raw trace element concentrations above the offset 5pt running mean. Intervals are labelled E – J, with N representing “normal” intervals.

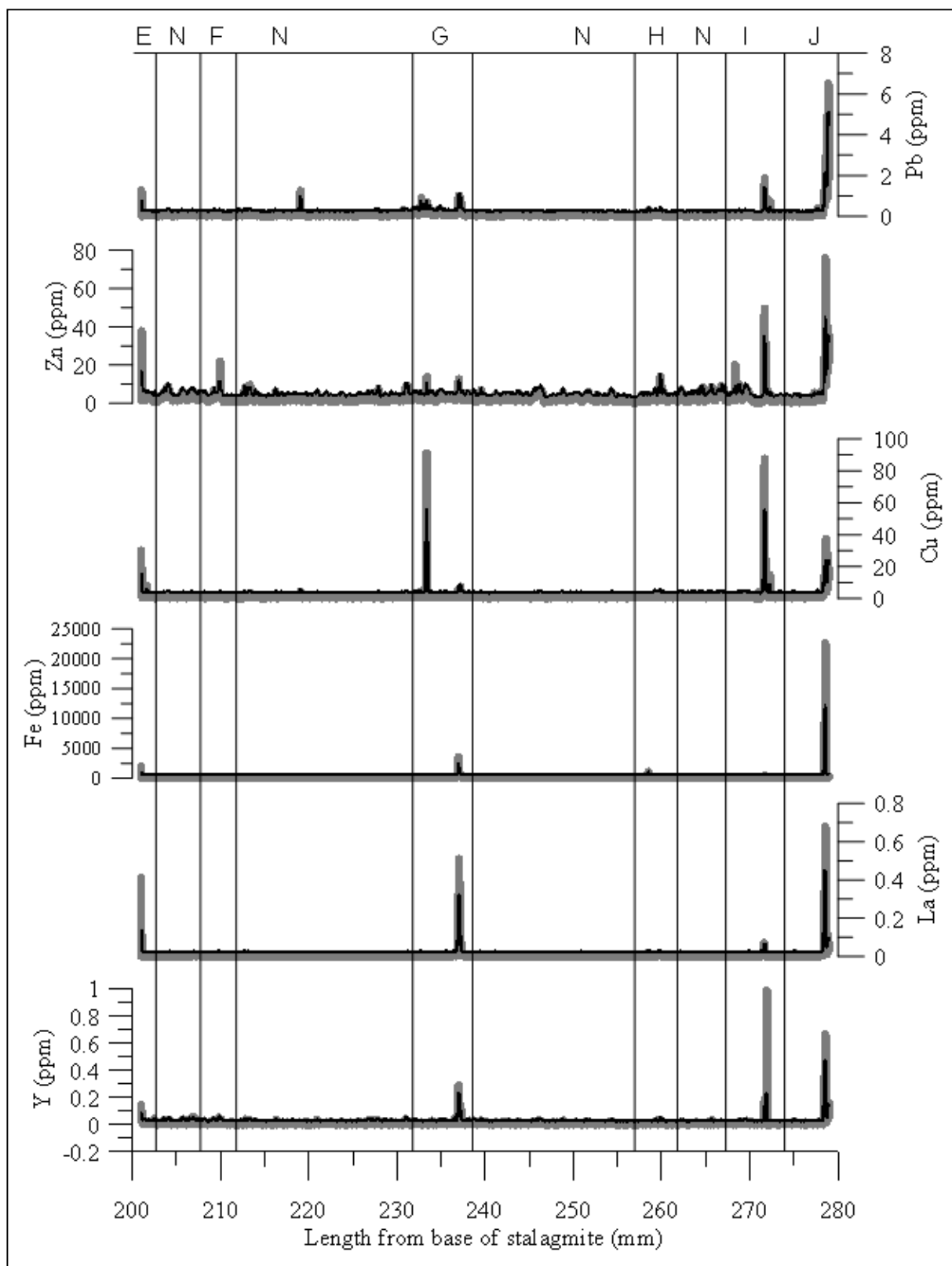


Figure 4.3d: Graphs of trace element concentrations up the length of the top section. Light grey line is raw trace element concentration data, black line is the 5pt running mean of the raw data offset by +1 SD. Intervals are marked where there is significant departure of raw trace element concentrations above the offset 5pt running mean. Intervals are labelled E – J, with N representing “normal” intervals.



The trace element concentrations up the base section show smaller, more regular fluctuations than the top section (Figure 4.3a-d). The top section has several much larger spikes in the concentration of some trace elements, with lower background levels. All the trace elements and the  $\delta^{13}\text{C}$  values of the calcite show a large enrichment at the tip of the stalagmite (Figure 4.3c-d).

The intervals of significant trace element enrichment were selected where raw values increase more than  $1\sigma$  from the 5-pt running mean. These intervals were looked at more closely to assist in interpretation of environmental processes and climate variation.

The Th concentrations from the trace element scans were also used to pin-point the parts of the M1 stalagmite most suitable for TIMS dating. Areas were marked with the lowest detrital Th concentrations, and preference was placed on those that would provide the most useful dates for an age model (Figure 4.4a-b). The increase in detrital Th at the tip of the stalagmite matches the increase seen in the other trace elements. The location of the intervals was marked against the figures below to determine if there was a pattern of trace element enrichment and layer colour, as the colour and thickness of the stalagmite layers are directly related to changes in hydrological balance in the cave (Figure 4.4a-b). It can be seen that intervals C, E, G, I, and J occur where there are white bands of calcite, and intervals A, B, D, F, and H generally occur where there are darker bands of calcite.

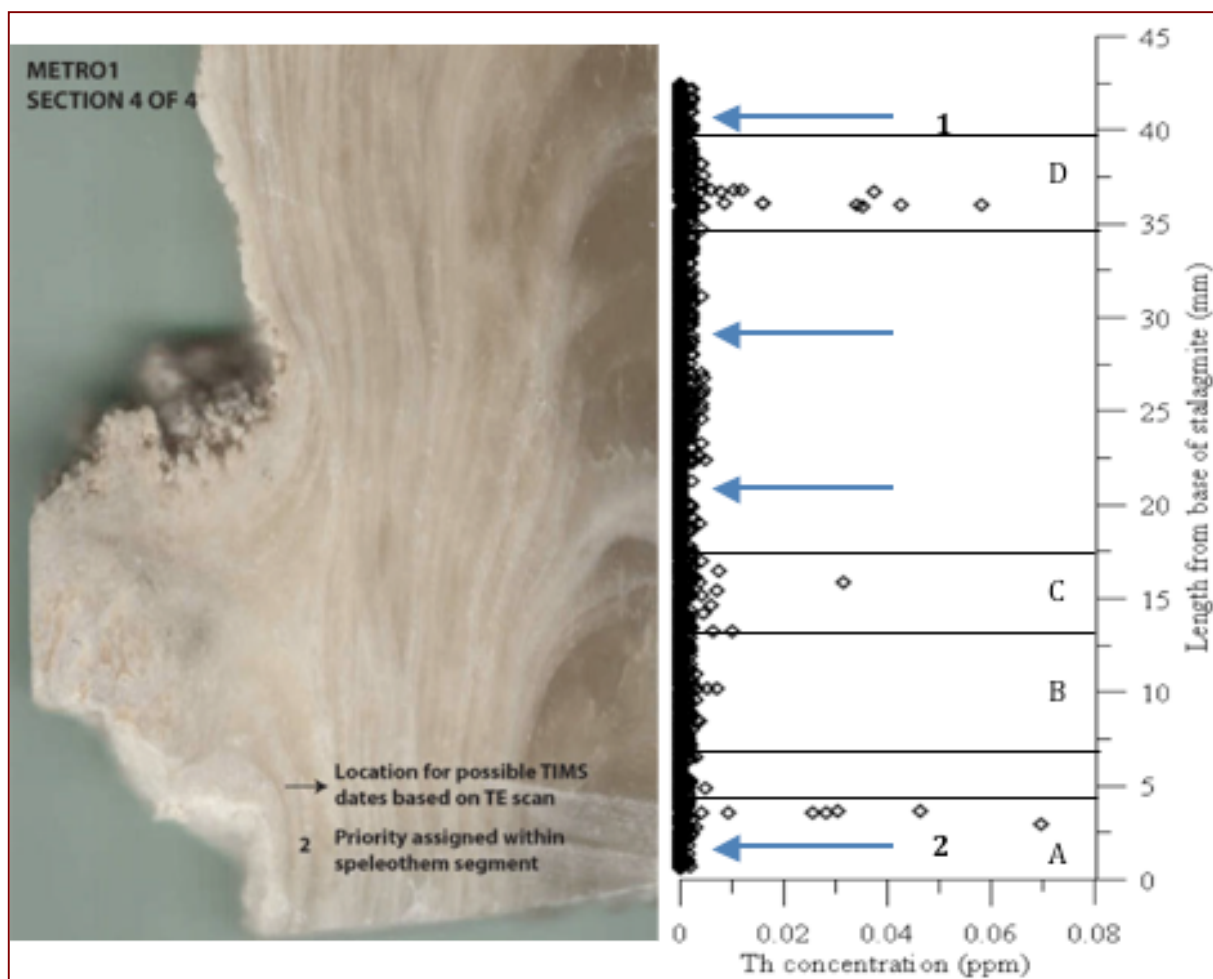


Figure 4.4a: The base section of the M1 stalagmite analysed for trace element concentration and for dating. The insert to the side shows the detrital Th concentration and the areas picked for dating. Points 1 and 2 are preferred sites for dates. The intervals of above normal trace element concentration from figures 4.3a-d are also plotted. Figure provided by Dr. Andrew Lorrey, NIWA.

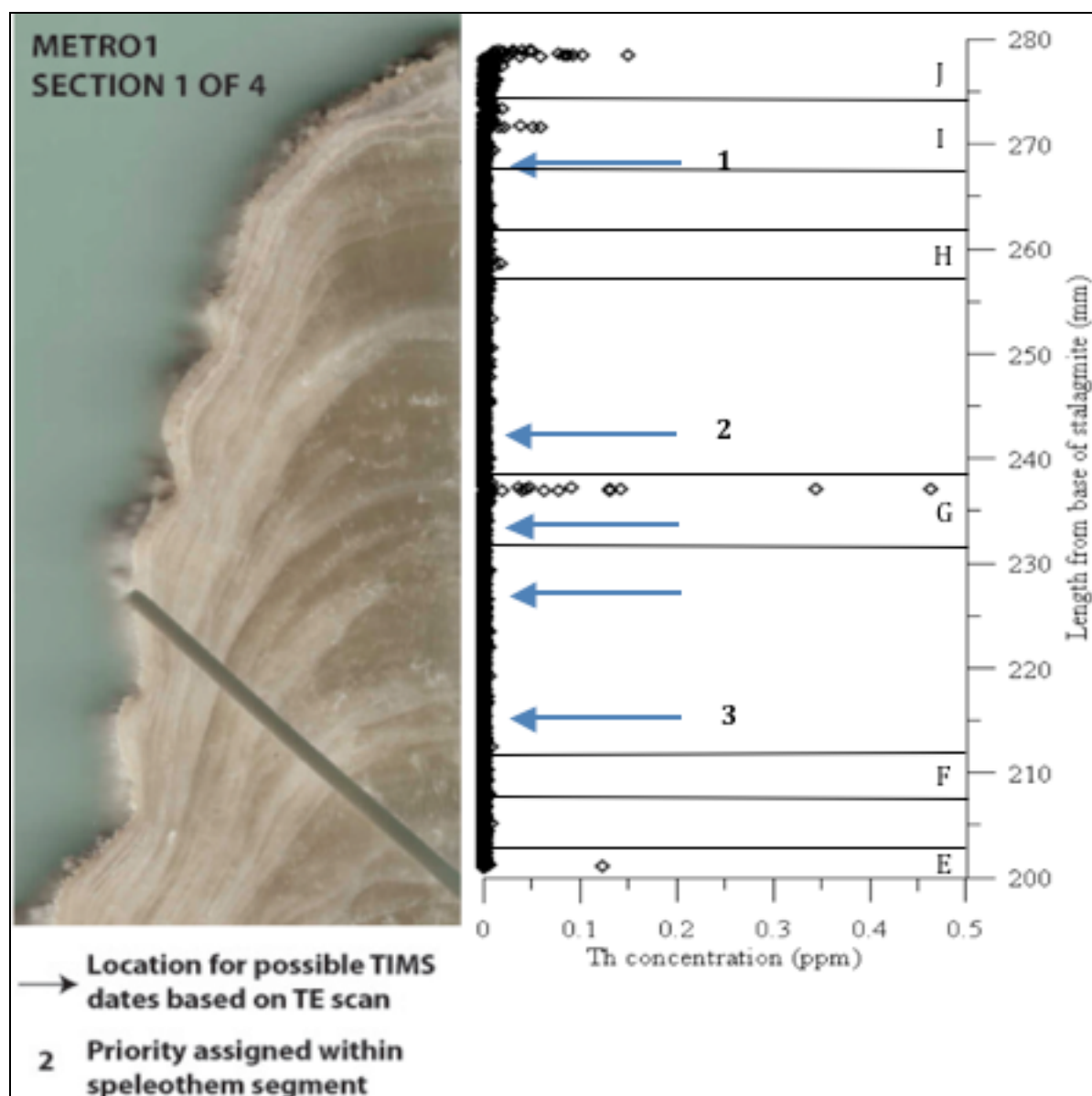


Figure 4.4b: The top section of the M1 stalagmite analysed for trace element concentration and for dating. The inserted graph shows the detrital Th concentration for the section, and the areas picked for dating. Points 1, 2 and 3 are preferred sites for dates. The intervals of above normal trace element concentration from figures 4.3a-d are also plotted. Figure provided by Dr. Andrew Lorrey, NIWA.

#### 4.5 Stable Isotopic Analysis of calcite

To develop a continuous high-resolution record of paleoclimate from the M1 stalagmite, calcite samples were drilled up the length of the growth axis (Figure 4.5). A resolution of 0.5mm was achieved using a hand-held Dremel drill with a 0.4mm carbide tip. Alternate samples were staggered to ensure continuous sampling of the calcite along the growth axis (Figure 4.5). This approach to sampling meant just over 550 samples were drilled. The calcite samples were analysed for stable carbon and oxygen isotopic composition in the University of

Canterbury Stable Isotope lab using a Thermo-Finnigan Gas Bench with a Thermo-Finnigan Delta V continuous-flow mass spectrometer. CO<sub>2</sub> was liberated from each sample by acidification using 100% phosphoric acid in a He atmosphere through a Thermo-Finnigan Gas Bench heated at 70°C (data included in Appendix 2). Precision (1 $\sigma$ ) of  $\delta^{18}\text{O}$  and  $\delta^{13}\text{C}$  values was better than  $\pm 0.1\text{‰}$ .



Figure 4.5: High-resolution scan of Metro 1 stalagmite showing the placement of all the drill holes for stable isotopic analysis of the calcite.

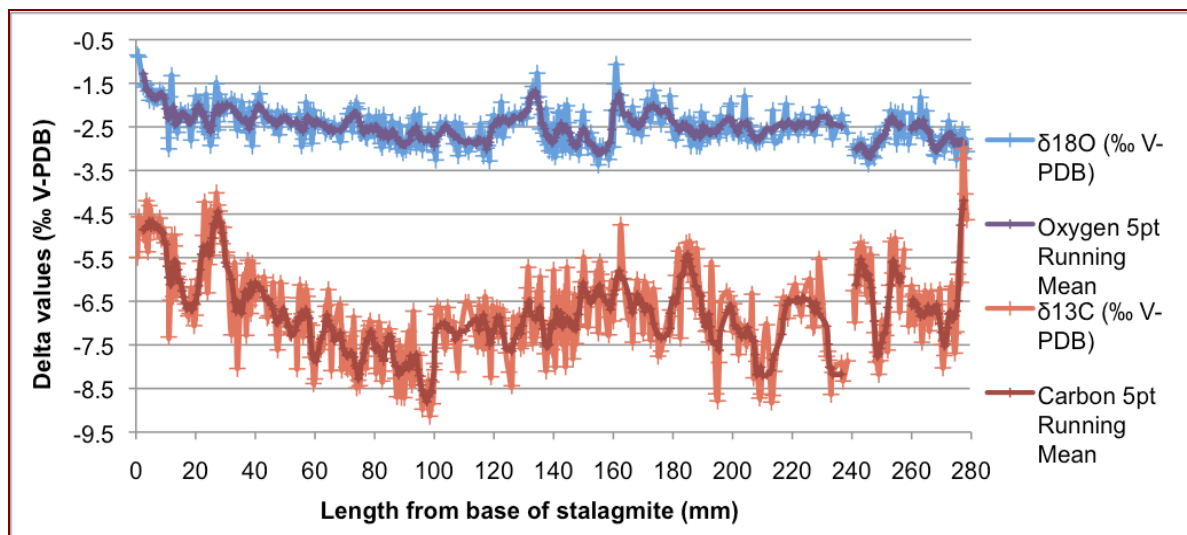


Figure 4.6: 557 data points of  $\delta^{18}\text{O}$  and  $\delta^{13}\text{C}$  values up the growth axis of the M1 stalagmite. Black lines indicate positions where Y concentrations increase (from left to right, in intervals C, D, E, G, and I).

The stable oxygen and carbon isotopic data show considerable variation over the growth of the M1 stalagmite, and there is a weak-moderate degree of correlation between them ( $r = 0.350$ ). The raw oxygen isotope values range from  $-0.85\text{‰}$  to  $-3.92\text{‰}$ , while raw carbon values range from  $-3.0\text{‰}$  to  $-9.14\text{‰}$ . Both stable isotopes show continuous small-scale oscillations, as well as some larger shifts. Most of the significant shifts in the oxygen and carbon records occur separately of each other, however, at 162mm up the stalagmite there is synchronous positive shift of close to  $2\text{‰}$  in the raw oxygen and  $2.5\text{‰}$  in the raw carbon. The  $\delta^{18}\text{O}$  values also show a positive increase at 135mm, and a negative shift at 250mm. The  $\delta^{13}\text{C}$

values are much more variable, however, significant positive and negative fluctuations occur both at the base of the M1 stalagmite within a negative trend, broken at 100mm by a shift to more positive values and a positive trend to 185mm, then large positive and negative fluctuations to the tip where the values rise to their highest in the stalagmite.

## **4.6 Fluid Inclusion Extraction Method**

### **4.6.1 Introduction**

When using stalagmites as a proxy of paleoclimate and past temperature it is essential to have an estimation of how the isotopic composition of the cave drip water has changed through time. In some cases this has been inferred from the composition of the modern water, with either some adjustment for past changes or a simple assumption that the composition has not changed (Williams et al. 2004). However, fossil cave drip water remains trapped in speleothems as fluid inclusions, so successful extraction and analysis of these would allow more accurate reconstructions of past climate. The two methods currently in use for extracting speleothem fluid inclusions both have advantages and disadvantages. In both, the minimum sample size of calcite is large (>300mg) and not easily comparable to the resolution achieved in the analysis of speleothem calcite (Vonhof et al. 2006; Verheyden et al. 2008).

Furthermore, there may be some isotopic fractionation associated with either incomplete extraction of water from the sample through crushing, or through isotopic exchange with CO<sub>2</sub> and/or anhydrous lime (CaO), which are by-products of high-temperature decrepitation (Vonhof et al. 2006; Verheyden et al. 2008). Given these drawbacks with current methods we have attempted to develop a new method to extract fluid inclusions that uses significantly smaller sample sizes, can be run reasonably efficiently, and that accurately analyses fluid inclusion  $\delta^{18}\text{O}$  and  $\delta\text{D}$  values.

The exploration of a new method to extract fluid inclusions from speleothems has occurred in progressive stages for this project. The two overall aims for this method were to reduce the sample size and the run time for speleothem calcite samples, and to produce consistent results with a good degree of reproducibility. These aims required a decrepitation chamber, but one that could be operated at temperatures that did not cause calcite to decompose. This would remove the possibility of oxygen isotopic fractionation through reactions with CaO (Sharp

1992). Removal of water from the samples by heating also presents the most effective way to extract all the water from small samples (Verheyden et al. 2008).

To test the precision and accuracy of the set-up, a series of analyses on liquid water of a known volume and isotopic composition were conducted to assess the water yield and quality of the data.

#### 4.6.2 Development Phase 1

The apparatus set-up initially designed for fluid inclusion extraction consisted of a tube furnace and a cold trap connecting a continuous flow of ultra-pure helium to a high-temperature thermal combustion elemental analyser (TC-EA) via a six-way Valco switching valve (Figure 4.7-A). The valve on top of the tube furnace could be changed to a septum to allow a direct injection of liquid water.

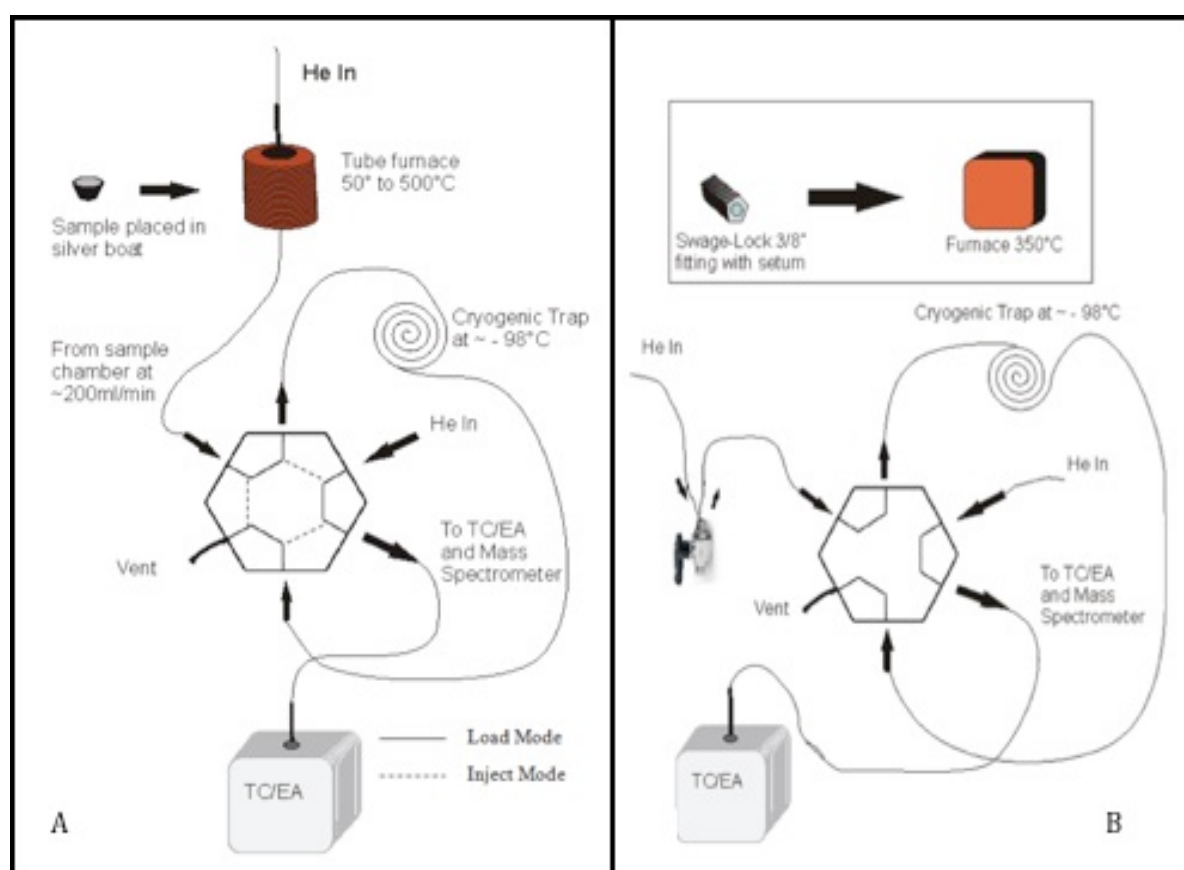


Figure 4.7: A – sketch of the first set-up for fluid inclusion extraction. B – sketch of the second set-up for fluid inclusion extraction.

A calcite sample could be placed in a ceramic tube, inside the tube furnace and heated incrementally to  $>500^{\circ}\text{C}$  under continuous ultra-high purity helium flow conditions (flow rate  $>150\text{ml/min}$ ) in order to liberate water trapped within the carbonate crystals. The tube furnace was first held at  $50^{\circ}\text{C}$  for  $\sim 1$  hour to bake out the sample and remove any atmospheric water. After incremental heating the tube furnace was held at  $500^{\circ}\text{C}$  for an hour. During heating, water was cryogenically focused onto a  $\sim 1\text{m}$  long  $1/16''$  (o.d.) stainless steel cold trap (dry ice + ethanol;  $-72^{\circ}\text{C}$ ) plumbed into a Valco six-way switching valve. This trapped the water liberated from the sample, and any  $\text{CO}_2$  was vented to the room. To introduce the trapped water to the TC-EA, the Valco valve was switched from “load” to “inject” mode, the cold trap was dropped and the stainless steel coils flash-heated to rapidly thaw the sample for standard continuous-flow pyrolysis isotope ratio determination (flow rate  $=100\text{ ml/min.}$ ; reactor  $=1450^{\circ}\text{C}$ ; GC  $=40^{\circ}\text{C}$ ) (Sharp et al. 2001).

With this configuration line blanks were run to check for leaks and any water inherent in the system. Only very low background levels of water ( $>20\text{mV}$ ) were found when cryo-trapping for 10 minutes. The background water was inferred to be from 0.001% impurities in the helium carrier flow. This was followed by direct injections of liquid water IAEA standards (GISP, SMOW and SLAP). The results from these tests show values for the different standards were both accurate and precise, although there were some skewed hydrogen peaks, most likely due to minor delays in the thawing and release of water from the cold trap (Figure 4.8). Yield curves were also established using the three IAEA standards, which showed a very strong correlation between water yield and sample size, suggesting water was not adsorbing to surfaces anywhere in the set-up (Figure 4.9). These yield curves also suggested that a minimum of 200 to 300 nanolitres of water was required to give a good signal.

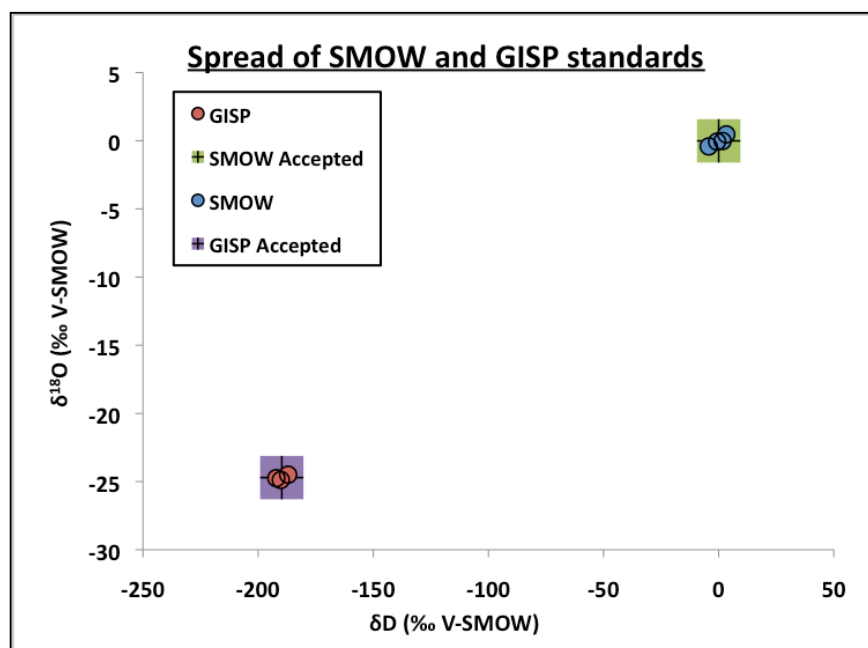


Figure 4.8: Samples of SMOW and GISP standard water analysed through the set-up for Method 1. All samples analysed fall within the accepted variability for the standard.

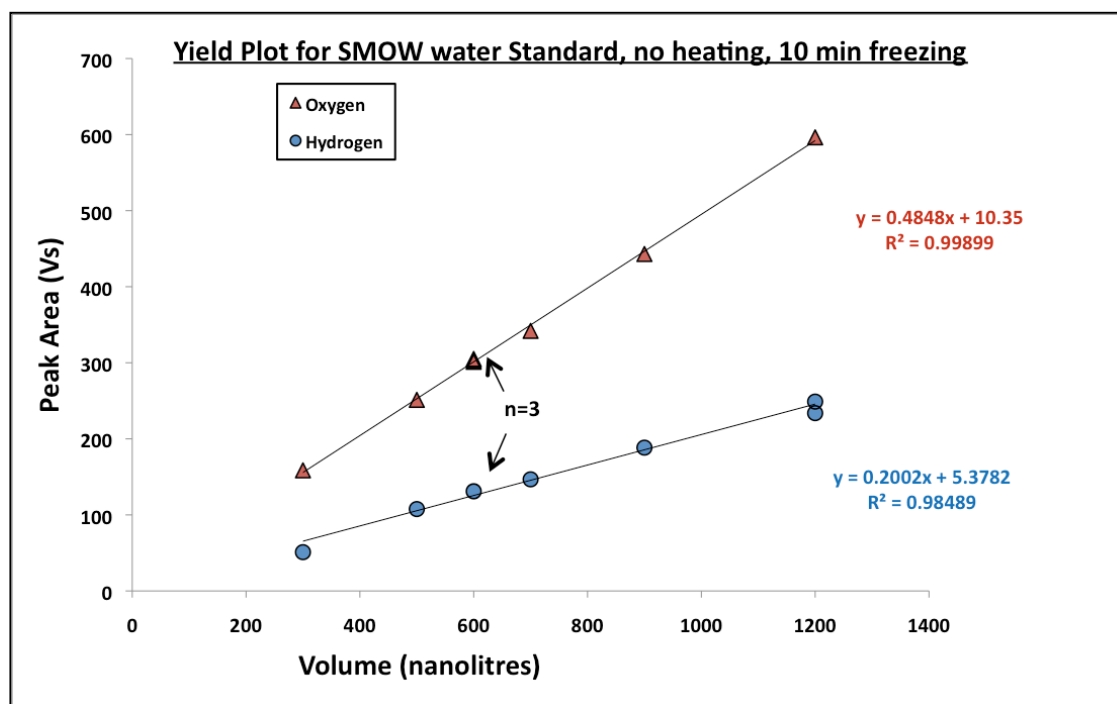


Figure 4.9: Yield plot produced using Method 1. Aliquots of SMOW standard water were analysed through the method described above, with increasing samples of water added.



Calcite samples were introduced from an undated Waitomo speleothem, and recorded water yields of about 300 nanolitres from 20 mg chunks of calcite and about 40 mg of powdered calcite. These samples were decrepitated at 500°C and multiple injections were made from the cold trap to the TC-EA over several hours. After 2 hours of decrepitation the temperature was raised to 1000°C to fully extract all the water possible out of the sample, and small water peaks persisted after 4.5 hours of decrepitation. In addition, the stable oxygen and hydrogen isotopic composition of these runs showed considerable variation, and only produced an average value near the local mean water line when all the water had been extracted (Figure 4.10).

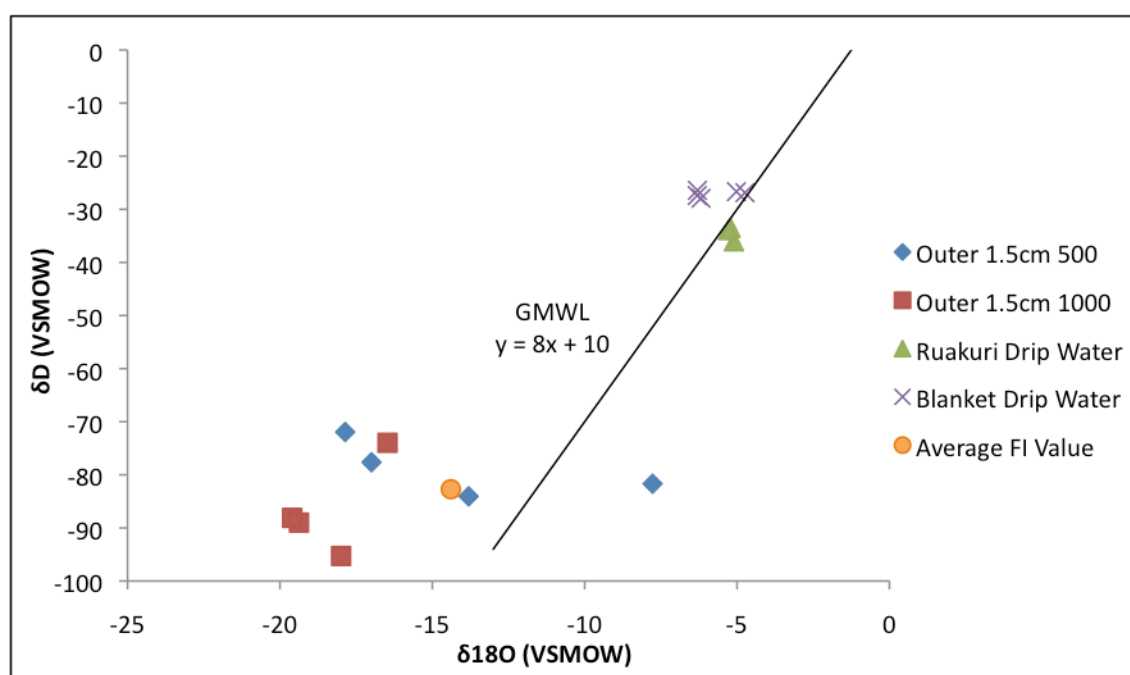


Figure 4.10: Plot of fluid inclusion data from one calcite sample from the Waitomo stalagmite. The fluid inclusion data from periodic cold trap injections are blue and red points (data provided by Kurt Joy, UC). The orange point is the average isotopic composition of all the water extracted from the sample over the total decrepitation time (about 4 hours). The global mean water line is plotted as a comparison to the Waitomo data.

Some of the large variability in our initial data is suspected to have been due to the production of lime, which starts to occur around 600°C, and also by the release of significant amounts of CO<sub>2</sub> which occurs above 400°C (Dennis et al. 2001; Rodriguez-Navarro et al. 2009). Also there can be fractionation of oxygen isotopes between CO<sub>2</sub> and the released water, which at higher temperatures can have an effect on the isotopic composition over enough time (Sharp 1992; Lecuyer & O'Neil 1994).

These tests confirmed the need to decrepitate at lower temperatures and suggested the processing set up in this study had the capability of producing accurate data from sample sizes about 10 times smaller than those previously reported in the literature. However, for this method to be usefully applied to cave speleothems a method of greatly reducing the run time per sample was needed.

#### **4.6.3 Development Phase 2**

The second method expanded on previous tests, with the aims of reducing the run time per sample and to produce consistent results. The results of the calcite chips trialled in Method One suggested that at least 5 – 6 hours of low-temperature decrepitation was required to release all the water from ~20 mg sample sizes. In order to provide this time it was decided to switch to a system where individual samples could be placed in a sample-chamber, dried, and sealed with a He atmosphere. The sample chamber could then be detached and placed in an oven off-line to decrepitate overnight. This way several samples could be prepared, left to decrepitate, and then run consecutively.

The new set-up consisted of a detachable sample chamber made of a Swage-lock ball-valve with a stainless steel fitting and end cap (Figure 4.7-B). The end cap is large enough to take calcite chips up to ~50 mg in size and when sealed, is leak tight. The chamber can be flushed with He using a two-way needle, which later can be used as the sampling needle. The sample chamber can be easily heated to 300°C – 400°C, and left at these temperatures for at least 12 hours.

After decrepitation individual sample chambers can be re-attached to a continuous flow of He through fittings containing a heat-resistant septum. Any gas in the sample chamber is pushed out using the two-way sampling needle via a continuous flow of ultra-pure He and through to a cold trap consisting of a ~1m long 1/16" (o.d.) stainless steel coils immersed in a dry ice + ethanol slushy (-72°C). The cold trap is plumbed into the Valco six-way switching valve, and from there the water can be introduced to the TC-EA and mass spectrometer by switching the Valco-valve and flash heating the cold trap.

Testing showed this set-up was leak-tight with only low background levels (>20mV) from slight impurities in the He carrier (0.001%), and had a high-sensitivity to water. The time to

run a 30 mg calcite chip after decrepitation overnight took about 15 minutes. A draw-back to this set-up was that liquid water samples could not be injected into the sample chamber, as the needle could not pass through the Swage-lock ball-valve. Consequently, the tests for yield and accuracy of water standards could not be carried out. However, two calcite chips from the younger, upper part of the Metro 1 stalagmite were analysed and compared to the stable isotopic composition of the same calcite layers, and to the measured drip water from the cave. Once decrepitation had been carried out overnight, the run time of the sample when it was reconnected to the continuous-flow system was 15 minutes. Even though the volume of water extracted from the sample was close to the expected, the fluid inclusion results were found to be very isotopically different from the calcite and the cave drip water, suggesting some isotopic fractionation was taking place during extraction (Figure 4.11). Peak heights recorded by the mass spectrometer suggested all the water was being extracted, however, there may have been issues with the temperature of the cold trap, or with the extraction of the sample gas through the two-way needle.

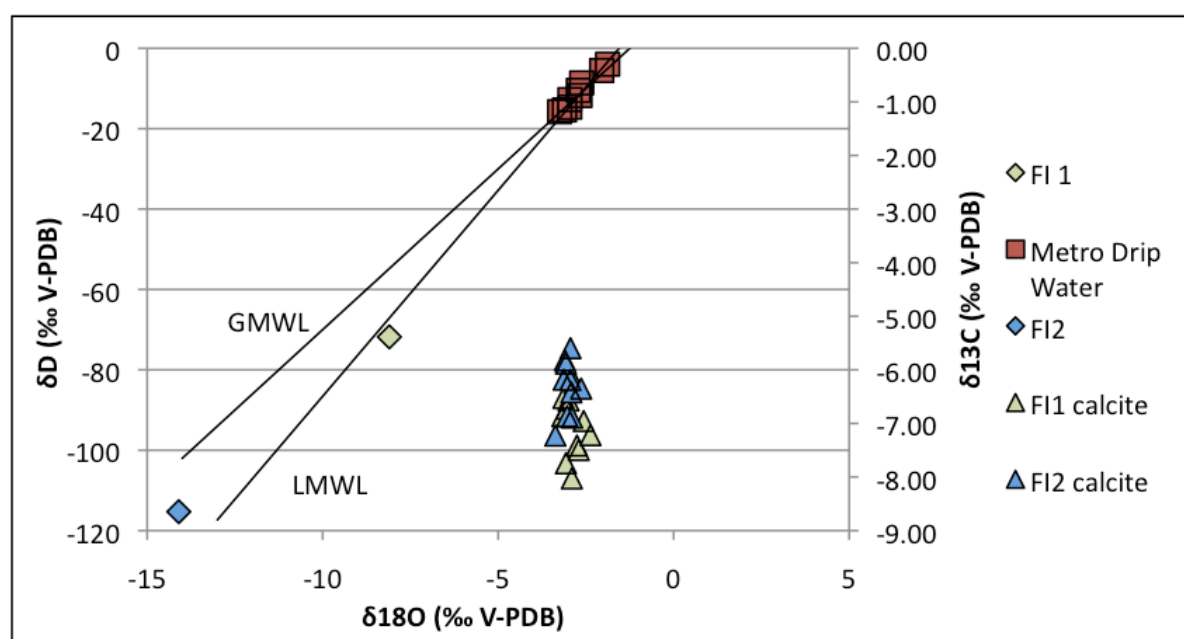


Figure 4.11: Fluid inclusion data ( $\delta D$  and  $\delta^{18}O$ ) from two 30mg calcite chips taken 270mm (F1) and 155mm (F2) from the base of the M1 stalagmite. The 10 points of calcite isotope data ( $\delta^{18}O$  and  $\delta^{13}C$ ) around these locations are also graphed, as are the modern cave drip water  $\delta^{18}O$  and  $\delta D$  for comparison. The GMWL and the LMWL from figure 4.2 are also shown.

#### 4.6.4 Summary

The exploration of a new method for extracting fluid inclusions from speleothem calcite has shown that a significant amount of testing is still required. The first set-up showed that injected liquid water samples could be fully recovered from the system, and accurately analysed for both hydrogen and oxygen stable isotopic composition. However, the release of water from decrepitated calcite chips is not straightforward, and contributes to inaccurate results from samples in the tests conducted so far. The future steps to be taken in the development of this method will be to alter the equipment to allow the injection and analysis of liquid water samples in a detachable sample chamber. Following a similar method to the second version, the samples could be sealed in a He atmosphere and left to decrepitate overnight at temperatures around 300°C and then reconnected to the on-line system. Ideally, the sample chamber could also be used as the cold trap, to reduce the possibility of isotopic fractionation occurring through a sampling needle. A variation could be to have two cold traps, one at liquid nitrogen temperatures and one ethanol-dry ice temperature, to ensure all water is frozen and passed through to the TC-EA. However, due to delays caused by the earthquakes in Canterbury during 2010 and 2011 these experiments will likely take place outside the time-frame of this thesis.

# Chapter 5 – Age Model for the M1 Stalagmite

## 5.1 Introduction

The development of an age model for the M1 stalagmite enables interpretation of possible climate history for the central West Coast, South Island. Radiometric dating facilitates determination of the rates of calcite precipitation over time. The growth rate of the stalagmite determines the temporal resolution of the climate change events possibly recorded by the carbonate chemistry (Baker et al. 1998). Because the growth rate is linked to the rate of drip water flow, changes in growth rate can also assist in identifying changes in karst hydrology (Baker et al. 1998; Genty et al. 2001).

Samples of the M1 stalagmite were sent to labs at both the University of Queensland, Australia, and Stanford University, California, USA, for radiometric dating. However, due to unforeseen circumstances, and measured low concentrations of radiogenic U and Th in the M1 calcite, sample analyses have been delayed for more than 6 months and dates are unavailable at the time of thesis submission. Once these dates become available the age model for the M1 stalagmite, presented below, will be refined and presented in a forthcoming manuscript.

## 5.2 Experimental Age Estimate

In the absence of radiometric dates, it is desirable to have a rough estimate of the age range over which the M1 stalagmite grew. As the stalagmite was still active at the time of collection, it is reasonable to assume the upper layers of calcite were deposited in the recent past. It may also be possible to gain a rough estimate of the growth rate of the M1 stalagmite by assessing the growth rates of other stalagmites collected in the region. It is likely that caves within the same rock units, in the same climate, and environmental conditions, will produce similar average stalagmite growth rates, although the variation about the average may be high due to the complex hydrology of caves and the heterogeneity of drip water flow paths.

Fortuitously, considerable work by Dr. Andrew Lorrey has involved age model construction for speleothems from caves in Punakaiki, West Coast, South Island. Punakaiki is only 30km

south of Metro cave, and the same rock units in which Metro cave has formed are found there. Like Metro cave, the caves around Punakaiki are within 10km of the coast, are surrounded by the same native New Zealand forest, and experience the same climatic conditions.

Consequently, the growth conditions of stalagmites in these caves is likely to be very similar to those in Metro cave. Given these assumptions the average growth rate of Punakaiki stalagmites was used to model the approximate growth rate for the M1 stalagmite. This is the best case scenario at the time of thesis submission.

Dr. Andrew Lorrey (co-supervisor to this thesis) kindly provided the average growth rate of six stalagmites in Punakaiki caves, based on the ages and growth models of a number of stalagmites. The deposition rate of each stalagmite was normalised relative to its length, to enable stalagmites with different growth rates and age ranges to be compared. The average growth rate of all the stalagmites (83 years per 1mm calcite) was then applied to the continuous stable isotope record from the M1 stalagmite to calculate the approximate age of each point (Figures 5.1-5.2).

M1 calcite  $\delta^{18}\text{O}$  values have been adjusted for ice volume following the record of global sea level change presented in the ICE-5G (VM2) model of global isostatic change following the LGM glaciation (Figure 5.1). This correction allows for changes in ocean stable isotope composition during the LGM and the late glacial/interglacial transition to be removed from the record (Figure 5.1) (Peltier 2004). The record has also been normalised to the Late-Holocene (4Ka) modern climate, to allow any departures from this in the recent part of the stalagmite record to be identified (Lorrey et al. 2008). The recently published stable isotope

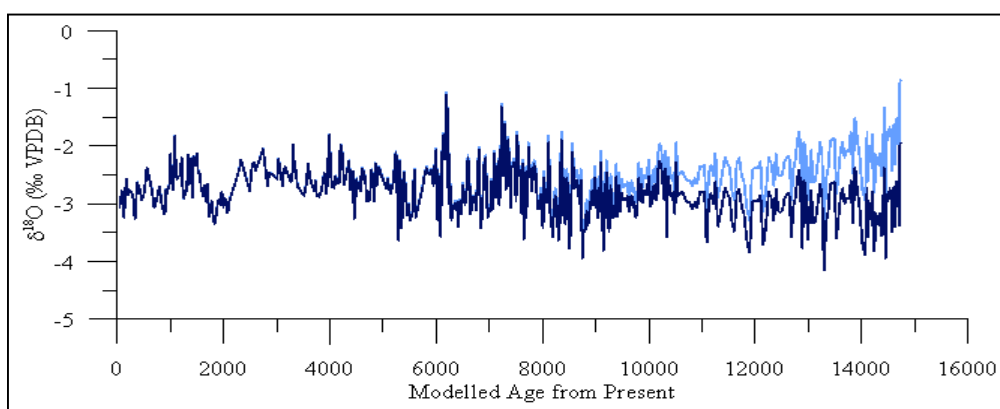


Figure 5.1: Plot of ice volume corrected (dark blue) M1 calcite  $\delta^{18}\text{O}$  values with uncorrected (light blue)  $\delta^{18}\text{O}$  values (Peltier 2004).

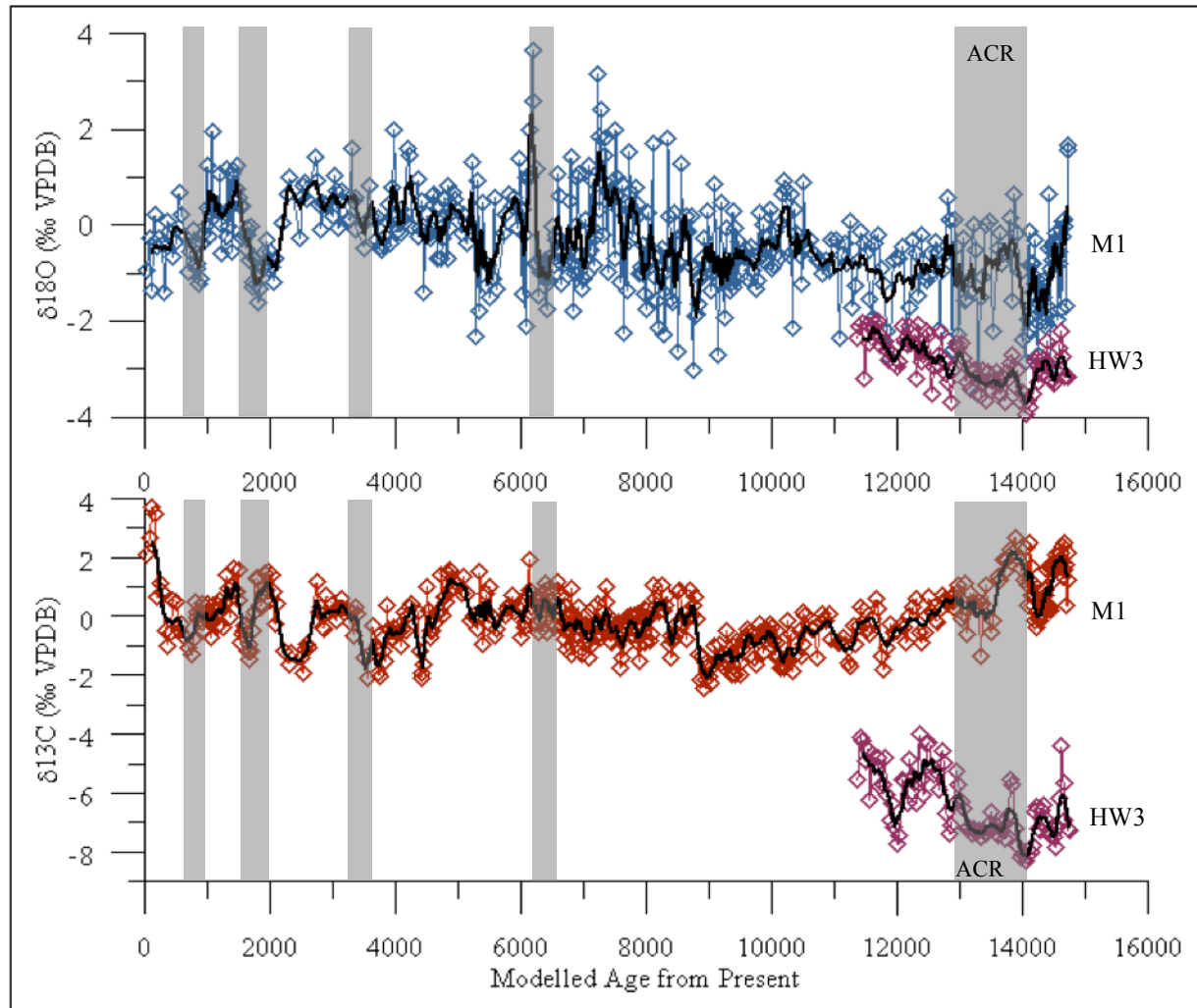


Figure 5.2: Experimental age model for the M1 stalagmite, based on the growth rates of stalagmites in Punakaiki caves 30km south of Metro cave. M1 Stable isotope record is normalised to the Late Holocene (4 Ka), and ice volume corrected following adjustments made according to the global ICE-5G (VM2) model (Peltier 2004). Holocene HW3 stable carbon and oxygen data were kindly provided by Dr. Tom Whittaker, and the age data from this stalagmite were not used in the average growth rate model to enable comparison with an independent time series (Whittaker et al. 2011). Grey bars mark cold periods in the Southern Alps identified through cosmogenic and  $^{10}\text{Be}$  dating (Schaefer et al. 2009; Kaplan et al. 2010; Putnam et al. 2010).

data from a Punakaiki stalagmite have been plotted for comparison to the M1 stable isotope data (Figure 5.2) (Whittaker et al. 2011).

Several recently published studies have helped to define periods of cooler climate in the South Island using cosmogenic and  $^{10}\text{Be}$  dating techniques (Schaefer et al. 2009; Kaplan et al. 2010; Putnam et al. 2010). Of note in the M1 stable isotope data are the links between also correspond with negative carbon peaks (Figure 5.2). The timing of negative peaks in both the HW3  $\delta^{18}\text{O}$  values and the M1  $\delta^{18}\text{O}$  values (as far as they overlap) is reasonably close (based on visual inspection), supporting the idea that the average growth rate of Punakaiki

stalagmites can be used for an experimental growth model for the M1 stalagmite (Figure 5.2). The general consistency of the negative stable isotope peaks with cold periods in the Southern Alps suggest the experimental age model may be a fairly good approximation of the age of the M1 stalagmite, although, as expected, the line-up is not exact in some places (Figure 5.2). A more conclusive analysis must remain pending radiometric age determination on M1.

The basal age of the M1 stalagmite potentially allows some additional insights into cave breakdown processes. The M1 stalagmite was growing on the rubble from a cave collapse, so theoretically the basal age of the stalagmite should give the minimum age for the collapse event. As the basal age of the M1 stalagmite is likely to be close to 14 Ka, this indicates the collapse event forming the rubble in Eureka Hall in Metro cave happened prior to this. However, because the processes of cave collapse are ongoing and are not necessarily linked to seismic events, the collapse in Eureka Hall could have occurred at any time after the formation of the chamber but before 14 Ka. Given the through flowing hydrology of the Metro cave system, it will be difficult to confidently ascribe the timing of cave collapse to paleoseismic events rather than cave instability associated with carbonate dissolution by surface waters.



# Chapter 6: Interpretation and Discussion

## 6.1 Introduction

Interpretation of the geochemical signals recorded by speleothems can be carried out in many different ways. Studies from many locations around the world have shown that processes in the local area exert a strong control on the preservation of climate information in a stalagmite. Two stalagmites from different locations may show similar signals, but may be influenced by spatial or temporal dependent processes in different ways, leading to distinct interpretations of past climate change (Mattey et al. 2010). Stable oxygen isotopes, with or without stable carbon isotopes, have been used as paleo-temperature proxies, while carbon isotopes have also been used to infer past vegetation changes and further linked to periodic wet/dry changes in precipitation (McDermott 2004; Williams et al. 2005; Lachniet 2009; Whittaker et al. 2011). Changes in trace element concentration have also been linked to temperature change, and elemental ratios of trace elements have been used to infer changes in processes such as prior calcite precipitation, changing partial pressure of CO<sub>2</sub> (pCO<sub>2</sub>) in cave air, and changing water sources (Borsato et al. 2007; Cruz et al. 2007; Fairchild & Treble 2009). In light of the many variables affecting stalagmite geochemistry it is beneficial to gain an understanding of the local environment around the cave, and to use as many different proxies as possible when using a single stalagmite for paleoclimate interpretations. Ultimately, the most robust interpretations will result from compilations, or stacks, of multiple high-quality speleothem proxy records.

This thesis combines the use of modern cave “environment” data with high-resolution stalagmite trace element and stable carbon and oxygen isotopic composition data to investigate intervals of change in the M1 stalagmite.

## 6.2 Interpreting Stable Isotopic Composition

### 6.2.1 Stable Oxygen Isotopes

A variety of environmental processes and conditions influence the stable isotopic composition of stalagmites. Processes outside the cave, including biological, pedospheric, and climatic/weather, cause fractionation of isotopes in the water before it percolates underground. Inside the cave several more processes further alter the isotopic composition of the water prior to carbonate formation. The processes influencing the stable oxygen isotope composition of a stalagmite can be summarised into three effects – the cave temperature effect, the precipitation effect, and the ocean source/ice volume effect.

The cave temperature effect describes the temperature related fractionation of oxygen isotopes that occurs when calcite is precipitated in a cave (McDermott 2004; Lachniet 2009). When this occurs under conditions of isotopic equilibrium between the drip water and the calcite,  $^{18}\text{O}$  is preferentially incorporated into the  $\text{CaCO}_3$  (Lachniet 2009). Several experimental studies have proposed fractionation factors describing the relationship for synthetic calcite, with the most commonly used one stating the  $d\delta^{18}\text{O}_{\text{ct}}/dT = -0.24$  at  $10^\circ\text{C}$  (O'Neil et al. 1969; Kim & O'Neil 1997). Because the slope of the cave temperature effect is negative, when there is a decrease in cave temperature, relatively more  $^{18}\text{O}$  is incorporated into the calcite resulting in more positive calcite  $\delta^{18}\text{O}$  values (Kim & O'Neil 1997).

Calcite may also precipitate out of isotopic equilibrium with the drip water, due to rapid kinetic fractionations of the oxygen and carbon isotopes (Hendy 1971). The most important variables that can lead to kinetic fractionation are the drip rate and the rate of  $\text{CO}_2$  degassing from the drip water (Lachniet 2009; Dreybrodt & Scholz 2011).  $\text{CO}_2$  naturally degasses from the drip water because cave air generally has relatively low  $p\text{CO}_2$  values, whereas the water has high  $p\text{CO}_2$  values due to critical zone processes above the cave. This carbon concentration gradient allows  $\text{CO}_2$  to degas from the water causing super-saturation of calcite due to elevated  $\text{Ca}^{2+}$  in the drip water (Fairchild et al. 2006a; Baldini et al. 2008). If there is a high  $p\text{CO}_2$  gradient, calcite precipitation occurs faster, and may sometimes result in calcite being formed before the drip water oxygen and carbon isotopes have equilibrated, leading to more positive  $\delta^{18}\text{O}$  and  $\delta^{13}\text{C}$  values in the speleothem (Baldini et al. 2008). A similar situation can occur if the rate at which drip water seeps through the karst is very fast, not allowing enough time for the oxygen isotopes to equilibrate with those from the dissolved limestone before

reaching the cave (Dreybrodt & Scholz 2011). Conversely if the drip rate is very slow, and each drop sits stagnant on top of the stalagmite for close to an hour or more, further CO<sub>2</sub> exchange with the cave air can cause stable isotope disequilibrium in the water (Dreybrodt & Scholz 2011). Consequently, the drip rate, the ventilation of the cave, and the residence time of water in the karst must all be favourable for the isotopic composition of rainwater and the climate signals it contains to be preserved in a stalagmite.

The  $\delta^{18}\text{O}$  value of unmodified rainwater entering the cave is the primary climate proxy recorded in stalagmites. These values are influenced by the isotopic composition of the ocean where the moisture was sourced, the amount of precipitation, the extent to which the precipitating air mass has moved across land, and how much elevation has been gained. Other important variables include the track path the air mass has followed before prior to rainfall, and the atmospheric temperature at the elevation from which the rain precipitated, both of which alter through time with changing circulation patterns. The temperature effect describes how changing the temperature at which water precipitates also changes the  $\delta^{18}\text{O}$  value of the rain. The global relationship between the  $\delta^{18}\text{O}$  value of rainfall and the temperature at which it precipitated at was described by Dansgaard in 1964, with a linear equation  $\delta^{18}\text{O} = 0.69(\text{MAT}) - 13.6\text{‰}$  (SMOW) (Dansgaard 1964). However, while the global slope is  $0.69\text{‰}/^{\circ}\text{C}$  many local regions depart significantly from this. Proposed New Zealand values for the precipitation effect ( $\Delta\delta^{18}\text{O}_p/dT$ ) have varied considerably. A study of stalagmites from two caves at a higher altitude site (Mt Arthur, North-west South Island) suggested that the slope of  $\Delta\delta^{18}\text{O}_p/dT$  was  $0.19\text{‰}/^{\circ}\text{C}$  (Hellstrom et al. 1998), whereas two other studies compared the weighted  $\delta^{18}\text{O}$  of precipitation and mean annual temperatures from the far north (Kaitiaia) and far south (Invercargill) with the result of  $\Delta\delta^{18}\text{O}_p/dT = 0.35\text{‰}/^{\circ}\text{C}$  (Williams et al. 2005) and  $\Delta\delta^{18}\text{O}_p/dT = 0.42\text{‰}/^{\circ}\text{C}$  (Whittaker 2008). The key issue with the variability in the rainfall temperature effect is whether the difference between the rainfall temperature effect and the cave temperature effect of carbonate formation is positive or negative (McDermott 2004). This is because the rainfall temperature effect acts in the opposite direction to the cave temperature effect. Thus, depending on the magnitude of the rainfall temperature effect stalagmite  $\delta^{18}\text{O}$  values could be interpreted in different ways (McDermott 2004). In the study from Mt Arthur the cave temperature – rainfall temperature effect difference was negative, so more negative calcite  $\delta^{18}\text{O}$  values were interpreted as warmer; while the studies from other South Island caves had a positive difference, so lower  $\delta^{18}\text{O}$  values were interpreted as cooler

(Hellstrom et al. 1998; Williams et al. 2005; Whittaker 2008). These study-specific differences highlight the complexity, and need for extreme care and caution, when interpreting temperature trends from speleothem  $\delta^{18}\text{O}$  values alone.

Another factor influencing meteoric water  $\delta^{18}\text{O}$  values over time are changes in global ice volume. The formation of continental ice during a glacial period requires the evaporation of water from the ocean, which is then deposited as snow contributing to ice caps. This leaves the ocean relatively enriched in  $^{18}\text{O}$  (Lachniet 2009). The opposite occurs in global greenhouse conditions with less ice at the poles, ultimately leading to increases in the  $\delta^{18}\text{O}$  value of global oceans due to ice melting. This is an important effect to consider when studying stalagmites that span the LGM and other cold periods, as the moisture delivered from the sea will have more positive  $\delta^{18}\text{O}$  values during periods of continental ice growth and preservation, resulting in  $^{18}\text{O}$  enriched water reaching the cave, relative to warm periods where ice volumes are lower (Williams et al. 2005). Estimating the degree to which ocean  $\delta^{18}\text{O}$  values increased during cold periods allows stalagmite  $\delta^{18}\text{O}$  values to be adjusted by the same amount to remove ice volume effects from the record (Williams et al. 2004, 2005).

### 6.2.2 Temperature reconstructions from the M1 stalagmite

A simple reconstruction of temperature from the M1 stable oxygen isotopes was carried out in order to evaluate the relative importance of temperature and other environmental processes. The commonly used equation from Kim & O'Neil (1997) was used, as was a new calcite-water fractionation equation proposed by Demeny et al. (2010) from stable isotopic analysis of naturally occurring calcite and travertine from various caves and deposits.

$$1000\ln\alpha(\text{calcite-H}_2\text{O}) = 18.03(10^3\text{T}^{-1}) - 32.42 \quad (\text{Kim \& O'Neil 1997})$$

$$1000\ln\alpha = 17500/\text{T} - 29.89 \quad (\text{Demeny et al. 2010})$$

As both these equations require that the value of drip water  $\delta^{18}\text{O}$  is known, the measured average drip water  $\delta^{18}\text{O}$  value from the M1 stalagmite feeder drip was used (-2.80‰ SMOW, n=4,  $\sigma=0.62$ ). For the purposes of this reconstruction, it was further assumed that the average isotopic composition of the drip water had not changed over the time of stalagmite growth.

This is a dubious assumption as the drip water  $\delta^{18}\text{O}$  was shown to vary by 12.9‰ from the average over fortnightly timescales. Thus, the reconstruction gives only an estimate of the amount of temperature change necessary to cause the observed M1  $\delta^{18}\text{O}$  record. The results produced a total temperature change over the growth period of the stalagmite of 8-9°C (Figure 6.1).

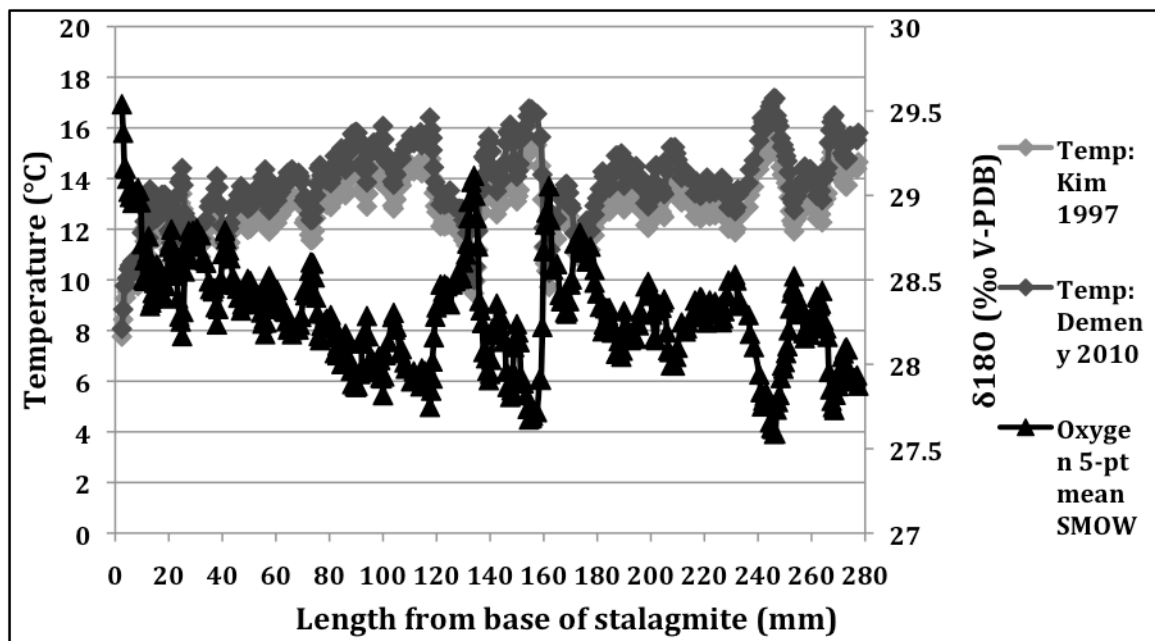


Figure 6.1: Temperature reconstruction using two different calcite-water fractionation equations (Kim & O'Neil 1997; Demeny et al. 2010) and the stable oxygen isotope data from the M1 stalagmite.

The suggestion that around 8°C of temperature change has occurred in the last 14-15 Ka is very unrealistic, as even at the height of the LGM in New Zealand temperatures are not thought to have dropped more than 4-6°C relative to today (Anderson & Mackintosh 2006; Barrows et al. 2007; Drost et al. 2007). This means that the assumption that cave drip water has remained at a constant average does not hold true, and it is also likely that temperature alone cannot account for all the variation in the stable oxygen isotope record. The likelihood of past variable cave drip water composition is enhanced by considering the high variability in the modern drip water collected from the cave during this study (Figure 4.2). The implication of past variation in cave drip water is that until there can be some quantification of these changes through time, it is very difficult to produce a realistic record of temperature from stalagmite oxygen isotope records alone.

### 6.2.3 Stable Carbon Isotopes

The changes in the stable carbon isotope composition of a stalagmite are also related to environmental and climatic changes. Above the cave, rainwater interacts with the vegetation and soil microbes, changing the dissolved carbon content of infiltrating waters. The exchange of CO<sub>2</sub> through decomposition of organic material results in the carbon in the water isotopically equilibrating with the local vegetation. The majority of carbon is present in the water as dissolved inorganic carbon (DIC), and depending on the pCO<sub>2</sub> of soil water is generally in the range of -14‰ to -18‰ in a C3 forest (McDermott et al. 2005). In times of dryness and water stress plants cause a fractionation of carbon isotopes through conserving and recycling water (Warren et al. 2001; Lambert & Aharon 2011). As such there can often be a seasonal change of  $\delta^{13}\text{C}$  – DIC values due to changing biomass productivity. Drier conditions put plants under stress and reduce productivity, leading to more positive DIC  $\delta^{13}\text{C}$  values, while wetter than normal conditions result in  $^{13}\text{C}$  depletion and more negative DIC  $\delta^{13}\text{C}$  values (Lambert & Aharon 2011).

Similarly, large changes in water  $\delta^{13}\text{C}$  values can occur when climate changes cause shifts in the type of vegetation growing in an area. In some areas changing climate allows a shift from C3 pathway dominated vegetation to C4 pathway dominated vegetation. The C4 photosynthetic pathway results in heavier carbon values being incorporated into the vegetation, typically in the range of -16 to -10‰ (McDermott et al. 2005). However, this is not likely to have occurred in New Zealand as the vegetation around Metro cave is dense native forest completely made up of C3 pathway plants, and C4 plants have almost certainly never grown in the area as there are only two rare native C4 pathway species which are both dune dwelling (Whittaker et al. 2011).

Despite the lack of C4 plants in New Zealand, the  $\delta^{13}\text{C}$  values (-9.14‰ to -3‰) from M1 calcite are significantly more positive than would be expected of water that has interacted with C3 plants. Some of this is likely due to the addition of carbon through the dissolution of local limestone, which equilibrates with the water as it seeps downwards. The degassing of CO<sub>2</sub> when the drip water enters the cave also increases the  $\delta^{13}\text{C}$  value by preferentially removing the lighter  $^{12}\text{C}$  isotopes (Frisia et al. 2011). Further degassing and equilibration to cave air occurs on the top of the stalagmite, again causing an increase in the  $\delta^{13}\text{C}$  values of

the calcite-forming water (Frisia et al. 2011). Consequently, the temporal changes in cave ventilation and  $p\text{CO}_2$  which affect the  $\delta^{18}\text{O}$  value of the water, also affect the  $\delta^{13}\text{C}$  composition (Dreybrodt & Scholz 2011; Frisia et al. 2011). In drier periods degassing of  $\text{CO}_2$  and prior precipitation can occur before the drip water enters the cave where the stalagmite is forming. This would result in water with more positive  $\delta^{13}\text{C}$  and  $\delta^{18}\text{O}$  values precipitating calcite on the stalagmite. Thus, it is possible that the co-variation of calcite  $\delta^{13}\text{C}$  and  $\delta^{18}\text{O}$  values across various growth periods may be used as a proxy for wet/dry periods of climate.

Consequently, in different scenarios of climate change (drier/warmer, wetter/cooler) there are competing processes driving both the  $\delta^{13}\text{C}$  and  $\delta^{18}\text{O}$  values of the stalagmite in different directions. Therefore it is necessary to work out which processes are dominating the stable carbon and oxygen isotope composition of the stalagmite in the local region (Quigley et al. 2010). For example, in dry conditions the temperature is usually warmer and there is more evaporation, which if the precipitation effect is dominant, where  $\Delta\delta^{18}\text{O}_p/dT = 0.35\text{‰/}^\circ\text{C}$  (Williams et al. 2005), results in more positive  $\delta^{18}\text{O}$  values in rainfall; whereas the warmer temperatures in the cave could result in more negative  $\delta^{18}\text{O}$  values through the cave temperature effect (Quigley et al. 2010).

### **6.3 Interpreting Trace Element Composition**

Speleothem trace element concentrations can be used as proxies for cave hydrological changes through time (Fairchild & Treble 2009). Trace elements and rare earth elements (REE) are incorporated into cave feed waters, and hence are affected by the many processes that modify cave drip water as it percolates through a karst system. Thus climatic changes causing relatively wetter and drier environmental conditions affect the concentrations of particular trace elements (Fairchild & Treble 2009). Hence, measuring trace element concentrations in a stalagmite can give insights into environmental controls such as temperature, trace element source and transport changes, vegetation changes, and rainfall amounts, independent of stable isotope compositions. Consequently, the trace element data from the top and bottom sections of the M1 stalagmite can be used to help interpret the stable isotope record and infer changes in climate affecting the local region around Metro cave through time.

In cave environments, aqueous trace element concentrations are influenced by inputs from atmospheric, bedrock, and detrital sediment sources, and also by the redox and pH state of the water. Dissolution and weathering of local bedrock and detrital sediment liberate trace element species into the soil and water (Borsato et al. 2007). Around Metro cave, Mg and Sr and other alkali earth elements (Ca, Ba) are most likely derived from dissolution of the limestone bedrock. However, aeolian inputs blown across the Tasman Sea from Australia can also be a significant source of aqueous phases (Marx et al. 2005; Fairchild & Treble 2009). Additionally, some elements can be leached from soil organics, while others are bound to various colloids which can be flushed from the soil and stream water depending on aqueous geochemical conditions, such as pH and redox state (Fairchild & Treble 2009). Colloids can be formed by many different particles such as clays, mineral precipitates, organic complexes, and even viruses and bacteria; while the charged surfaces of these particles allow other trace elements to bond to them (Kretzschmar & Schäfer 2005). Iron-rich colloids are often associated with trace elements such as Pb, Th and U, while other elements such as Zn, Cu and Yttrium (Y) are associated with inorganic and organic complexes (Pokrovsky & Schott 2002; Borsato et al. 2007). Some studies have found that the close association of Y with organic complexes means it is often found in higher concentrations in stalagmite calcite bands with higher UV-fluorescent properties (Borsato et al. 2007). Colloids are sensitive to high and low water flow and some, such as Fe-Ca rich colloids in particular, can be strongly retained in karst fractures (Mavrocordatos et al. 2000). Periods of high precipitation tend to wash more colloids into karstic systems where they can be incorporated into stalagmites (Fairchild & Treble 2009).

Increases in concentration and co-variation of particular trace elements in a stalagmite can be used as indicators for certain processes and climate conditions. For example, when prior calcite precipitation occurs, the proportion of trace element cations relative to  $\text{Ca}^{2+}$  in the remaining solution increases. Thus, when more carbonate is precipitated at the stalagmite there can be a strong enrichment and co-variation of Mg and Sr (Fairchild & Treble 2009). Prior carbonate precipitation can occur when seeping drip water encounters air with lower  $\text{pCO}_2$  than the soil, and tends to be enhanced during dry periods when there are more aerated zones in the karst, as the drip water can degas and become supersaturated with calcite ions prior to reaching the stalagmite (Tooth & Fairchild 2003). Sr concentrations in stalagmite calcite have been shown to be linked with stalagmite growth rates under certain conditions, with more Sr incorporated during times of increased calcite precipitation, and less when



growth rates are slower; although at lower overall growth rates this pattern is less obvious (Borsato et al. 2007). Speleothem Mg has been used as a paleo-rainfall proxy, and some studies have used Mg concentrations to reconstruct changes in ENSO severity and associated shifts in water balance (Treble et al. 2003; Treble et al. 2005). The co-variation of Mg concentration with changes in speleothem  $\delta^{13}\text{C}$  and/or  $\delta^{18}\text{O}$  values can indicate that the calcite geochemistry has been strongly influenced by changes in water balance, allowing interpretation of a stalagmite record in terms of cave hydrological change (Hellstrom & McCulloch 2000; Verheyden et al. 2000; Cruz et al. 2007).

Changes in cave hydrology can also be inferred from changing Fe concentration in stalagmites. The concentration of Fe in the M1 stalagmite shows a regular cyclical pattern up the growth axis (Figure 6.2). Compared to the bottom section, the average concentration of Fe is much lower, and the peaks much higher in the top section of the stalagmite (Figure 6.2). The influx of Fe into the cave environment is through the entrainment of dissolved Fe and Fe-bearing sediment and colloids into the groundwater. Fe in river water is mainly present as dissolved species such as colloids and trace element complexes with dissolved organic and inorganic ligands, other suspended particulates in the form of Fe-oxides, clays, and high molecular weight organic compounds (Sholkovitz & Copland 1981; Bergquist & Boyle 2006). Colloids and small detrital particles are easily mobilised from soil, and the weathering of bedrock in the watershed also contributes to the Fe load in the streams contributing to Metro cave and the groundwater of the karst aquifer. Another possible source of Fe is from airborne dust (Marx 2005). Although the total concentration of Fe in rainfall in more remote areas of New Zealand is low, due to the lack of significant anthropogenic inputs, the majority of rainwater Fe is present as particulates, suggesting it has a solid crustal source (Halstead et al. 2000). This is supported by the Australian provenance of airborne dust deposited on West Coast alpine glaciers in the Southern Alps (Marx et al. 2005). Australian dust differs from New Zealand sourced loess and dust in that the higher concentrations of heavy trace metals such as Pb and Cu reflect higher anthropogenic contamination (Marx 2005; Marx et al. 2005). The long distances between Australia and New Zealand allows scavenging of these metals and others (Zn, Sb, and Cd), resulting in higher trace metal concentrations (Marx et al. 2005). The frequent occurrence of Australian dust storms over New Zealand suggests this has been an important source of trace metals in West Coast systems throughout the Quaternary (McTainsh 1989; McTainsh & Lynch 1996). Thus it is possible that the periods with higher Fe concentration in the M1 stalagmite relate to increased westerly wind strength.

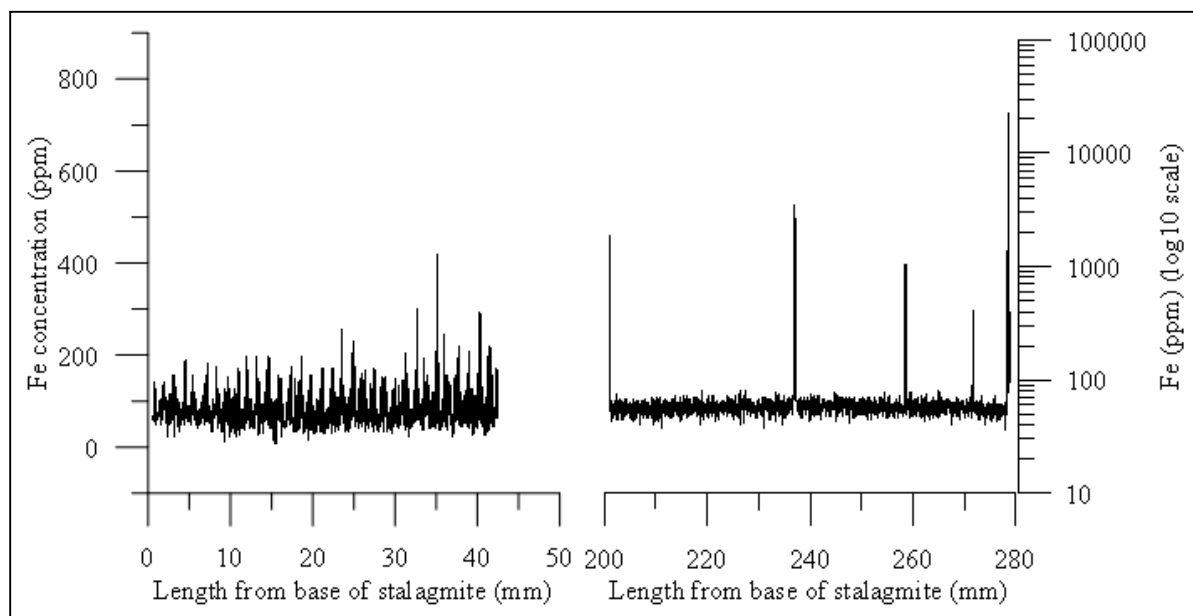


Figure 6.2: Fe concentration in the base (left) and top (right) sections of the M1 stalagmite. Note the log-scale in the top section (right). There has clearly been a shift between the base and top sections from larger magnitude oscillations to smaller scale oscillations, lower concentration, and larger peak spikes.

#### 6.4 M1 Trace Element Dilution/Enrichment Models

The M1 trace element record exhibits periods where concentrations are well above background levels. These intervals are clearest in the conservative elements Y and La, but are also observable in Cu, Pb, Zn, U, and Th concentrations, and to a lesser extent in Fe, Sr, Ba, and Mg. The periods with marked increases in trace element concentration is shown in the graphs where the raw data increases more than 1 standard deviation above the 5pt running mean of the data (indicated by the thin black line) (Figure 4.3a-d). To explore dilution/enrichment patterns, trace element concentrations were plotted against concentrations of the conservative tracer, Y (Figure 6.3a-b). Several intervals have been shown on the graphs with different symbols to highlight the similarities and differences between intervals of growth in the M1 stalagmite. Intervals B, C, H, and I were chosen for plotting because they are not at the very top or bottom of the stalagmite where there may be some distortion of the stalagmite layers, but they include intervals of growth from both analysed sections of the stalagmite. All the trace element species measured show a large increase in concentration at the very tip of the stalagmite, so interval J (the tip) was also plotted to compare with other intervals. Intervals considered “normal”, where peaks do not significantly increase above background levels, were plotted as part of the overall data on each dilution/enrichment plot.

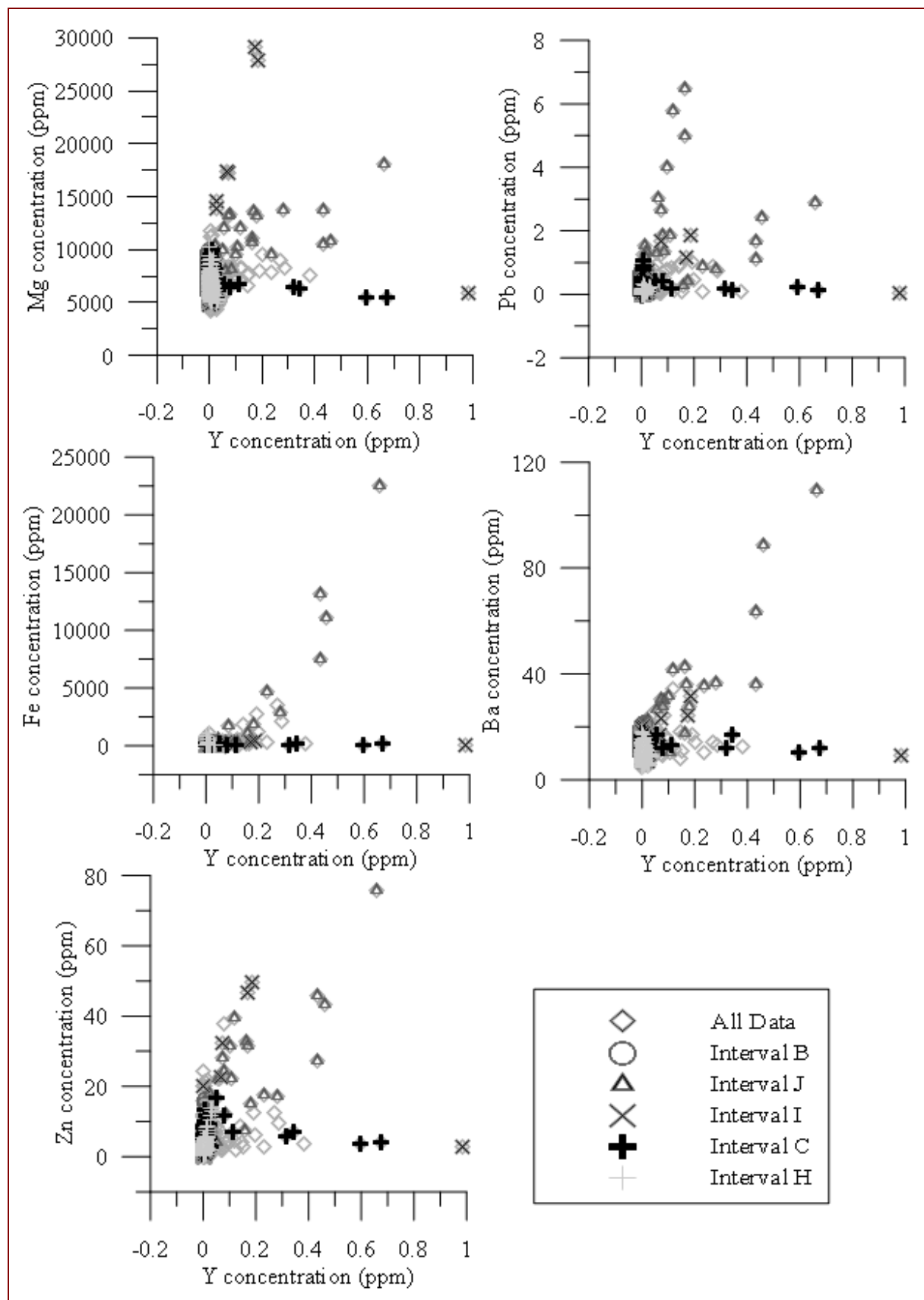


Figure 6.3a: Dilution/enrichment plots of trace elements against Y concentration in ppm. Five separate intervals are plotted over all the data from the top and bottom sections of the M1 stalagmite. Intervals B and C are from the base of the M1 stalagmite and intervals H, I, and J are from the top section.

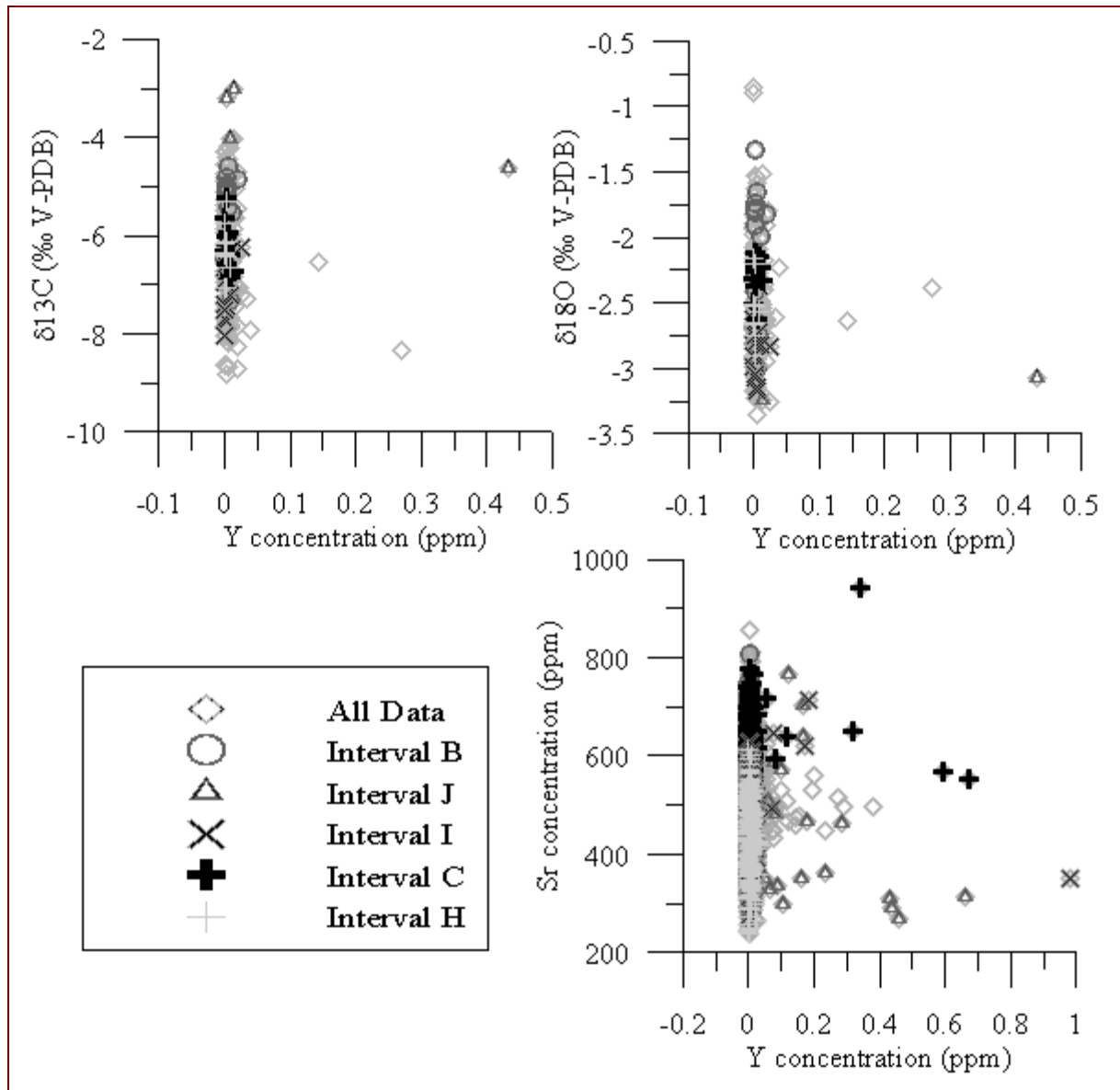


Figure 6.3b: Dilution/enrichment plots of stable oxygen and carbon isotopes and trace elements (Sr) against Y concentration in ppm. Five separate intervals are plotted over all the data from the top and bottom sections of the M1 stalagmite. Intervals B and C are from the base of the M1 stalagmite and intervals H, I, and J are from the top section.

Figures 6.3a-b present the concentrations of these trace elements at the growth intervals indicated (B, C, H, I, J). Intervals B and H occupy very similar areas in all graphs for all the trace elements, and in most graphs interval B is obscured by interval H. These two intervals are characterised by an increase only in the various trace element concentrations, with little variation in Y. This suggests that during these periods of stalagmite growth processes were occurring that increased the concentrations of most trace elements, but not of the conservative elements Y and La. Intervals C and I are similar in that they both show large increases of Y in all the plots. The increase in the other trace element concentrations is usually more than that

observed in intervals B and H. However, interval I tends to show higher trace element concentrations than interval C. The very tip of the M1 stalagmite (interval J) most often shows a simultaneous increase in y-axis and x-axis trace elements. Whereas intervals C and I suggest that Y and the other trace elements are both increasing during the period of growth, but not simultaneously.

The general patterns observed in the graphs presented in Figures 6.3a-b include:

1. When the stable isotope composition is plotted against Y the intervals (B, C, H, I, J) all overlap more than the in the trace element plots in Figure 6.3a.
2. In the plots of stable isotope composition against Y, the only interval to show increases in Y is interval J – the very tip of the M1 stalagmite.
3. Intervals C and I have more negative stable isotope values than intervals B and H (from the bottom and top sections of the M1 stalagmite).
4. Interval J differs between the two stable isotope plots in that it occupies the most positive  $\delta^{13}\text{C}$  values, but the most negative  $\delta^{18}\text{O}$  values.
5. Intervals B and H show changes in Sr concentration, but little increase in Y, while intervals C and I and J show considerable increases in Y.
6. Interval J is the only period of growth in the M1 stalagmite that shows simultaneous increases in trace element and Y concentrations in any of the plots.
7. In all the plots, intervals B and H consistently show increases in trace element/stable isotope concentrations, but not Y concentrations, while intervals C and I show increases in both trace element/stable isotope concentrations and Y concentrations.

Overall the plots in Figures 6.3a-b indicate that growth intervals in the M1 stalagmite similar to B and H are characterised by increases in some trace element concentrations, but not in the conservative Y and La, and by more positive stable isotope values. Growth intervals similar to C and I are characterised by significant increases in Y as well as other trace element concentrations, and by more negative stable isotope values. Interval J is the only interval to show simultaneous increases in both trace element concentrations and Y concentrations.

## 6.5 Paleoclimate from the M1 Stalagmite

As trace element concentrations in a stalagmite are derived, in a large part, from their aqueous concentration in cave drip waters, interpretation of trace element profiles centre on changes in hydro-climatic conditions. At the most basic level, wetter periods could decrease elemental concentrations by dilution, whereas the converse would occur during drier periods.

Alternatively, wetter conditions might introduce larger quantities of mobile elements and colloids through pulses of water entering the cave system, or increased weathering of bedrock and mobilised sediment.

Despite the more intuitive interpretation that trace element concentrations are diluted during wet conditions and enriched during dry conditions, the literature supports the alternative explanation of increased mobilisation of dissolved and particulate bound trace elements and REE during wetter than normal conditions (Kretzschmar & Schäfer 2005; Borsato et al. 2007; Zhou et al. 2008a). Consequently, the intervals where all the trace element concentrations increase in the M1 stalagmite could be driven by shifts to wetter climate. A period of time with more intense rainfall would cause more colloids to be washed through the soil into the cave system (Ingri et al. 2000; Borsato et al. 2007). As Y and other REE readily form complexes with carbonate in slightly acidic to basic water conditions, these elements are very mobile and the aqueous concentration of such complexes in river water can be increased five to twentyfold during weathering (Wood 1990; Sholkovitz & Shen 1995). Other particulate bound and dissolved trace elements would also be expected to increase as pulses of water and wetter than normal conditions increase the sediment load into the cave system (Pokrovsky & Schott 2002; Treble et al. 2003; Kretzschmar & Schäfer 2005). This would promote higher concentrations of dissolved, colloid, and organically bound elements (particularly Y) in the precipitating calcite (Zhou et al. 2008a). These periods of carbonate formation should also be associated with higher growth rates and thicker layers in the stalagmite, as more water entering the cave generally means drip rates are faster. Intervals C, E, G, I, and J mostly correspond with the white layers of calcite, although D does not (Figures 4.4a-b). In addition, these intervals all mostly correspond with negative peaks in both the oxygen and carbon isotope record in the M1 calcite. The negative peaks in the M1 stable carbon and oxygen isotope values are interpreted to represent wetter and colder conditions. Increased annual precipitation increases the water balance and input of organic material to the cave, producing more negative calcite  $\delta^{13}\text{C}$  values. Also, a colder, wetter climate produces more negative

oxygen stable isotope values when the precipitation effect is more dominant than the cave temperature effect.

Conversely, the intervals where Y and La do not increase may be the result of drier climate. This would result in slower seepage of water through to the cave, promoting more mixing of water in the karst, and a higher likelihood of prior calcite precipitation (Fairchild & Treble 2009). The removal of  $\text{Ca}^{2+}$  ions through the precipitation of calcite prior to the drip water reaching the stalagmite would result in water relatively enriched in some of the trace element species reaching the stalagmite. The evaporation of stream water and cave seepage water would also increase the relative concentrations of some trace elements. The slower seepage flow through to the cave would lead to a slower drip rate at the stalagmite. Intervals A, B, F, and H tend to correspond with thinner, darker layers of calcite. These intervals also generally correspond with more positive peaks in the calcite stable carbon and oxygen isotope record. The more positive peaks in the stable isotope composition of the M1 calcite are interpreted to represent warmer, drier conditions in the Metro cave region. Drier conditions increase the water stress on local vegetation, resulting in carbon entering the cave system with more positive  $\delta^{13}\text{C}$  values. In addition, there is also usually more evaporation in warm, dry periods promoting more positive water  $\delta^{18}\text{O}$  values.

These interpretations of the M1 stable isotope record suggest that cooler, wetter conditions occurred on the West Coast around 14.5 Ka, with the most negative oxygen isotope values occurring at 14 Ka. This time period coincides with the Antarctic Cold Reversal (ACR), and the same negative peaks can be seen in the HW3 record (Figure 6.4). The M1 stable isotope values increase by  $\sim 1\%$  after 13.8 Ka, but another prominent negative peak in both the carbon and oxygen isotope values close to 12 Ka indicates a return to cooler, wetter conditions. The peak at 12 Ka is also present in the HW3 record (Figure 6.4). From 12 Ka to 10 Ka the M1 oxygen isotope values show a warming trend, however, the carbon isotope values indicate steadily wetter conditions prevailed until 9 Ka. Just after 9 Ka the oxygen isotope values indicate another cold, wet point was reached, and for close to a further 4000 years the oxygen isotope values are highly variable, with several oscillations between more positive and more negative values. Although the M1 carbon isotope values remain relatively positive during this period, suggesting drier conditions, it seems likely that temperature may have varied somewhat, and imply the glacial advances recorded in the Southern Alps 6.6 Ka to 6.2 Ka may have been more pronounced on the West Coast (Alloway et al. 2007; Schaefer

et al. 2009). From 4 Ka to the present the M1 stable isotope record indicates several cold, wet periods occurred, most of which correspond well with dated glacial advances (Figure 6.4). Although the absolute timing and duration of the cold periods recorded throughout the M1 calcite stable isotope record cannot yet be determined, the sequence of climatic changes is similar to those proposed from other proxy records (Suggate 1990; Mayewski et al. 2004; Williams et al. 2005; Whittaker et al. 2011). The large positive increase in calcite carbon isotope values at the very tip of the M1 stalagmite likely reflects a shift to relatively drier conditions, but may also indicate increased disturbances to the forest over the past few centuries.

This interpretation of the M1 stalagmite stable isotope record corroborates those drawn from other recently published stalagmite records, which suggest that changes in annual precipitation and the atmospheric temperature of rainfall precipitation are the most important controls of West Coast stalagmite geochemistry (Williams et al. 2010; Whittaker et al. 2011).

Furthermore, the interpretation of periodic changes in precipitation on the West Coast are linked to changes in atmospheric westerly circulation patterns and strength, as it is through changes in westerly wind strength that changes in precipitation on the West Coast occur (Clare et al. 2002; Lorrey et al. 2007; Whittaker et al. 2011). Increases in westerly wind flow over the South Island of New Zealand are primarily driven through the northward migration of both the Subtropical and Sub-polar Fronts over millennial timescales, which both increase the annual precipitation on the West Coast, and are associated with cooler temperatures (Vandergoes & Fitzsimons 2003; Carter et al. 2008; Whittaker et al. 2011). Annual precipitation is also affected on shorter timescales by changes in IPO mode and ENSO (Salinger & Mullan 1999; Salinger et al. 2001; Lorrey et al. 2007). However, these more detailed interpretations are precluded by the current lack of absolute age dates for the M1 stalagmite.



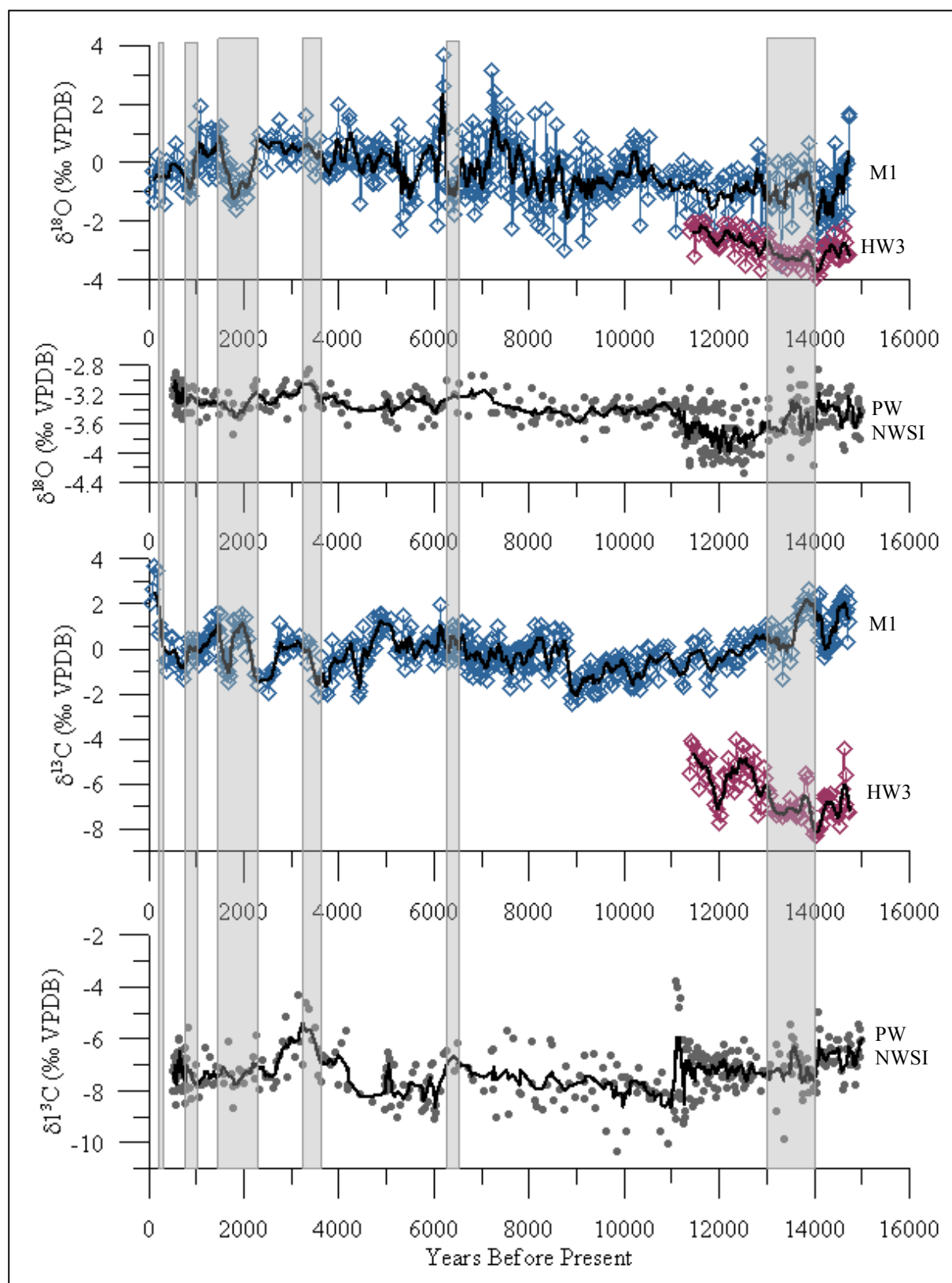


Figure 6.4: Comparison of the M1 stable oxygen and carbon isotope record with stable isotope records from a Punakaiki stalagmite (HW3) and the North West South Island Master speleothem record (PW NWSI) (Williams et al. 2010; Whittaker et al. 2011). Data were kindly provided by Dr. Tom Whittaker for HW3, and by Prof. Paul Williams for the NWSI Master record. Grey bars represent periods of known Holocene glacial advances in the Southern Alps (Schaefer et al. 2009; Kaplan et al. 2010; Putnam et al. 2010).

## **6.6 Discussion of M1 Paleoclimate**

### **6.6.1 Comparison with Two South Island Stalagmite Records**

Temperature and precipitation are both key controls on climate in the West Coast region. These are heavily influenced by the ocean and atmospheric circulation patterns occurring to the west of New Zealand, as the West Coast of the South Island lies directly in the Southern Hemisphere westerly wind path. In determining which has the stronger effect on stalagmite stable isotope geochemistry, it is necessary to consider the time period over which the stalagmite has grown. The M1 stalagmite most likely started forming around 14 Ka, and its continuous laminated texture suggests it has grown continuously since then. This period of time follows the warming that occurred post-LGM, and was generally equitable compared to the LGM, however, several significant climate reversals are also known to have occurred, both in the Southern Hemisphere, and in the Northern Hemisphere (McGlone et al. 2004; Vandergoes et al. 2005; Thackray 2008). Although radiometric dates for the M1 stalagmite and the growth rate of the stalagmite are still unknown, the experimental age model presented in Chapter 5 compares favourably with other published stalagmite records from the same region (Whittaker et al. 2011), supporting the estimated maximum age of 14 Ka (Figure 6.4).

Changes in climate (temperature and precipitation) cause competing changes in calcite stable oxygen isotope composition through the cave temperature effect, the rainfall precipitation effect, and the changes to annual precipitation amounts. Although temperature has an important effect on stalagmite geochemistry, it cannot be the dominant control, as the amount of variation observed in the M1 calcite stable oxygen isotope values is too high to be accounted for by temperature alone (Figure 6.1). In addition, the estimated change in temperature over the last 14 Ka is between -1°C to -4°C (Singer et al. 1998; Anderson & Mackintosh 2006; Carter et al. 2008), which is not enough to account for all the variation observed in the M1 oxygen isotope record. Therefore, changes in: precipitation amount; the atmospheric temperature at which rain is precipitating; and, the balance between precipitation and evaporation (P/E) in the region are the most likely primary controls on the variation of M1 stalagmite geochemistry.

The impact of precipitation and water balance changes on the West Coast is supported by the patterns of dilution/enrichment in the calcite trace element concentrations (Figures 6.3a-b).

The negative peaks in the M1 oxygen isotope record, especially in the recent calcite near the tip of the stalagmite where the age is more certain, agree well with the suggested periods of glacial advances in the Southern Alps (Schaefer et al. 2009; Kaplan et al. 2010). The oldest part of the M1 stable oxygen isotope record fits well with the negative peaks recorded in the HW3 stalagmite from Punakaiki (Figure 6.4) (Whittaker et al. 2011), which also suggests that the base of the stalagmite is close to 14 Ka in age.

Large portions of the M1 and HW3 oxygen isotope records overlap, with prominent negative peaks occurring at close to the same time (Figure 6.4). In the HW3 record, the negative oxygen and carbon isotope peaks are interpreted as representing cooler, wetter periods, with precipitation effects dominating cave temperature effects (Whittaker et al. 2011), and the similarity between the two records suggests the M1 stalagmite contains similar responses to environmental and climatic changes in the region. The carbon isotope records from the two stalagmites are more distinct than the oxygen isotope records, however, several negative and positive peaks occur about the same time (Figure 6.4). This suggests that local processes particular to the cave systems are contributing to differences in  $\delta^{13}\text{C}$  DIC values, but also that the two stalagmites are influenced by regional drivers of climate change. The two records also show similar amounts of variation in the calcite stable isotope composition. This is likely to proceed from the fact that these are both records from single stalagmites, which capture the variability of hydrological processes through the epikarst in their respective cave systems. While the M1 and HW3 stable isotope records are largely similar, there are some notable differences as well. These likely stem from the variability in drip water flow paths and differences in particular local environmental conditions in the two cave systems, despite only ~30km distance between the caves.

In contrast to the HW3 record, the M1 stable isotope record has fewer similarities with the master record from Williams et al. (2010), which is a composite series of 8 stalagmites from North West Nelson (Figure 6.4). Although the timing of some cold periods in both records is similar, especially at 12 Ka and 2 Ka (Figure 6.4), others do not line up quite so closely. There are also significant differences in the amount of variation in the two stable isotope records, particularly in the oxygen isotope values. The M1 stalagmite oxygen isotope values vary over close to 7‰ (after ice volume corrections) while the NWSI record varies over ~1.4‰, with the master series showing smaller scale changes. This reflects the differences between single stalagmite records and records compiled from several stalagmites. The M1

stalagmite shows much more of the natural variation present in the local area, while the composite master record indicates the more general trends in larger-scale regional climate. Because the M1 stable isotope record is from a single stalagmite, the isotopic variation present in the record allows local climatic changes, particularly during the Late Holocene, to appear more pronounced. As a result single stalagmite records may show more clearly the smaller-scale climatic changes that have occurred in the local region of their cave, allowing more detailed investigations of local climate.

### **6.6.2 Modern Geochemical Variability versus Past Variability**

Most paleoclimate research/proxies report on changes relative to the modern environment. While the average modern climate is well known for all the regions of New Zealand, the details of modern climatic variability in cave systems are not so well understood. It is well known that variations in processes in the modern cave environment have a strong impact on the geochemical signal recorded in stalagmite calcite (Mickler et al. 2004; McDermott et al. 2005; Fairchild et al. 2006b), and that this variability in the cave region must be understood in order to reach the best possible interpretations from a stalagmite climate proxy record. However, in general many studies of stalagmite records have assumed the modern cave environment is relatively stable, reflecting the annual average climate, and that this has also been in the case in the past (McDermott 2004; Williams et al. 2005). However, data gathered during this study suggests that there is significantly more variability in the modern environment than previously assumed. This is a key contribution of this research.

The large variation observed in the modern stable isotope composition of local rainwater, cave drip water, DIC, and modern calcite, suggest the modern cave environment in New Zealand can be extremely dynamic. The general assumption that the  $\delta^{18}\text{O}$  value of drip water from which a stalagmite precipitates is close to the mean annual  $\delta^{18}\text{O}$  value of rainfall in the region applied by others (Williams 2005), is called into question by this research. The drip water collected from Metro cave during this study over two months in the winter showed there can be significant fractionation of stable oxygen isotope values as water filters down into the cave. Not only was there close to 2‰ difference between the average rainfall oxygen isotope value and the average cave drip water oxygen isotope value, but over the two month period the cave drip water varied by ~1.4‰ (Figure 4.2). There was an even larger variation (~5‰) in the drip water DIC carbon isotope values, as well a large range of carbon and

oxygen values in the top 5 samples from the stalagmite tip (calcite carbon range  $\sim 3\text{‰}$ , calcite oxygen range  $\sim 1.6\text{‰}$ ). These large variations suggest that in any one year there is considerable variability in the annual average rainfall and drip water stable isotope values, and that this is transferred through to the stalagmite. This suggests that there may be some doubt as to a single stalagmite preserving the annual average rainfall  $\delta^{18}\text{O}$  value in recently formed calcite.

The large stable isotope variation in the modern environment implies that there has been considerable variation in the past. Furthermore, this suggests that climate change events can only be easily discerned from a stalagmite record where the normal variability has been accounted for. The large isotopic variability associated with the dynamic nature of processes in Metro cave raises questions about whether equilibrium conditions can have occurred during the formation of the M1 stalagmite. Nevertheless, the Metro cave environment has been conducive to forming a highly laminated stalagmite, with growth axis calcite that passes Hendy Tests. This implies that there is still significantly more to be learnt about the formation of speleothems and the influence of climate in temperate, mid-latitude cave systems.

## **6.7 Summary**

Considering the results discussed in this study, the methods of simplifying the complex processes affecting stalagmite formation and geochemistry by making assumptions of cave environment stability and isotopic equilibrium only serve to reduce the scope of information that can be extracted from a stalagmite. Our understanding of cave environmental conditions and processes is still incomplete, hence interpretations of stalagmite records still tend to carry high uncertainty and should be read with extreme caution. Therefore, in order to understand climatic changes in one particular region, from a single stalagmite, records must be used in conjunction with considerable local modern environmental data. A record of the  $\delta^{18}\text{O}$  value of local precipitation, along with the  $\delta^{18}\text{O}$  value of cave drip water, DIC stable isotope composition, cave temperature and humidity changes over a year or more (depending on the growth rate of the stalagmite) would be the ideal method for assisting interpretations of climate in a local area from a stalagmite record. Data of cave air and soil  $\text{pCO}_2$ , and their  $\delta^{13}\text{C}$  values, would also assist in determining changes in stalagmite growth caused by changes in degassing rates and cave air circulation. These data would not only allow the modern

variability and cave system processes to be better understood, but would also enhance our understanding of geochemical variation in older calcite, and would contribute to more detailed interpretations of past climatic change.

## Chapter 7: Conclusions and Future Opportunities

This thesis presents a new high-resolution stable isotope and trace element record for a single stalagmite from Metro cave, West Coast, New Zealand. This research was undertaken in order to advance our understanding of both regional climatic changes during the Late Quaternary on the West Coast, South Island, New Zealand, and to elucidate the climate signals preserved in stalagmites. Importantly, this study demonstrates the utility of using multiple proxies of environmental conditions through combined use of trace element concentrations and carbonate stable isotopic compositions (the second such study in New Zealand; (Hellstrom & McCulloch 2000). Additional novel contributions of this research include an investigation of new stalagmite fluid inclusion analytical approaches.

The combined M1 calcite stable isotope and trace element record shows that precipitation and water balance changes are the primary drivers of changes in calcite geochemistry of stalagmites on the West Coast of the South Island. The M1 stalagmite record suggests that environmental change in the South Island through the Late Quaternary was strongly controlled by changes in atmospheric circulation and westerly wind strength. The South Island of New Zealand is sensitive to the position of the Subtropical and Subpolar Fronts, and the north/south migration of these during colder and warmer periods in the Southern Hemisphere leads to strengthening and weakening of westerly wind flow over the Southern Alps of the South Island. In turn, this affects not only the amount of rainfall in the West Coast region, but also the air temperature at which condensation occurs. In colder periods, stronger westerly winds bring more cool moist air over the South Island. The cooler temperature of rainfall precipitation and the higher annual rainfall amounts are recorded in stalagmite calcite stable isotope composition as negative shifts in both stable oxygen and carbon  $\delta$ -values. The calcite trace element concentrations reinforce these shifts in cave water balance through increases of specific trace elements during wetter and drier periods depending on mobility and source. Yttrium concentrations in stalagmite calcite are conservative, and only increase when water borne colloids containing Yttrium (and other trace elements) are flushed through the cave system during relatively wet periods. During dry periods, Yttrium concentrations do not increase. However, some other trace elements do, in particular the trace metals. These metals most likely increase through evaporation of water and precipitation of calcite during seepage, which leads to relative enrichment of trace metal concentration in the drip water. Warmer,

drier periods also result in more positive calcite  $\delta^{18}\text{O}$  and  $\delta^{13}\text{C}$  values through higher levels of evaporation, warmer temperatures, and increased water stress on local vegetation, and changes in soil respiration rates.

Although the stable isotope and trace element records from the M1 stalagmite indicate several different periods of abrupt climate change, the reliance of the age model on an average growth rate calculated from other stalagmites in nearby cave systems precludes high levels of confidence in the timing of these events. While the occurrence of negative stable isotope peaks with known periods of glacial advance suggests the age model applied is reasonably appropriate, the uncertainty is too large to compare the timing of events in the M1 stalagmite to other records. Samples of the M1 stalagmite are still being worked on, and hopefully U-Th dates or calibrated  $^{14}\text{C}$  ages will be available in the near future.

The interpretation of stalagmite stable isotope and trace element concentrations is complex. Cave environments are sensitive to multiple processes in the local area. Each of the processes will affect stalagmite geochemistry to certain degrees. As is the case with all proxy methods, key assumptions must be made regarding cave conditions at the time of speleothem formation. These include the widely held assumption that the cave environment is relatively stable and that drip water represent the annual rainfall stable oxygen isotope composition. Additionally, it is often assumed that isotopic equilibrium between the drip water and the precipitating calcite was achieved, despite the well-known occurrence of disequilibrium effects on some speleothems. When estimates of past changes in temperature are sought, a further assumption that the isotopic composition of the water entering the cave has not changed substantially over time generally has to be made. In order to assess these assumptions data including cave temperature, relative humidity, cave drip water stable isotope composition and DIC isotope composition, and local precipitation stable isotope composition were gathered and analysed, and compared with modern calcite stable isotope composition.

The modern data gathered from Metro cave demonstrate that there is high variability in the modern environment. This variability is manifest in the M1 records. Importantly, such highly variable cave drip water stable isotope values question the validity of the assumption that local rainfall isotope compositions are recorded in calcite geochemistry, as well as whether isotopic equilibrium between the drip water and precipitating calcite is ever achieved. However, despite these concerns, the environmental conditions in Metro cave have still



produced the highly laminated M1 stalagmite, and growth axis calcite from the M1 stalagmite passes Hendy Test criteria, suggesting it can still be used for paleoclimate interpretations under current conventions of interpretation. The two-month monitoring of modern conditions in Metro cave in this thesis is the first such analysis for a New Zealand system (to my knowledge), and has raised many questions that perhaps could be addressed by a longer-term monitoring study.

In attempting to determine if the high variability observed in modern stable isotopes in the cave system has also occurred in the past, a new method for extracting and analysing calcite fluid inclusions was explored. Other current methods use large samples of calcite, 300mg and more, that average the stable oxygen and hydrogen isotope composition of fluid inclusions over many layers of calcite. Also, if samples of this size are crushed or heated to decrepitation temperatures, they are likely to bias measurements of fluid inclusion water to larger inclusions, and inclusions that can escape the solid sample relatively quickly. In order for a reasonable comparison between calcite stable isotope composition and fluid inclusion stable isotope composition to be made, the fluid inclusions must be extracted and analysed at a resolution much closer to that of the calcite samples (0.5mm). In this study we succeeded in extracting and analysing the stable oxygen and hydrogen composition of fluid inclusions from calcite samples as small as 30mg. However, while the injected test samples of liquid IAEA water standards GISP and SMOW returned stable isotope values that were both accurate and precise, the calcite chips analysed from the M1 stalagmite returned highly negative isotope values. This was most likely due to some isotopic fractionation occurring during release of the fluid inclusion water from the calcite chip, and further isotopic fractionation may also have occurred through the use of a two-way sampling needle, or problems with the temperature of the cold trap. These methods will be explored further in subsequent research, as the potential of a method for extracting higher resolution fluid inclusion samples from speleothem calcite will not only allow investigations into past isotopic variation in source drip water, but will also allow more quantitative reconstructions of past temperature. By using fluid inclusion oxygen isotope values a more detailed record of past changes in cave drip water isotope composition can be formed, allowing a quantitative solution to the temperature equations of Kim & O'Neil (1997) and Demeny et al. (2010).

In summary, this thesis presents an original high-resolution multi-proxy stalagmite record that most likely spans the last 14 Ka to the present. The exploratory work on a new method to

extract and analyse fluid inclusions from speleothem calcite has produced highly encouraging preliminary results, and will hopefully lead to new insights into past drip water variability and the processes of equilibrium and kinetic stable isotope fractionation in stalagmite calcite. Ultimately, the use of single stalagmite records allows for more detailed interpretation of local paleoenvironmental changes when they are complimented by a thorough understanding of the geochemical variation in the modern environment through extensive site monitoring.

## **Thesis References:**

- CliFlo: NIWA's National Climate Database on the Web.
- Alloway BV, Lowe DJ, Barrell DJA, Newnham RM, Almond PC, Augustinus PC, Bertler NAN, Carter L, Litchfield NJ, McGlone MS and others 2007. Towards a climate event stratigraphy for New Zealand over the past 30 000 years (NZ-INTIMATE project). *Journal of Quaternary Science* 22(1): 9-35.
- Anderson B, Mackintosh A 2006. Temperature change is the major driver of late-glacial and Holocene glacier fluctuations in New Zealand. *Geology* 34(2): 121-124.
- Anderson B, Lawson W, Owens I, B G 2006. Past and future mass balance of 'Ka Roimata o Hine Hukatere' Franz Josef Glacier, New Zealand. *Journal of Glaciology* 52(179): 597-607.
- Ayliffe LK, Marianelli PC, Moriarty KC, Wells RT, McCulloch MT, Mortimer GE, Hellstrom JC 1998. 500 ka precipitation record from southeastern Australia: Evidence for interglacial relative aridity. *Geology* 26(2): 147-150.
- Baker A, Genty D, Dreybrodt W, Barnes WL, Mockler N, Grapes J 1998. Testing theoretically predicted stalagmite growth rate with recent annually laminated samples: Implications for past stalagmite deposition. *Geochimica et Cosmochimica Acta* 62(3): 393-404.
- Baldini J, Baldini LM, McDermott F, Clipson N 2006. Carbon Dioxide sources, sinks, and spatial variability in shallow temperate zone caves: Evidence from Ballynamintra cave, Ireland. *Journal of Cave and Karst Studies* 68(1): 4-11.
- Baldini J, McDermott F, Hoffmann DL, Richards DA, Clipson N 2008. Very high-frequency and seasonal cave atmosphere PCO<sub>2</sub> variability: Implications for stalagmite growth and oxygen isotope-based paleoclimate records. *Earth and Planetary Science Letters* 272: 118-129.
- Baldini JUL, McDermott F, Baker A, Baldini LM, Matthey DP, Bruce Railsback L 2005. Biomass effects on stalagmite growth and isotope ratios: A 20th century analogue from Wiltshire, England. *Earth and Planetary Science Letters* 240: 486-494.
- Barrows TT, Stone JO, Fifield LK, Cresswell RG 2002. The timing of the Last Glacial Maximum in Australia. *Quaternary Science Reviews* 21: 159-173.
- Barrows TT, Juggins S, De Deckker P, Calvo E, Pelejero C 2007. Long-term sea surface temperature and climate change in the Australian–New Zealand region. *Paleoceanography* 22(PA2215): 1-17.
- Beck JW, Récy J, Taylor F, Edwards RL, Cabioch G 1997. Abrupt changes in early Holocene tropical sea surface temperature derived from coral records. *Nature* 385: 705-707.
- Bergquist BA, Boyle EA 2006. Iron isotopes in the Amazon River system: Weathering and transport signatures. *Earth and Planetary Science Letters* 248: 54-68.
- Borsato A, Frisia S, Fairchild IJ, Somogyi A, Susini J 2007. Trace element distribution in annual stalagmite laminae mapped by micrometer-resolution X-ray fluorescence: Implications for incorporation of environmentally significant species. *Geochimica et Cosmochimica Acta* 71: 1494-1512.
- Bowen GJ, Wilkinson B 2002. Spatial distribution of  $\delta^{18}\text{O}$  in meteoric precipitation. *Geology* 30(4): 315-318.
- Broecker WS 2003. Does the trigger for abrupt climate change reside in the ocean or in the atmosphere? *Science* 300(5625): 1519-1522.
- Buffett BA 2000. Clathrate hydrates. *Annual Review of Earth and Planetary Sciences* 28: 477-507.
- Carter L, Manighetti B, Ganssen G, Northcote L 2008. Southwest Pacific modulation of abrupt climate change during the Antarctic Cold Reversal–Younger Dryas. *Palaeogeography, Palaeoclimatology, Palaeoecology* 260: 284-298.

- Chinn TJ 1996. New Zealand glacier responses to climate change of the past century. *New Zealand Journal of Geology and Geophysics* 39: 415-428.
- Chinn TJ, Winkler S, Salinger MJ, Haakensen N 2005. Recent glacier advances in Norway and New Zealand; A comparison of their glaciological and meteorological causes. *Geografiska Annaler* 87(1): 141-157.
- Clare GR, Fitzharris BB, Chinn TJ, Salinger MJ 2002. Interannual variation in End-Of-Summer snowlines of the Southern Alps of New Zealand, and relationships with Southern Hemisphere atmospheric circulation and sea surface temperature patterns. *International journal of Climatology* 22: 107-120.
- Clark PU, Mix AC 2002. Ice sheets and sea level of the Last Glacial Maximum. *Quaternary Science Reviews* 21: 1-7.
- Crawford SJ 1994. Hydrology and geomorphology of the Paparoa karst, North Westland, New Zealand. Unpublished thesis, University of Auckland, Auckland. 266 p.
- Cruz FWJ, Burns SJ, Jercinovic M, Karmann I, Sharp WD, Vuille M 2007. Evidence of rainfall variations in Southern Brazil from trace element ratios (Mg/Ca and Sr/Ca) in a Late Pleistocene stalagmite. *Geochimica et Cosmochimica Acta* 71: 2250-2263.
- Dansgaard W 1964. The O18-abundance in fresh water. *Geochimica et Cosmochimica Acta* 6: 241-260.
- Dansgaard W, Johnsen SJ, Clausen HB, Dahl-Jensen D, Gundestrup NS, Hammer CU, Hvidberg CS, Steffensen JP, Sveinbjörnsdottir AE, Jouzel J and others 1993. Evidence for general instability of past climate from a 250-kyr ice-core record. *Nature* 364: 218-220.
- Darling WG 2004. Hydrological factors in the interpretation of stable isotopic proxy data present and past: a European perspective. *Quaternary Science Reviews* 23: 743-770.
- Davis MB, Shaw RG 2001. Range shifts and adaptive responses to Quaternary climate change. *Science* 292: 673-679.
- Demény A, Kele S, Siklosy Z 2010. Empirical equations for the temperature dependence of calcite-water oxygen isotope fractionation from speleothems. *Rapid Communications in Mass Spectrometry* 24(24): 3521-3526.
- Dennis PF, Rowe PJ, Atkinson TC 2001. The recovery and isotopic measurement of water from fluid inclusions in speleothems. *Geochimica et Cosmochimica Acta* 65(6): 871-884.
- Denton GH, Heusser CJ, Lowell TV, Moreno PI, Andersen BG, Huessner LE, Schlüchter C, Marchant DR 1999. Interhemispheric linkage of paleoclimate during the last glaciation. *Geografiska Annaler* 81 A(2): 107-153.
- Desmarchelier JM, Goede A, Ayliffe LK, McCulloch MT, Moriarty K 2000. Stable isotope record and its palaeoenvironmental interpretation for a late Middle Pleistocene speleothem from Victoria Fossil Cave, Naracoorte, South Australia. *Quaternary Science Reviews* 19: 763-774.
- Diaz HF, Hoerling MP, Eischeid JK 2001. ENSO variability, teleconnections and climate change. *International journal of Climatology* 21: 1845-1862.
- Dorale JA, Liu Z 2009. Limitations of Hendy Test criteria in judging the paleoclimate suitability of speleothems and the need for replication. *Journal of Cave and Karst Studies* 71(1): 73-80.
- Dorale JA, Lawrence E, Ito E, LA G 1998. Climate and vegetation history of the midcontinent from 75 to 25 ka: A speleothem record from Crevice Cave, Missouri, USA. *Science* 282(5395): 1871-1874.
- Dreybrodt W 1980. Deposition of calcite from thin films of natural calcareous solutions and the growth of speleothems. *Chemical Geology* 29: 89-105.

- Dreybrodt W, Scholz D 2011. Climatic dependence of stable carbon and oxygen isotope signals recorded in speleothems: From soil water to speleothem calcite. *Geochimica et Cosmochimica Acta* 75: 734-752.
- Drost F, Renwick J, Bhaskaran B, Oliver H, McGregor J 2007. A simulation of New Zealand's climate during the Last Glacial Maximum. *Quaternary Science Reviews* 26: 2505-2525.
- Edwards R, Chen JH, Wasserburg GJ 1987.  $^{238}\text{U}$ -  $^{234}\text{U}$ - $^{230}\text{Th}$ -  $^{232}\text{Th}$  systematics and the precise measurement of time over the past 500,000 years. *Earth and Planetary Science Letters* 81: 175-192.
- Eggins SM, Grun R, McCulloch MT, Pike AWG, Chappell J, Kinsley L, Mortimer G, Shelley M, Murray-Wallace CV, Spotl C and others 2005. In situ U-series dating by laser-ablation multi-collector ICPMS: new prospects for Quaternary geochronology. *Quaternary Science Reviews* 24: 2523-2538.
- EPICA Community Members 2004. Eight glacial cycles from an Antarctic ice core. *Nature* 429: 623-628.
- Epstein S, Buchsbaum R, Lowenstam HA, Urey HC 1953. Revised carbonate-water isotopic temperature scale. *Bulletin of the Geological Society of America* 64: 1315-1325.
- Evans JL, Allan RJ 1992. El Nino/southern oscillation modification to the structure of the monsoon and tropical cyclone activity in the Australasian region. *International journal of Climatology* 12(6): 611-623.
- Fairchild IJ, Treble PC 2009. Trace elements in speleothems as recorders of environmental change. *Quaternary Science Reviews* 28: 449-468.
- Fairchild IJ, Frisia S, Borsato A, Tooth AF 2006a. Speleothems. In: Nash DJ, McLaren S J ed. *Geochemical Sediments and Landscapes*. Oxford, Blackwells.
- Fairchild IJ, Frisia S, Borsato A, Tooth A 2007. Speleothems. In: Nash DJ, McLaren S J ed. *Geochemical sediments and landscapes*, Blackwell Publishing Ltd. Pp. 200-245.
- Fairchild IJ, Borsato A, Tooth AF, Frisia S, Hawkesworth CJ, Huang Y, McDermott F, Spiro B 2000. Controls on trace element Sr-Mg compositions of carbonate cave waters: implications for speleothem climatic records. *Chemical Geology* 166: 255-269.
- Fairchild IJ, Smith CL, Baker A, Fuller L, Spotl C, Matthey D, McDermott F, EIMF 2006b. Modification and preservation of environmental signals in speleothems. *Earth Science Reviews* Submitted in 2005.
- Ford DC, Williams PW 1989. *Karst geomorphology and hydrology*. London, Boston: Unwin Hyman. 601 p.
- Fornaca-Rinaldi G, Panichi C, Tongiorgi E 1968. Some causes of the variation of the isotopic composition of carbon and oxygen in cave concretions. *Earth and Planetary Science Letters* 4: 321-324.
- Frappier A, Sahagian D, Gonzalez LA, Carpenter SJ 2002. El Nino events recorded by stalagmite carbon isotopes. *Science* 298(5593): 565.
- Frappier A, Sahagian D, Carpenter SJ, Gonzalez LA, Frappier BR 2007. Stalagmite stable isotope record of recent tropical cyclone events. *Geology* 35(2): 111-114.
- Fricke HC, O'Neil JR 1999. The correlation between  $^{18}\text{O}/^{16}\text{O}$  ratios of meteoric water and surface temperature: its use in investigating terrestrial climate change over geologic time. *Earth and Planetary Science Letters* 170: 181-196.
- Friedman I, Harris JM, Smith GI, Johnson CA 2002. Stable isotope composition of waters in the Great Basin, United States 1. Air-mass trajectories. *Journal of Geophysical Research* 107(D19): 4400-4414.
- Frisia S, Borsato A, Fairchild IJ, McDermott F 2000. Calcite fabrics, growth mechanisms, and environments of formation in speleothems from the Italian Alps and Southwestern Ireland. *Journal of Sedimentary Research* 70(5): 1183-1196.

- Frisia S, Fairchild IJ, Fohlmeister J, Miorandi R, Spötl C, Borsato A 2011. Carbon mass-balance modelling and carbon isotope exchange processes in dynamic caves. *Geochimica et Cosmochimica Acta* 75: 380-400.
- Gascoyne M 1992. Paleoclimate determination from cave calcite deposits. *Quaternary Science Reviews* 11: 609-632.
- Genty D, Quinif Y 1996. Annually laminated sequences in the internal structure of some Belgian stalagmites - Importance for paleoclimatology. *Journal of Sedimentary Research* 66(1): 275-288.
- Genty D, Baker A, Vokal B 2001. Intra- and inter-annual growth rate of modern stalagmites. *Chemical Geology* 176: 191-212.
- Genty D, Plagnes V, Causse C, Cattani O, Stievenard M, Falourd S, Blamart D, Ouahdi R, Van-Exter S 2002. Fossil water in large stalagmite voids as a tool for paleoprecipitation stable isotope composition reconstitution and paleotemperature calculation. *Chemical Geology* 184: 83-95.
- Ghisetti FC, Sibson RH 2006. Accommodation of compressional inversion in north-western South Island (New Zealand): Old faults versus new? *Journal of Structural Geology* 28: 1994-2010.
- Gillieson D 1996. *Caves: Processes, development, management*. Oxford, Blackwell Publishers Ltd.
- Goede A, Green DC, Harmon RS 1986. Late Pleistocene palaeotemperature record from a Tasmanian speleothem. *Australian Journal of Earth Sciences* 33(3): 333-342.
- Goldstein RH 2001a. Clues from fluid inclusions. *Science* 294(5544): 1009-1011.
- Goldstein RH 2001b. Fluid inclusions in sedimentary and diagenetic systems. *Lithos* 55: 159-193.
- Gomez B, Carter L, Trustrum NA, Palmer AS, Roberts AP 2004. El Niño–Southern Oscillation signal associated with middle Holocene climate change in intercorrelated terrestrial and marine sediment cores, North Island, New Zealand. *Geology* 32(8): 653-656.
- Griffiths M, Drysdale RN, Vonhof HB, Gagan MK, Zhao J-X, Ayliffe LK, Hantoro WS, Hellstrom JC, Cartwright I, Frisia S and others 2010. Younger Dryas–Holocene temperature and rainfall history of southern Indonesia from  $\delta^{18}\text{O}$  in speleothem calcite and fluid inclusions. *Earth and Planetary Science Letters* 95: 30-36.
- Halstead MJR, Cunninghame RG, Hunter KA 2000. Wet deposition of trace metals to a remote site in Fiordland, New Zealand. *Atmospheric Environment* 34: 665-676.
- Harmon RS, Schwarcz HP, O'Neil JR 1979. D/H ratios in speleothem fluid inclusions: A guide to variations in the isotopic composition of meteoric precipitation? *Earth and Planetary Science Letters* 42: 254-266.
- Harmon RS, Schwarcz HP, Gascoyne M, Hess JW, Ford DC 2007. Paleoclimate information from speleothems: The present as a guide to the past. In: Sasowsky ID, Mylroie J ed. *Studies of Cave Sediments: Physical and Chemical Records of Paleoclimate*. New York, Kluwer Academic/Plenum Publishers. Pp. 199-226.
- Hartman G, Danin A 2010. Isotopic values of plants in relation to water availability in the Eastern Mediterranean region. *Oecologia* 162(4): 837-852.
- Hellstrom J 2003. Rapid and accurate U/Th dating using parallel ion-counting multi-collector ICP-MS. *Journal of Analytical Atomic Spectrometry* 18: 1346-1351.
- Hellstrom J 2006. U–Th dating of speleothems with high initial  $^{230}\text{Th}$  using stratigraphical constraint. *Quaternary Geochronology* 1: 289-295.
- Hellstrom J, McCulloch M, Stone J 1998. A detailed 31,000-year record of climate and vegetation change, from the isotope geochemistry of two New Zealand speleothems. *Quaternary Research* 50(167-178).

- Hellstrom JC, McCulloch MT 2000. Multi-proxy constraints on the climatic significance of trace element records from a New Zealand speleothem. *Earth and Planetary Science Letters* 179: 287-297.
- Hendy CH 1971. The isotopic geochemistry of speleothems - I. The calculation of the effects of different modes of formation on the isotopic composition of speleothems and their applicability as palaeoclimatic indicators *Geochimica et Cosmochimica Acta* 35: 801-824.
- Hendy CH, Wilson AT 1968. Paleoclimatic data from speleothems. *Nature* 219: 48-51.
- Higgins P, MacFadden BJ 2004. "Amount Effect" recorded in oxygen isotopes of Late Glacial horse (*Equus*) and bison (*Bison*) teeth from the Sonoran and Chihuahuan deserts, southwestern United States. *Palaeogeography, Palaeoclimatology, Palaeoecology* 206: 337-353.
- Hooker BL, Fitzharris BB 1999. The correlation between climatic parameters and the retreat and advance of Franz Josef Glacier, New Zealand. *Global and Planetary Change* 22: 39-48.
- Ingri J, Widerlund A, Land M, Gustafsson Ö, Andersson P, Öhlander B 2000. Temporal variations in the fractionation of the rare earth elements in a boreal river; the role of colloidal particles. *Chemical Geology* 166: 23-45.
- Isla FI 1989. Holocene sea-level fluctuation in the Southern Hemisphere. *Quaternary Science Reviews* 8: 359-368.
- Ivy-Ochs S, Schlüchter C, Kubik PW, Denton GH 1999. Moraine exposure dates imply synchronous Younger Dryas glacier advances in the European Alps and in the Southern Alps of New Zealand. *Geografiska Annaler* 81A(2): 313-323.
- Jansen E, Overpeck J, Briffa KR, Duplessy J-C, Joos F, Masson-Delmotte V, Olago D, Otto-Bliesner B, Peltier WR, Rahmstorf S and others 2007. Palaeoclimate. In: Solomon S, Qin D, Manning M, Chen Z, Marquis M, Averyt KB, Tignor M, Miller HL ed. *Climate Change 2007: The Physical Science Basis. Contribution of Working Group I to the Fourth Assessment Report of the Intergovernmental Panel on Climate Change*. Cambridge, United Kingdom and New York, NY, USA, Cambridge University Press.
- Kaplan MR, Schaefer JM, Denton GH, Barrell DJA, Chinn TJH, Putnam AE, Andersen BG, Finkel RC, Schwartz R, Doughty AM 2010. Glacier retreat in New Zealand during the Younger Dryas stadial. *Nature* 467: 194-197.
- Kendall AC, Broughton PL 1978. Origin of fabrics in speleothems composed of columnar calcite crystals. *Journal of Sedimentary Petrology* 48(2): 519-538.
- Kidson JW 2000. An analysis of New Zealand synoptic types and their use in defining weather regimes. *International journal of Climatology* 20: 299-316.
- Kim S-T, O'Neil JR 1997. Equilibrium and nonequilibrium oxygen isotope effects in synthetic carbonates. *Geochimica et Cosmochimica Acta* 61(16): 3461-3475.
- Kretzschmar R, Schäfer T 2005. Metal retention and transport on colloidal particles in the environment. *Elements* 1: 205-210.
- Lacazette A 1990. Application of linear elastic fracture mechanics to the quantitative evaluation of fluid-inclusion decrepitation. *Geology* 18: 782-785.
- Lachniet MS 2009. Climatic and environmental controls on speleothem oxygen-isotope values. *Quaternary Science Reviews* 28: 412-432.
- Lambert WJ, Aharon P 2011. Controls on dissolved inorganic carbon and  $\delta^{13}\text{C}$  in cave waters from DeSoto Caverns: Implications for speleothem  $\delta^{13}\text{C}$  assessments. *Geochimica et Cosmochimica Acta* 75: 753-768.
- Lauritzen S-E, Lundberg J 1999. Speleothems and climate: a special issue of *The Holocene*. *The Holocene* 9(6): 643-647.

- Lecuyer C, O'Neil JR 1994. Stable isotope compositions of fluid inclusions in biogenic carbonates. *Geochimica et Cosmochimica Acta* 58: 353-363.
- Little TA, Cox S, Vry JK, Batt G 2005. Variations in exhumation level and uplift rate along the oblique-slip Alpine fault, central Southern Alps, New Zealand. *Geological Society of America Bulletin* 117(5/6): 707-723.
- Lorrey A, Fowler AM, Salinger J 2007. Regional climate regime classification as a qualitative tool for interpreting multi-proxy palaeoclimate data spatial patterns: A New Zealand case study. *Palaeogeography, Palaeoclimatology, Palaeoecology* 253: 407-433.
- Lorrey A, Williams P, Salinger J, Martin T, Palmer J, Fowler A, Zhao J-X, Neil H 2008. Speleothem stable isotope records interpreted within a multi-proxy framework and implications for New Zealand palaeoclimate reconstruction. *Quaternary International* 187: 52-75.
- Marra MJ, Smith EGC, Shulmeister J, Leschen R 2004. Late Quaternary climate change in the Awatere Valley, South Island, New Zealand using a sine model with a maximum likelihood envelope on fossil beetle data. *Quaternary Science Reviews* 23: 1637-1650.
- Marra MJ, Shulmeister J, Smith EGC 2006. Reconstructing temperature during the Last Glacial Maximum from Lyndon Stream, South Island, New Zealand using beetle fossils and maximum likelihood envelopes. *Quaternary Science Reviews* 25: 1841-1849.
- Marx SK, Kamber BS, McGowan HA 2005. Provenance of long-travelled dust determined with ultra-trace-element composition: a pilot study with samples from New Zealand glaciers. *Earth Surface Processes and Landforms* 30: 699-716.
- Marx SK, McGowan HA 2005. Dust transportation and deposition in a superhumid environment, West Coast, South Island, New Zealand. *Catena* 59(2): 147-171.
- Matthey DP, Fairchild IJ, Atkinson TC, Latin J-P, Ainsworth M, Durell R 2010. Seasonal microclimate control of calcite fabrics, stable isotopes and trace elements in modern speleothem from St. Michaels Cave, Gibraltar. *Tufas and Speleothems: Unravelling the Microbial and Physical Controls*. London, Geological Society of London.
- Matthews A, Ayalon A, Bar-Matthews M 2000. D/H ratios of fluid inclusions of Soreq cave (Israel) speleothems as a guide to the Eastern Mediterranean Meteoric Line relationships in the last 120 ky. *Chemical Geology* 166: 183-191.
- Mavrocordatos D, Mondy-Couture C, Atteia O, Leppard GG, Perret D 2000. Formation of a distinct class of Fe-Ca(-C<sub>org</sub>)-rich particles in a complex peat-karst system. *Journal of Hydrology* 237(3-4): 234-247.
- Mayewski PA, Rohling EE, Stager JC, Karlen W, Maasch KA, Meeker LD, Meyerson EA, Gasse F, van Kreveland S, Holmgren K and others 2004. Holocene climate variability. *Quaternary Research* 62: 243-255.
- McCarroll D, Loader NJ 2004. Stable isotopes in tree rings. *Quaternary Science Reviews* 23: 771-801.
- McDermott F 2004. Palaeo-climate reconstruction from stable isotope variations in speleothems: a review. *Quaternary Science Reviews* 23: 901-918.
- McDermott F, Schwarcz H, Rowe PJ 2005. Isotopes in Speleothems. In: Leng MJ ed. *Isotopes in Palaeoenvironmental Research*. Dordrecht, Springer. Pp. 307.
- McGarry S, Bar-Matthews M, Matthews A, Vaks A, Schilman B, Ayalon A 2004. Constraints on hydrological and paleotemperature variations in the Eastern Mediterranean region in the last 140 ka given by the dD values of speleothem fluid inclusions. *Quaternary Science Reviews* 23: 919-934.
- McGarry SF, Baker A 2000. Organic acid fluorescence: applications to speleothem palaeoenvironmental reconstruction. *Quaternary Science Reviews* 19: 1087-1101.



- McGlone MS 1995. Lateglacial landscape and vegetation change and the Younger Dryas climate oscillation in New Zealand. *Quaternary Science Reviews* 14: 867-881.
- McGlone MS 2002. The Late Quaternary peat, vegetation and climate history of the Southern Oceanic Islands of New Zealand. *Quaternary Science Reviews* 21: 683-707.
- McGlone MS, Turney CSM, Wilmshurst JM 2004. Late-glacial and Holocene vegetation and climatic history of the Cass Basin, central South Island, New Zealand. *Quaternary Research* 62: 267-279.
- McGlone MS, Newnham RM, Moar NT 2010. The vegetation cover of New Zealand during the Last Glacial Maximum: Do pollen records under-represent woody vegetation? *Terra Australis* 32: 49-68.
- McTainsh GH 1989. Quaternary aeolian dust processes and sediments in the Australian region. *Quaternary Science Reviews* 8: 235-253.
- McTainsh GH, Lynch AW 1996. Quantitative estimates of the effect of climate change on dust storm activity in Australia during the Last Glacial Maximum. *Geomorphology* 17: 263-271.
- Mickler PJ, Stern LA, Banner JL 2006. Large kinetic isotope effects in modern speleothems. *Geological Society of America Bulletin* 118(1/2): 65-81.
- Mickler PJ, Banner JL, Stern L, Asmerom Y, Edwards RL, Ito E 2004. Stable isotope variations in modern tropical speleothems: Evaluating equilibrium vs. kinetic isotope effects. *Geochimica et Cosmochimica Acta* 68(21): 4381-4393.
- Mix AC, Bard E, Schneider R 2001. Environmental processes of the ice age: land, oceans, glaciers (EPILOG). *Quaternary Science Reviews* 20: 627-657.
- Moar NT 1980. Late Otiran and Early Aranuiian grassland in central South Island. *New Zealand Journal of Ecology* 3: 4-12.
- Moar NT, Suggate RP 1996. Vegetation history from the Kaihinu (last) Interglacial to the Present, West Coast, South Island, New Zealand. *Quaternary Science Reviews* 15: 521-547.
- Mullan AB 1995. On the linearity and stability of Southern Oscillation-climate relationships for New Zealand. *International Journal of Climate* 15: 1365-1387.
- Nathan S, Rattenbury MS, Suggate RP (compilers) 2002. *Geology of the Greymouth area: scale 1:250,000*. Lower Hutt, Institute of Geological & Nuclear Sciences. 58 p.
- Nelson CS, Hendy IL, Neil HL, Hendy CH, Weaver PPE 2000. Last glacial jetting of cold waters through the Subtropical Convergence zone in the Southwest Pacific off eastern New Zealand, and some geological implications. *Palaeogeography, Palaeoclimatology, Palaeoecology* 156: 103-121.
- Newnham RM, Lowe DJ, Williams PW 1999. Quaternary environmental change in New Zealand: a review. *Progress in Physical Geography* 23(4): 567-610.
- Newnham RM, Vandergoes MJ, Hendy CH, Lowe DJ 2007. A terrestrial palynological record for the last two glacial cycles from southwestern New Zealand. *Quaternary Science Reviews* 26: 517-535.
- NZSS 2011. New Zealand Speleological Society. Retrieved 12/5/2011 <http://www.caves.org.nz>
- O'Neil JR, Clayton RN, Mayeda TK 1969. Oxygen isotope fractionation in divalent metal carbonates. *The Journal of Chemical Physics* 51(12): 5547-5558.
- Oerlemans J 1992. Climate sensitivity of glaciers in southern Norway: application of an energy-balance model to Nigardsbren, Hellstugubren and Alftobren. *Journal of Glaciology* 38(129): 223-232.
- Oerlemans J 2005. Extracting a climate signal from 169 glacier records. *Science* 308: 675-677.

- Parmesan C 2006. Ecological and evolutionary responses to Recent climate change. *Annual Review of Ecology, Evolution, and Systematics* 37: 637-669.
- Peltier WR 2004. Global glacial isoostasy and the surface of the Ice-Age Earth: The ICE-5G (VM2) model and GRACE. *Annual Review of Earth and Planetary Sciences* 32: 111-149.
- Pillans B 1991. New Zealand Quaternary stratigraphy: and overview. *Quaternary Science Reviews* 10: 405-418.
- Pokrovsky OS, Schott J 2002. Iron colloids/organic matter associated transport of major and trace elements in small boreal rivers and their estuaries (NW Russia). *Chemical Geology* 190: 141-179.
- Polag D, Scholz D, Muhlinghaus C, Spötl C, Schroder-Ritzrau A, Segl M, Mangini A 2010. Stable isotope fractionation in speleothems: Laboratory experiments. *Chemical Geology* 279: 31-39.
- Putnam A, Denton GH, Schaefer JM, Barrell DJA, Andersen BG, Finkel RC, Schwartz R, Doughty AM, Kaplan MR, Schlüchter C 2010. Glacier advance in southern middle-latitudes during the Antarctic Cold Reversal. *Nature Geoscience* 3: 700-704.
- Quigley MC, Horton T, Hellstrom JC, Cupper ML, Sandiford M 2010. Holocene climate change in arid Australia from speleothem and alluvial records. *The Holocene* 20(7): 1-12.
- Rabassa J, Coronato AM, Salemme M 2005. Chronology of the Late Cenozoic Patagonian glaciations and their correlation with biostratigraphic units of the Pampean region (Argentina). *Journal of South American Earth Sciences* 20: 81-103.
- Ramseyer K, Miano TM, D'Orazio V, Wildberger A, Wagner T, Geister J 1997. Nature and origin of organic matter in carbonates from speleothems, marine cements and coral skeletons. *Organic Geochemistry* 26(5/6): 361-378.
- Richards DA, Dorale JA 2003. Uranium-series chronology and environmental applications of speleothems. *Reviews in Mineralogy and Geochemistry* 52(1): 407-460.
- Rodriguez-Navarro C, Ruiz-Agudo E, Luque A, Rodriguez-Navarro AB, Ortega-Huertas M 2009. Thermal decomposition of calcite: Mechanisms of formation and textural evolution of CaO nanocrystals. *American Mineralogist* 94: 578-593.
- Romanov D, Kaufmann G, Dreybrodt W 2008. Modeling stalagmite growth by first principles of chemistry and physics of calcite precipitation. *Geochimica et Cosmochimica Acta* 72: 423-437.
- Rother H, Shulmeister J 2006. Synoptic climate change as a driver of late Quaternary glaciations in the mid-latitudes of the Southern Hemisphere. *Climate of the Past* 2: 11-19.
- Salinger MJ, Mullan AB 1999. New Zealand climate: Temperature and precipitation variations and their links with atmospheric circulation 1930-1994. *International Journal of Climatology* 19: 1049-1071.
- Salinger MJ, Renwick JA, Mullan AB 2001. Interdecadal Pacific Oscillation and South Pacific climate. *International Journal of Climatology* 21: 1705-1721.
- Schaefer JM, Denton GH, Barrell DJA, Ivy-Ochs S, Kubik PW, Anderson BG, Phillips FM, Lowell TV, Schluchter C 2006. Near-synchronous interhemispheric termination of the last glacial maximum in mid-latitudes. *Science* 312: 1510-1513.
- Schaefer JM, Denton GH, Kaplan M, Putnam A, Finkel RC, Barrell DJA, Anderson BG, Schwartz R, Mackintosh A, Chinn T and others 2009. High-frequency Holocene glacier fluctuations in New Zealand differ from the Northern signature. *Science* 324: 622-625.

- Schwarcz HP, Rink WJ 2001. Dating methods for sediments of caves and rockshelters with examples from the Mediterranean region. *Geoarchaeology: An International Journal* 16(4): 355-371.
- Schwarcz HP, Harmon RS, Thompson P, Ford DC 1976. Stable isotope studies of fluid inclusions in speleothems and their paleoclimatic significance. *Geochimica et Cosmochimica Acta* 40: 657-665.
- Sharp ZD 1992. In situ laser microprobe techniques for stable isotope analysis. *Chemical Geology* 101: 3-19.
- Sharp ZD 2007. *Principles of Stable Isotope Geochemistry*. Upper Saddle River, NJ, Pearson Prentice Hall. 344 p.
- Sharp ZD, Atudorei V, Durakiewicz T 2001. A rapid method for determination of hydrogen and oxygen isotope ratios from water and hydrous minerals. *Chemical Geology* 178: 197-210.
- Sholkovitz E, Shen G 1995. The incorporation of rare earth elements in modern coral. *Geochimica et Cosmochimica Acta* 59(13): 2749-2756.
- Sholkovitz ER, Copland D 1981. The coagulation, solubility and adsorption properties of Fe, Mn, Cu, Ni, Cd, Co and humic acids in a river water. *Geochimica et Cosmochimica Acta* 45: 181-189.
- Shulmeister J, Lees B 1995. Pollen evidence from tropical Australia for the onset of an ENSO-dominated climate at c. 4000 BP. *The Holocene* 5(1): 10-18.
- Shulmeister J, Rodbell DT, Gagan MK, Seltzer GO 2006. Inter-hemispheric linkages in climate change: paleo-perspectives for future climate change. *Climate of the Past* 2: 167-185.
- Shulmeister J, McLea WL, Singer C, McKay RM, Hosie C 2003. Late Quaternary pollen records from the Lower Cobb Valley and adjacent areas, North-West Nelson, New Zealand. *New Zealand Journal of Botany* 41: 503-533.
- Siegel FR, Reams MW 1966. Temperature effect on precipitation of calcium carbonate from calcium bicarbonate solutions and its application to cavern environments. *Sedimentology* 7: 241-248.
- Singer C, Shulmeister J, McLea B 1998. Evidence against a significant Younger Dryas cooling event in New Zealand. *Science* 281(5378): 812-814.
- Smith N ed. 2004. *The New Zealand cave atlas - Volume 2, South Island*. Waitomo, New Zealand Speleological Society.
- Spötl C, Mangini A 2002. Stalagmite from the Austrian Alps reveals Dansgaard-Oeschger events during isotope stage 3: Implications for the absolute chronology of Greenland ice cores. *Earth and Planetary Science Letters* 203: 507-518.
- Spötl C, Matthey D 2006. Stable isotope microsampling of speleothems for palaeoenvironmental studies: A comparison of microdrill, micromill and laser ablation techniques. *Chemical Geology* 235: 48-58.
- Stirling CH, Esat TM, McCulloch MT, Lambek K 1995. High-precision U-series dating of corals from Western Australia and implications for the timing and duration of the Last Interglacial. *Earth and Planetary Science Letters* 135: 115-130.
- Sugden DE, Bentley MJ, Cofaigh CÓ 2006. Geological and geomorphological insights into Antarctic ice sheet evolution. *Philosophical Transactions of the Royal Society of London A* 364: 1607-1625.
- Suggate RP 1990. Late Pliocene and Quaternary glaciations of New Zealand. *Quaternary Science Reviews* 9: 175-197.
- Suggate RP, Almond PC 2005. The Last Glacial Maximum (LGM) in western South Island, New Zealand: implications for the global LGM and MIS 2. *Quaternary Science Reviews* 24: 1923-1940.

- Svensson U, Dreybrodt W 1992. Dissolution kinetics of natural calcite minerals in CO<sub>2</sub>-water systems approaching calcite equilibrium. *Chemical Geology* 100: 129-145.
- Thackray GD 2008. Varied climatic and topographic influences on Late Pleistocene mountain glaciation in the western United States. *Journal of Quaternary Science* 23(6-7): 671-681.
- Thompson P, Schwarcz HP, Ford DC 1976. Stable isotope geochemistry, geothermometry, and geochronology of speleothems from West Virginia. *Geological Society of America Bulletin* 87: 1730-1738.
- Tooth AF, Fairchild IJ 2003. Soil and karst aquifer hydrological controls on the geochemical evolution of speleothem-forming drip waters, Crag Cave, southwest Ireland. *Journal of Hydrology* 273: 51-68.
- Treble P, Shelley JMG, Chappell J 2003. Comparison of high resolution sub-annual records of trace elements in a modern (1911-1992) speleothem with instrumental climate data from southwest Australia. *Earth and Planetary Science Letters* 216: 141-153.
- Treble PC, Chappell J, Gagan MK, McKeegan KD, Harrison TM 2005. In situ measurement of seasonal  $\delta^{18}\text{O}$  variations and analysis of isotopic trends in a modern speleothem from southwest Australia. *Earth and Planetary Science Letters* 233: 17-32.
- Turney CSM, McGlone MS, Wilmshurst JM 2003. Asynchronous climate change between New Zealand and the North Atlantic during the last deglaciation. *Geology* 31(3): 223-226.
- Ujiie K, Yamaguchi A, Taguchi S 2008. Stretching of fluid inclusions in calcite as an indicator of frictional heating on faults. *Geology* 36(2): 111-114.
- van Breukelen MR, Vonhof HB, Hellstrom JC, Wester WCG, Kroon D 2008. Fossil dripwater in stalagmites reveals Holocene temperature and rainfall variation in Amazonia. *Earth and Planetary Science Letters* 275: 54-60.
- Van den Kerkhof AM, Hein UF 2001. Fluid inclusion petrography. *Lithos* 55: 27-47.
- Vandergoes MJ, Fitzsimons S 2003. The Last Glacial–Interglacial Transition (LGIT) in south Westland, New Zealand: paleoecological insight into mid-latitude Southern Hemisphere climate change. *Quaternary Science Reviews* 22: 1461-1476.
- Vandergoes MJ, Dieffenbacher-Krall AC, Newnham RM, Denton GH, Blaauw M 2008. Cooling and changing seasonality in the Southern Alps, New Zealand during the Antarctic Cold Reversal. *Quaternary Science Reviews* 27: 589-601.
- Vandergoes MJ, Newnham R, Preusser F, Hendy C, Lowell T, Fitzsimons S, Hogg A, Kasper H, Schlüchter C 2005. Regional insolation forcing of late Quaternary climate change in the Southern Hemisphere. *Nature* 436: 242-245.
- Verheyden S, Genty D, Cattani O, van Breukelen MR 2008. Water release patterns of heated speleothem calcite and hydrogen isotope composition of fluid inclusions. *Chemical Geology* 247: 266-281.
- Verheyden S, Keppens E, Fairchild IJ, McDermott F, Weis D 2000. Mg, Sr and Sr isotope geochemistry of a Belgian Holocene speleothem: implications for paleoclimate reconstructions. *Chemical Geology* 169: 131-144.
- Vonhof HB, Atkinson TC, van Breukelen MR, Postma O 2007. Fluid inclusion hydrogen and oxygen isotope analyses using the “Amsterdam Device”: a progress report. *Geophysical Research Abstracts*.
- Vonhof HB, van Breukelen MR, Postma O, Rowe PJ, Atkinson TC, Kroon D 2006. A continuous-flow crushing device for on-line  $\delta^2\text{H}$  analysis of fluid inclusion water in speleothems. *Rapid Communications in Mass Spectrometry* 20: 2553-2558.
- Warren CR, McGrath J, Adams M 2001. Water Availability and Carbon Isotope Discrimination in Conifers. *Oecologia* 127(4): 476-486.

- Whitehead NE, Ditchburn RG, Williams PW, McCabe WJ 1999. 231Pa and 230Th contamination at zero age: a possible limitation on U/Th series dating of speleothem material. *Chemical Geology* 156: 359-366.
- Whittaker TE 2008. High-resolution speleothem-based paleoclimate records from New Zealand reveal robust teleconnection to North Atlantic during MIS 1-4. Unpublished thesis, University of Waikato, Hamilton. 249 p.
- Whittaker TE, Hendy CH, Hellstrom JC 2011. Abrupt millennial-scale changes in intensity of Southern Hemisphere westerly winds during marine isotope stages 2 – 4. *Geology* 39(5): 455-458.
- Williams PW ed. 1980. Metro Cave: A Survey of Scientific and Scenic Resources, NZ Forest Service. 85 p.
- Williams PW 1982. Speleothem dates, Quaternary terraces and uplift rates in New Zealand. *Nature* 298: 257-260.
- Williams PW 1996. A 230 ka record of glacial and interglacial events from Aurora Cave, Fiordland, New Zealand. *New Zealand Journal of Geology and Geophysics* 39: 225-241.
- Williams PW 2008. The role of the epikarst in karst and cave hydrogeology: a review. *International Journal of Speleology* 31(1): 1-10.
- Williams PW, Neil HL, Zhao J-X 2010. Age frequency distribution and revised stable isotope curves for New Zealand speleothems: palaeoclimatic implications. *International Journal of Speleology* 39(2): 99-112.
- Williams PW, Marshall A, Ford DC, Jenkinson AV 1999. Palaeoclimatic interpretation of stable isotope data from Holocene speleothems of the Waitomo district, North Island, New Zealand. *The Holocene* 9(6): 649-657.
- Williams PW, King DNT, Zhao J-X, Collerson KD 2004. Speleothem master chronologies: combined Holocene 18O and 13C records from the North Island of New Zealand and their palaeoenvironmental interpretation. *The Holocene* 14(2): 194-208.
- Williams PW, King DNT, Zhao J-X, Collerson KD 2005. Late Pleistocene to Holocene composite speleothem 18O and 13C chronologies from South Island, New Zealand—did a global Younger Dryas really exist? *Earth and Planetary Science Letters* 230: 301-317.
- Wing AL, Harrington GJ, Smith FA, Boch JJ, Boyer DM, Freeman KH 2005. Transient floral change and rapid global warming at the Paleocene-Eocene boundary. *Science* 310(5750): 993-996.
- Wood SA 1990. The aqueous geochemistry of the rare-earth elements and yttrium. *Chemical Geology* 82: 159-186.
- Woodhead J, Hellstrom J, Maas R, Drysdale R, Zanchetta G, Devine P, Taylor E 2006. U–Pb geochronology of speleothems by MC-ICPMS. *Quaternary Geochronology* 1: 208-221.
- Woodhead J, Reisz R, Fox D, Drysdale R, Hellstrom J, Maas R, Cheng H, Edwards RE 2010. Speleothem climate records from deep time? Exploring the potential with an example from the Permian. *Geology* 38(5): 455-458.
- Worthy TH, Holdaway RN 1993. Quaternary fossil faunas from caves in the Punakaiki area, West Coast, South Island, New Zealand. *Journal of the Royal Society of New Zealand* 23: 147-254.
- Yonge CJ 1982. Stable isotope studies of water extracted from speleothems. Unpublished thesis, McMaster University. 298 p.
- Yonge CJ, Ford DC, Gray J, Schwarcz HP 1985. Stable isotope studies of cave seepage water. *Chemical Geology* 58: 97-105.

- Zachos J, Pagani M, Sloan L, Thomas E, Billups K 2001. Trends, rhythms, and aberrations in global climate 65 Ma to present. *Science* 292(5517): 686-693.
- Zhao J-X, Xia Q, Collerson KD 2001. Timing and duration of the Last Interglacial inferred from high resolution U-series chronology of stalagmite growth in Southern Hemisphere. *Earth and Planetary Science Letters* 184: 635-644.
- Zhou H, Wang Q, Zhao J, Zheng L, Guan H, Feng Y, Greig A 2008a. Rare earth elements and yttrium in a stalagmite from Central China and potential paleoclimatic implications. *Palaeogeography, Palaeoclimatology, Palaeoecology* 270: 128-138.
- Zhou H, Chi B, Lawrence M, Zhao J-X, Yan J, Greig A, Feng Y 2008b. High-resolution and precisely dated record of weathering and hydrological dynamics recorded by manganese and rare-earth elements in a stalagmite from Central China. *Quaternary Research* 69: 438-446.